

## Electronic Supporting Information

### Enhancement of catalytic hydrolysis activity for organophosphates by the Metal-Organic Framework MOF-808-NH<sub>2</sub> via post-synthetic modification.

Sergio J. Garibay,<sup>1,2</sup> Trenton M. Tovar,<sup>2</sup> Ivan Iordanov,<sup>2</sup> Gregory W. Peterson,<sup>2</sup> and Jared B. DeCoste<sup>2\*</sup>

---

<sup>1</sup>Leidos, Inc., 3465 Box Hill Corporate Center Drive, Abingdon, Maryland 21009, United States, USA.

<sup>2</sup>DEVCOM Chemical and Biological Center, 5183 Blackhawk Road, Aberdeen Proving Ground, Maryland 21010, USA.

---

\*Corresponding authors: [jared.b.decoste2.civ@mail.mil](mailto:jared.b.decoste2.civ@mail.mil)

**Abstract:** Metal-organic frameworks (MOFs) necessitate buffers or basic amine moieties for high activity and turnover in the hydrolysis of organophosphates. While polymeric amine buffers can be integrated with a MOF, all solid-state formulations suffer from active site poisoning of the secondary building units (SBUs) within MOFs which inhibits further catalytic turnover. Herein, we developed a simple soaking procedure with a basic aqueous solution that reactivates the active sites of spent MOFs after organophosphate catalysis. Moreover, we develop amine functionalized MOF-808 derivatives through de novo synthesis with H<sub>3</sub>-BTC-NH<sub>2</sub> (BTC = 1,3,5-benzenetricarboxylic acid) and post-synthetic modification (PSM) that are highly active for organophosphate hydrolysis under non-buffered aqueous conditions.

**DOI:**

## Experimental Procedures

All reagents were purchased from commercial sources and used without further purification. H<sub>3</sub>-BTC-NH<sub>2</sub> was synthesized according to published procedures.<sup>1</sup>

<sup>1</sup>H-NMR spectra were recorded on Varian FT-NMR spectrometer (300 MHz) and data were analysed with Mestre Nova software. Samples (~10 mg) were digested using ~60 μL of D<sub>2</sub>SO<sub>4</sub> and 600 μL of DMSO-d<sub>6</sub>.

<sup>31</sup>P-NMR spectra were recorded on Varian FT-NMR spectrometer (400 MHz) and data were analysed with Mestre Nova software.

Powder X-ray diffraction (PXRD) data were measured at room temperature on a PXRD data were also measured on a Rigaku Miniflex 600 diffractometer at 30kV, 15mA (CuKα1 radiation, λ = 1.54056 Å) with a scan speed of 5°/min and a step size of 0.05 in 2θ at room temperature.

Nitrogen isotherm measurements were carried out on a Micromeritics ASAP 2420 instrument at 77 K. Samples were activated at specified temperatures under vacuum on a Micromeritics Smart VacPrep instrument until an outgas rate below 0.05 mmHg/min was achieved.

Thermogravimetric analyses were performed under a stream of air using a TA Instrument Q600 SDT running from room temperature to 600 °C with a scan rate of 5 °C/min.

pH measurements were measured with EMD Millipore™ MColorpHast™ 1.09535.0001 Non-Bleeding pH-Indicator Strips.

### MOF-808 synthesis, activation and SALI modification

**Zr-MOF-808-PA:** ZrCl<sub>4</sub> (117 mg, 0.5 mmol), BTC (35 mg, 0.168 mmol) and propanoic acid (3.7 mL, 49 mmol) were mixed in 10 mL of DMF in an 8-dram vial and ultrasonically dissolved. The clear solution was incubated in an oven at 120 °C for 24 h. After cooling down to room temperature, the white polycrystalline material was isolated by centrifuge (5 min, 7500 rpm) and solvent exchanged with fresh DMF three times (10 mL each) followed by methanol three times (10 mL). Zr-MOF-808-PA was collected by centrifugation and dried in a vacuum oven at 80 °C for 1 h.

The as synthesized MOF-808-PA was suspended in 12 mL DMF or acetone and 0.5 mL of 4 M aqueous HCl was added to an 8-dram vial and heated in an oven at 100°C or 50°C (DMF and acetone, respectively) for 18 h. After cooling to room temperature, the powder was isolated by centrifugation and washed with DMF three times (10 mL each) and acetone three times (10 mL each). MOF-808-act was collected by centrifugation and dried in a vacuum oven at 80 °C for 1 h, and then activated at 120 °C for 18 h using Micromeritics Smart VacPrep instrument as described above.

**Hf-MOF-808-PA:** HfCl<sub>4</sub> (160 mg, 0.5 mmol), BTC (35 mg, 0.168 mmol) and propanoic acid (3.7 mL, 49 mmol) were mixed in 10 mL of DMF in an 8-dram vial and ultrasonically dissolved. The clear solution was incubated in an oven at 120 °C for 24 h. After cooling down to room temperature, the white polycrystalline material was isolated by centrifuge (5 min, 7500 rpm) and solvent exchanged with fresh DMF three times (10 mL each) followed by methanol three times (10 mL). Hf-MOF-808-PA was collected by centrifugation and dried in a vacuum oven at 80 °C for 1 h.

The as synthesized Hf-MOF-808-PA was suspended in 12 mL DMF or acetone and 0.5 mL of 4 M aqueous HCl was added to an 8-dram vial and heated in an oven at 100°C or 50°C (DMF and acetone, respectively) for 18 h. After cooling to room temperature, the powder was isolated by centrifugation and washed with DMF and/or acetone three

times (10 mL each). Hf-MOF-808-HCl-act was collected by centrifugation and dried in a vacuum oven at 80 °C for 1 h.

**Zr-MOF-808-AA:** ZrCl<sub>4</sub> (117 mg, 0.5 mmol), BTC (35 mg, 0.168 mmol) and acetic acid (2.8 mL, 49 mmol) were mixed in 10 mL of DMF in an 8-dram vial and ultrasonically dissolved. The clear solution was incubated in an oven at 120 °C for 24 h. After cooling down to room temperature, the white polycrystalline material was isolated by centrifuge (5 min, 7500 rpm) and solvent exchanged with fresh DMF three times (10 mL each) followed by methanol three times (10 mL). Zr-MOF-808-AA was collected by centrifugation and dried in a vacuum oven at 80 °C for 1 h.

**Zr-MOF-808-TFA:** ZrCl<sub>4</sub> (117 mg, 0.5 mmol), BTC (35 mg, 0.168 mmol) and trifluoroacetic acid (3.8 mL, 49 mmol) were mixed in 10 mL of DMF in an 8-dram vial and ultrasonically dissolved. The clear solution was incubated in an oven at 120 °C for 24 h. After cooling down to room temperature, the white polycrystalline material was isolated by centrifuge (5 min, 7500 rpm) and solvent exchanged with fresh DMF three times (10 mL each) followed by methanol three times (10 mL). MOF-808-P was collected by centrifugation and dried in a vacuum oven at 80 °C for 1 h.

**Zr-MOF-808-SALI-DMP:** Zr-MOF-808-HCl-act (43 mg, 0.032 mmol) and dimethylphosphate (3.6 uL, 0.04 mmol) were mixed in 7 mL of water in an 8-dram vial. The clear solution was incubated at room temperature (~35 °C) for 24 h. The material was solvent exchanged with water three times (10 mL each) followed by methanol three times (10 mL). Zr-MOF-808-SALI-DMP was collected by centrifugation and dried in a vacuum oven at 80 °C for 1 h.

**Hf-MOF-808-SALI-DMP:** Hf-MOF-808-HCl-act (30 mg, 0.016 mmol) and dimethylphosphate (2 uL, 0.02 mmol) were mixed in 7 mL of water in a 8-dram vial. The clear solution was incubated at room temperature (~35 °C) for 24 h. The material was solvent exchanged with water three times (10 mL each) followed by methanol three times (10 mL). Hf-MOF-808-SALI-DMP was collected by centrifugation and dried in a vacuum oven at 80 °C for 1 h.

**Synthesis of Zr-MOF-808-SALI-[BA-morph]:** Zr-MOF-808-HCl-acetone-act (55 mg, 0.04 mmol) and 4-(morpholinomethyl)benzoic acid (171 mg, 0.78 mmol) were mixed in 8 mL of DMF in an 8-dram vial and ultrasonically dissolved. The vial was incubated in an oven at 80 °C for 18 h. After cooling down to room temperature, material was isolated by centrifuge (5 min, 7500 rpm) and solvent exchanged with fresh DMF three times (10 mL each) followed by methanol three times (10 mL). MOF-808-SALI-[BA-Morph]<sub>2</sub>[PA]<sub>1</sub> was collected by centrifugation and dried in a vacuum oven at 80 °C for 1 h.

**Synthesis of Hf-MOF-808-SALI-[BA-morph]<sub>3</sub>:** Hf-MOF-808-HCl-DMF-act (158 mg, 0.087 mmol) and 4-(morpholinomethyl)benzoic acid (155 mg, 0.7 mmol) were mixed in 8 mL of DMF in an 8-dram vial and ultrasonically dissolved. The clear solution was incubated in an oven at 70 °C for 18 h. After cooling down to room temperature, material was isolated by centrifuge (5 min, 7500 rpm) and solvent exchanged with fresh DMF three times (10 mL each) followed by methanol three times (10 mL). Hf-MOF-808-SALI-[BA-morph]<sub>3</sub>[PA]<sub>1</sub> was collected by centrifugation and dried in a vacuum oven at 80 °C for 1 h.

**Synthesis of Zr-MOF-808-SALI-[BA-CH<sub>2</sub>NH<sub>2</sub>]<sub>3</sub>[BA-CH<sub>2</sub>-NH<sub>3</sub><sup>+</sup>]<sub>1</sub>[PA]<sub>1</sub>:** Zr-MOF-808-HCl-DMF-act (50 mg, 0.04 mmol) and 4-(aminomethyl)benzoic acid (107 mg, 0.7 mmol) were mixed in 8 mL of H<sub>2</sub>O in an 8-dram vial and ultrasonically dissolved. The clear solution was incubated in an oven at 80 °C for 48 h. After cooling down to room temperature, material was isolated by centrifuge (5 min, 7500 rpm) and solvent exchanged with fresh H<sub>2</sub>O three times (10 mL each) followed by methanol three times (10 mL). MOF-808-SALI-[BA-CH<sub>2</sub>NH<sub>2</sub>]<sub>3</sub>[BA-CH<sub>2</sub>-NH<sub>3</sub><sup>+</sup>]<sub>1</sub>[PA]<sub>1</sub> was collected by centrifugation and dried in a vacuum oven at 80 °C for 1 h.

**Hf-MOF-808-SALI-[BA-CH<sub>2</sub>NH<sub>2</sub>]<sub>2</sub>[BA-CH<sub>2</sub>-NH<sub>3</sub><sup>+</sup>]<sub>2</sub>:** Hf-MOF-808-HCl-DMF-act (127 mg, 0.07 mmol) and 4-(aminomethyl)benzoic acid (210 mg, 1.4 mmol) were mixed in 16 mL of H<sub>2</sub>O in an 8-dram vial and ultrasonically dissolved. The clear solution was incubated in an oven at 70 °C for 18 h. After cooling down to room temperature, material was isolated by centrifuge (5 min, 7500 rpm) and solvent exchanged with fresh H<sub>2</sub>O three times (10 mL each) followed by methanol three times (10 mL). MOF-808-SALI-[BA-CH<sub>2</sub>NH<sub>2</sub>]<sub>2</sub>[BA-CH<sub>2</sub>-NH<sub>3</sub><sup>+</sup>]<sub>2</sub>[PA]<sub>1</sub> was collected by centrifugation and dried in a vacuum oven at 80 °C for 1 h.

**Zr-MOF-808-SALI-[BA-AO]<sub>2</sub>:** Zr-MOF-808-HCl-acetone-act (55 mg, 0.04 mmol) and 4-(N'-Hydroxycarbamimidoyl)benzoic acid (140 mg, 0.78 mmol) were mixed in 8 mL of DMF in an 8-dram vial and ultrasonically dissolved. The clear solution was incubated in an oven at 80 °C for 18 h. After cooling down to room temperature, material was isolated by centrifuge (5 min, 7500 rpm) and solvent exchanged with fresh DMF three times (10 mL each) followed by methanol three times (10 mL). Zr-MOF-808-SALI-[BA-AO]<sub>2</sub>[PA]<sub>1</sub> was collected by centrifugation and dried in a vacuum oven at 80 °C for 1 h.

**Hf-MOF-808-SALI-[BA-AO]<sub>3</sub>:** Hf-MOF-808-HCl-DMF-act (150 mg, 0.082 mmol) and 4-(N'-Hydroxycarbamimidoyl)benzoic acid (148 mg, 0.82 mmol) were mixed in 8 mL of DMF in an 8-dram vial and ultrasonically dissolved. The clear solution was incubated in an oven at 70 °C for 18 h. After cooling down to room temperature, material was isolated by centrifuge (5 min, 7500 rpm) and solvent exchanged with fresh DMF three times (10 mL each) followed by methanol three times (10 mL). Hf-MOF-808-SALI-[BA-AO]<sub>3</sub>[PA]<sub>1</sub> was collected by centrifugation and dried in a vacuum oven at 80 °C for 1 h.

**Zr-MOF-808-NH-TFA:** ZrCl<sub>4</sub> (117 mg, 0.5 mmol), H<sub>3</sub>-BTC-NH<sub>2</sub> (38 mg, 0.168 mmol) and trifluoroacetic acid (1.8 mL, 23.5 mmol) were mixed in 10 mL of DMF in an 8-dram vial and ultrasonically dissolved. The clear solution was incubated in an oven at 120 °C for five days. After cooling down to room temperature, the white polycrystalline material was exchanged with fresh DMF three times (10 mL each) followed by methanol three times (10 mL). Zr-MOF-808-NH-TFA was dried in a vacuum oven at 80 °C for 1 h.

**Zr-MOF-808-NH-TFA-HCl-act:** The as synthesized Zr-MOF-808-NH-TFA (70 mg) was suspended in 12 mL acetone and 1 mL of 4 M aqueous HCl was added to an 8-dram vial and heated in an oven at 50 °C for 18 h. After cooling to room temperature, the powder was solvent exchanged with water three times (10 mL each) and acetone three times (10 mL each). Zr-MOF-808-NH-TFA-HCl-act was dried in a vacuum oven at 80 °C for 1 h.

**Zr-MOF-808-NH<sub>2</sub>-K<sub>2</sub>CO<sub>3</sub>-act:** The as synthesized Zr-MOF-808-NH-TFA (62 mg, 0.034 mmol) was suspended in an aqueous K<sub>2</sub>CO<sub>3</sub> solution (9.2 mM, 10 mL) was added to an 8-dram vial and heated in an oven at 90°C for 18 h. After cooling to room temperature, the powder was solvent exchanged with water three times (10 mL each) and

methanol three times (10 mL each). Zr-MOF-808-NH<sub>2</sub> was dried in a vacuum oven at 80 °C for 1 h, and then activated at 100 °C for 18 h.

**Hf-MOF-808-NH-TFA:** HfCl<sub>4</sub> (160 mg, 0.5 mmol), H<sub>3</sub>-BTC-NH<sub>2</sub> (38 mg, 0.168 mmol) and trifluoroacetic acid (1.8 mL, 23.5 mmol) were mixed in 10 mL of DMF in an 8-dram vial and ultrasonically dissolved. The clear solution was incubated in an oven at 120 °C for five days. After cooling down to room temperature, the white polycrystalline material was exchanged with fresh DMF three times (10 mL each) followed by methanol three times (10 mL each). Hf-MOF-808-NH-TFA was dried in a vacuum oven at 80 °C for 1 h.

**Hf-MOF-808-NH<sub>2</sub>-K<sub>2</sub>CO<sub>3</sub>-act:** The as synthesized Hf-MOF-808-NH-TFA (240 mg, 0.094 mmol) was suspended in 10 mL water and an aqueous K<sub>2</sub>CO<sub>3</sub> solution (9.2 mM, 10 mL) was added to an 8-dram vial and heated in an oven at 90°C for 18 h. After cooling to room temperature, the powder was solvent exchanged with water three times (10 mL each) and methanol three times (10 mL each). Hf-MOF-808-NH<sub>2</sub> was dried in a vacuum oven at 80 °C for 1 h, and then activated at 100 °C for 18 h.

**Zr-MOF-808-NH-Morph:** Zr-MOF-808-NH<sub>2</sub>-K<sub>2</sub>CO<sub>3</sub>-act (90 mg, 0.068 mmol), 4-(2-chloroethyl)morpholine (14 mg, 0.1 mmol) and K<sub>2</sub>CO<sub>3</sub> (13 mg, 0.092 mmol) were mixed in 10 mL of CH<sub>3</sub>CN in an 8-dram vial. The solution was incubated in an oven at 75 °C for 18 h. After cooling down to room temperature, material was solvent exchanged with fresh H<sub>2</sub>O three times (10 mL each) followed by methanol three times (10 mL). Zr-MOF-808-NH-Morph was dried in a vacuum oven at 80 °C for 1 h.

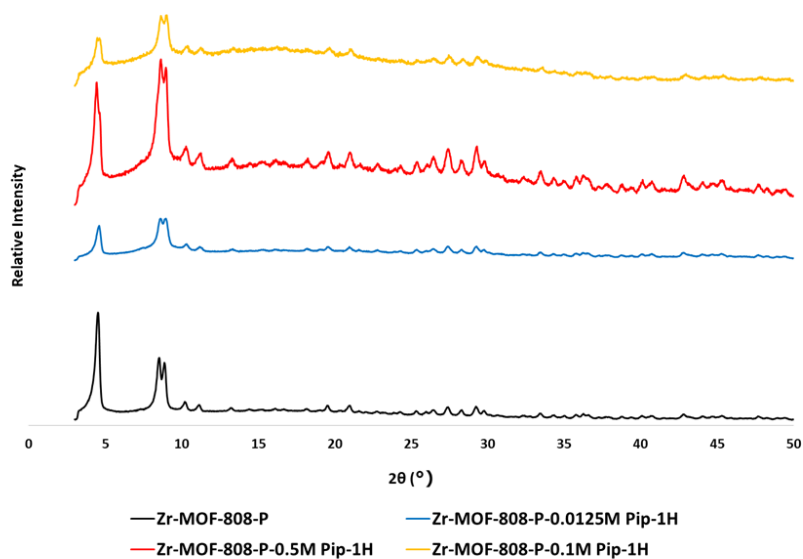


**Figure S1.** PXRD patterns of Zr-MOF-808-PA (black, bottom), after 24 h treatment with 0.0125 M piperidine aqueous solution (blue), 0.5 M piperidine aqueous solution (red), 0.1 M piperidine aqueous solution (yellow, top).

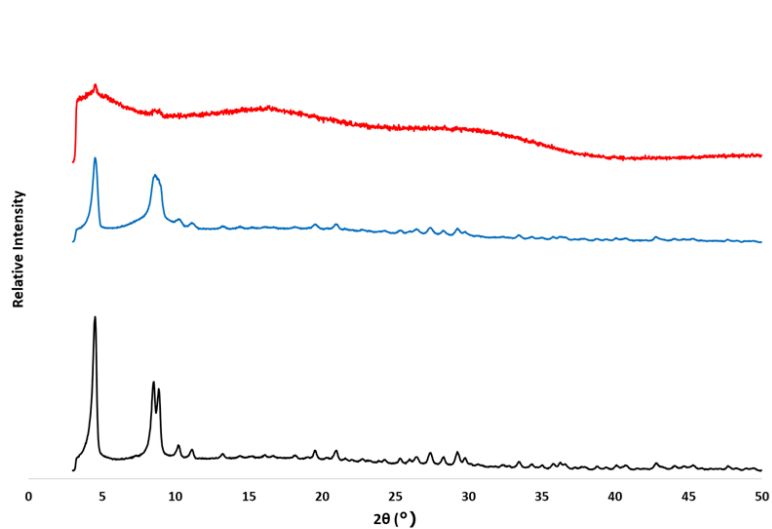


**Figure S2.** PXR D patterns of Hf-MOF-808-PA (black, bottom), after 24 h treatment with 0.0125 M piperidine aqueous solution (blue, middle), 0.1 M piperidine aqueous solution (red).

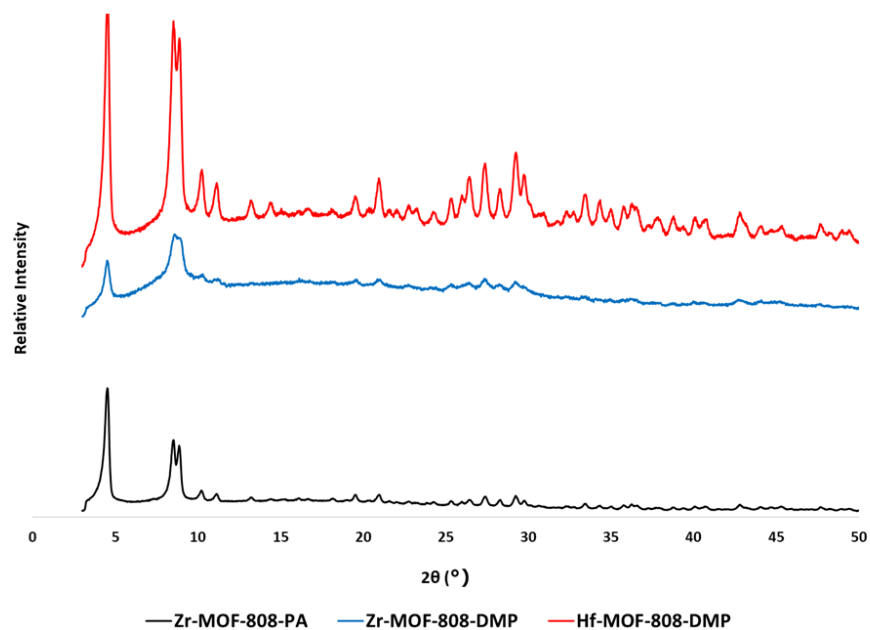


**Figure S3.** PXR D patterns of Zr-MOF-808-PA (bottom), Zr-MOF-808-DMP (middle) and Hf-MOF-808-DMP (top).

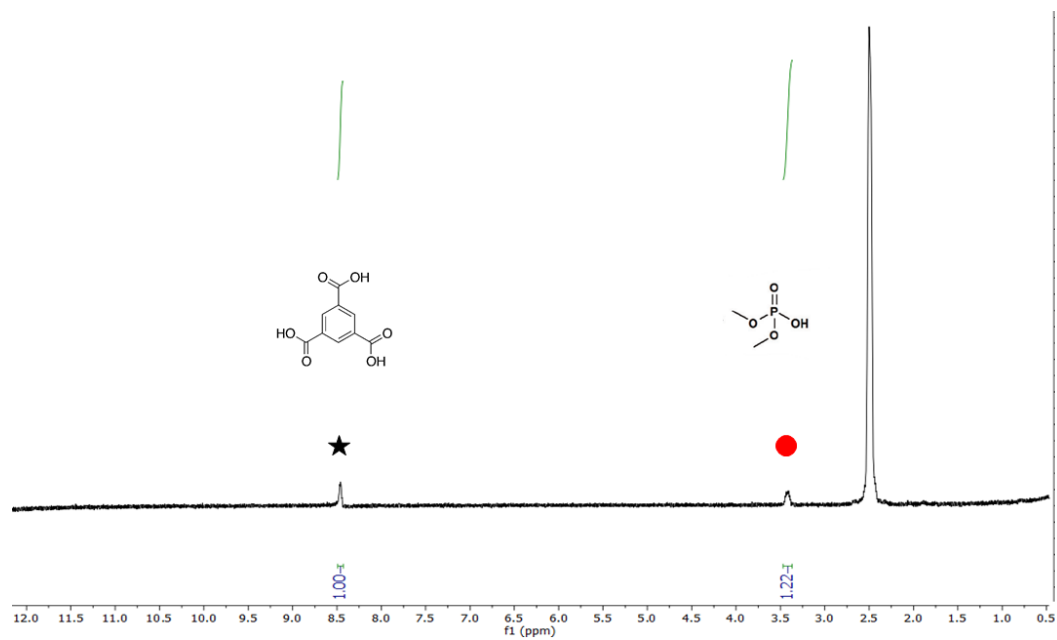


**Figure S4.**  $^1\text{H}$  NMR spectrum of digested Zr-MOF-808-SALI-DMP in  $d_6$ -DMSO.

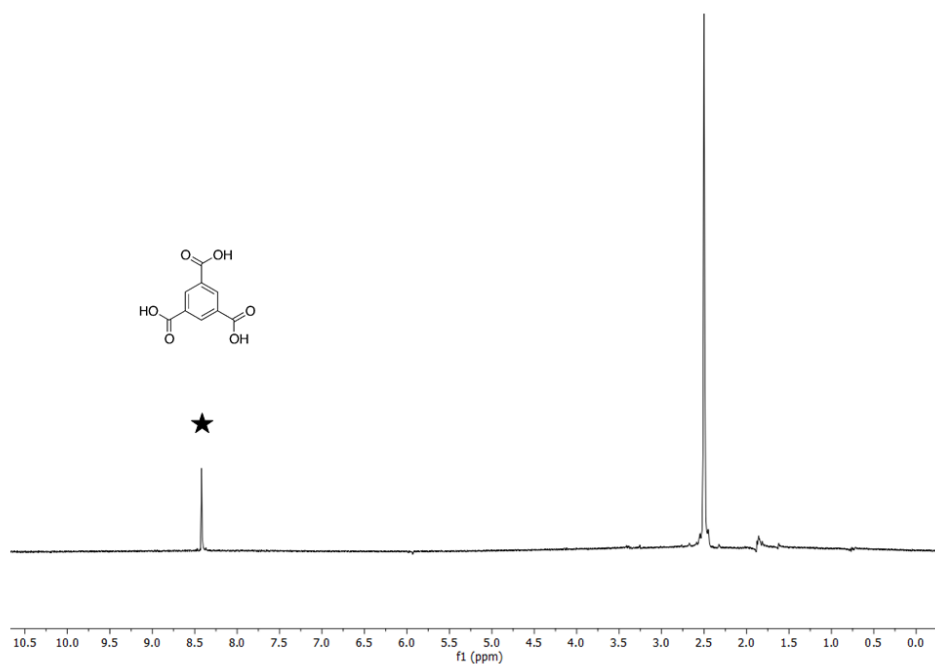


**Figure S5.**  $^1\text{H}$  NMR spectrum of digested Zr-MOF-808-SALI-DMP treated with piperidine in  $d_6$ -DMSO.

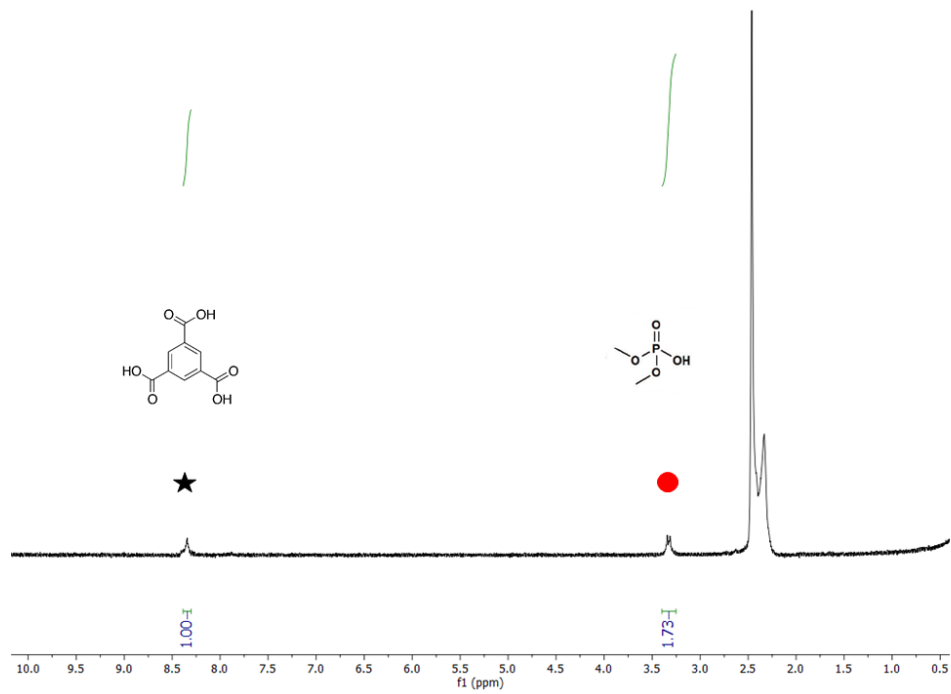


**Figure S6.** <sup>1</sup>H NMR spectrum of digested Hf-MOF-808-SALI-DMP in *d*<sub>6</sub>-DMSO.

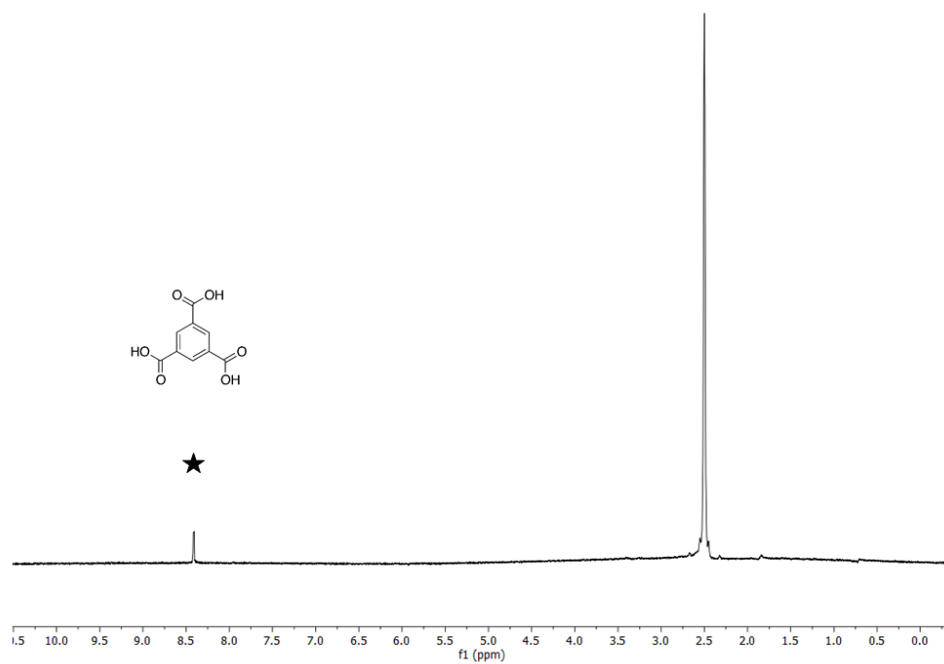


**Figure S7.** <sup>1</sup>H NMR spectrum of digested Hf-MOF-808-SALI-DMP treated with piperidine in *d*<sub>6</sub>-DMSO.



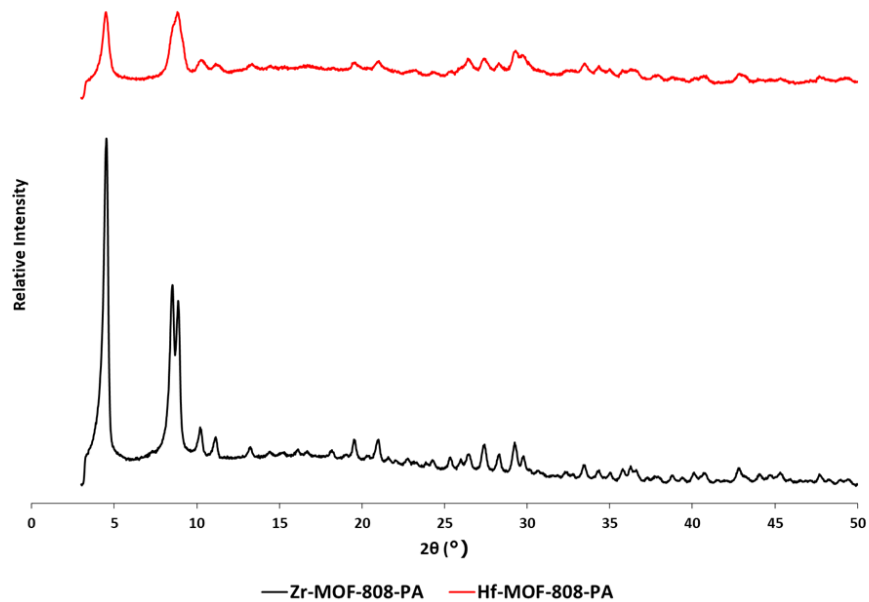


Figure S8. PXRD patterns of Zr-MOF-808-PA (bottom), and Hf-MOF-808-PA (top).

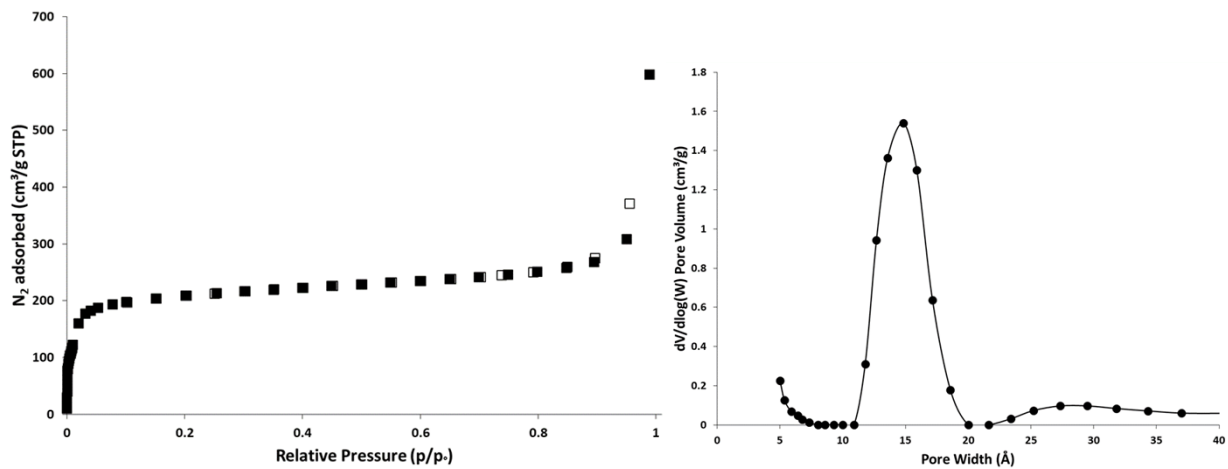


Figure S9.  $N_2$  isotherms (left) and pore size distribution (right) of Hf-MOF-808-PA. Adsorption = filled, desorption = empty markers.

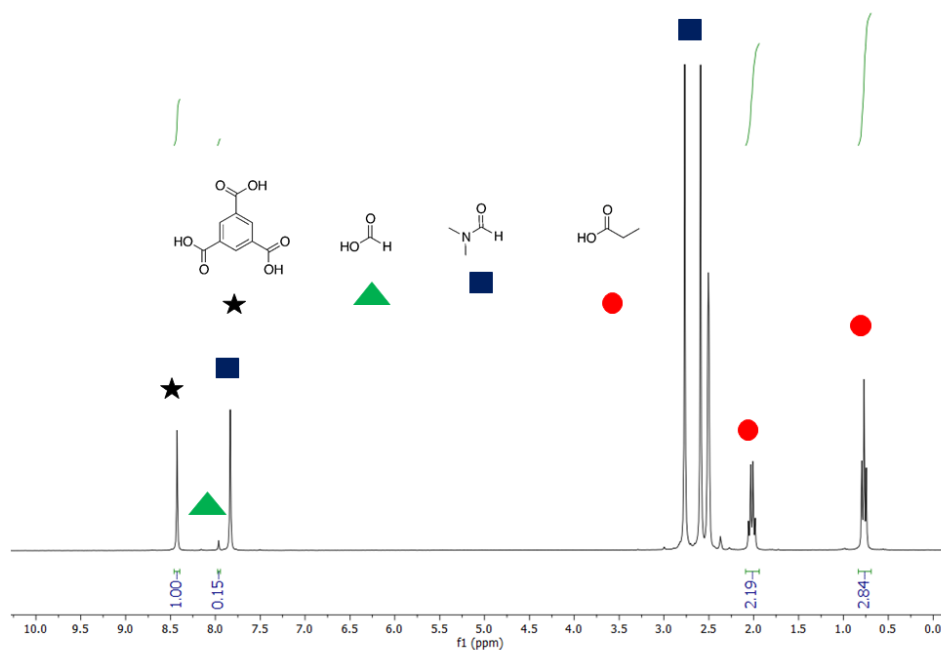


Figure S10.  $^1\text{H}$  NMR spectrum of digested Hf-MOF-808-PA in  $d_6$ -DMSO.

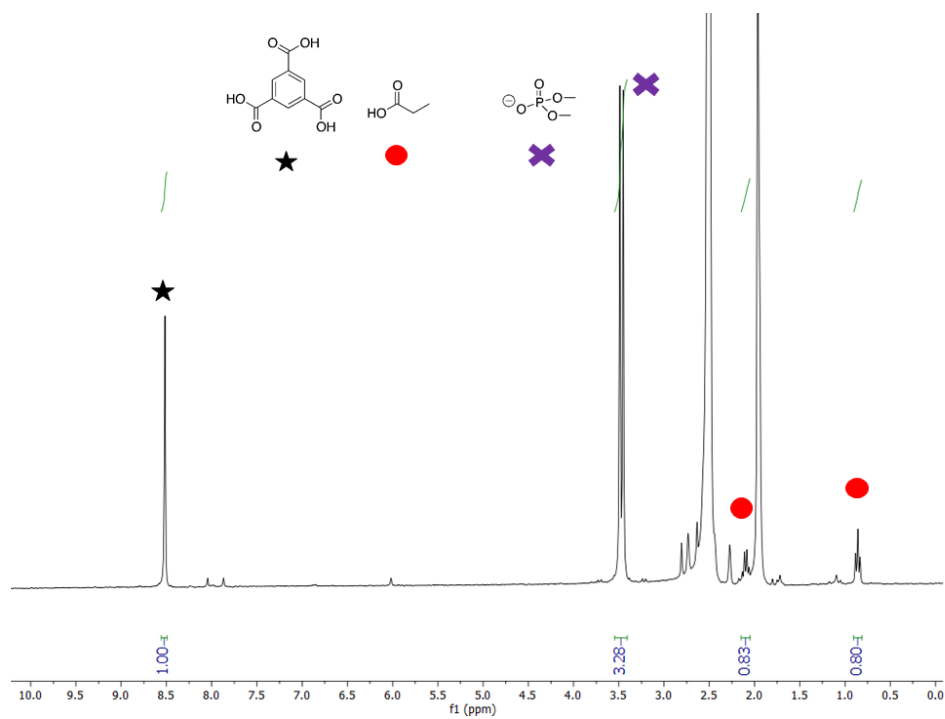
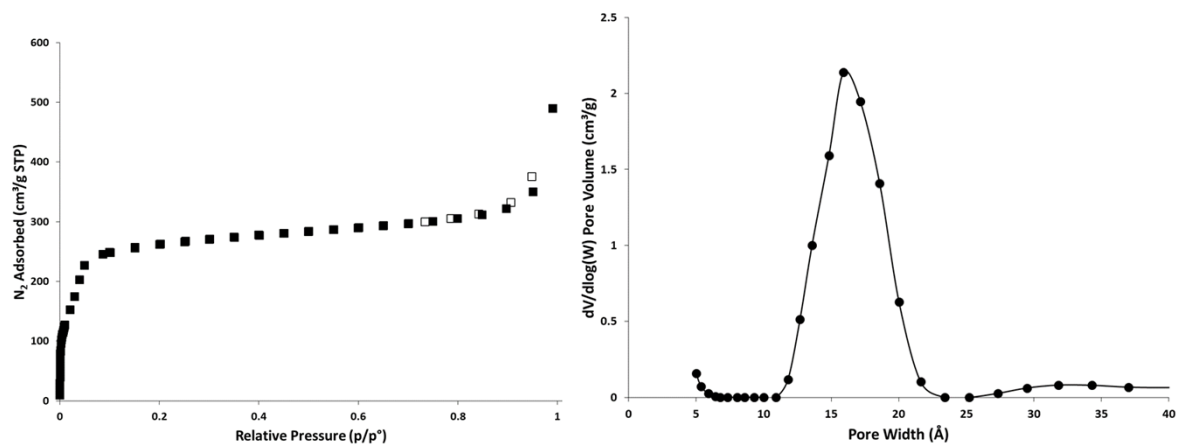
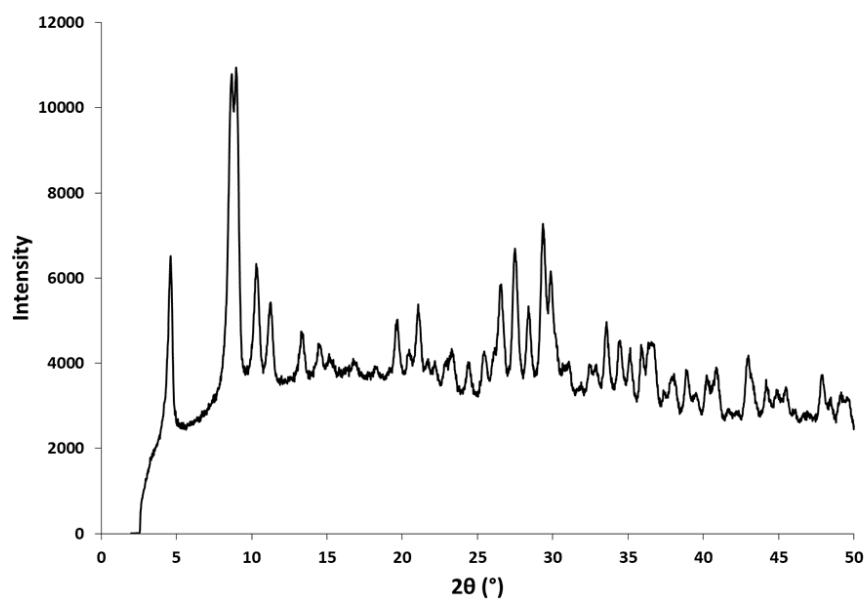


Figure S11.  $^1\text{H}$  NMR spectrum of digested Hf-MOF-808-PA after DMNP hydrolysis in  $d_6$ -DMSO.



**Figure S12.** N<sub>2</sub> isotherms (left) and pore size distribution (right) of Hf-MOF-808-HCl-DMF. Adsorption = filled, desorption = empty markers.



**Figure S13.** PXRD pattern of Hf-MOF-808-HCl-DMF.

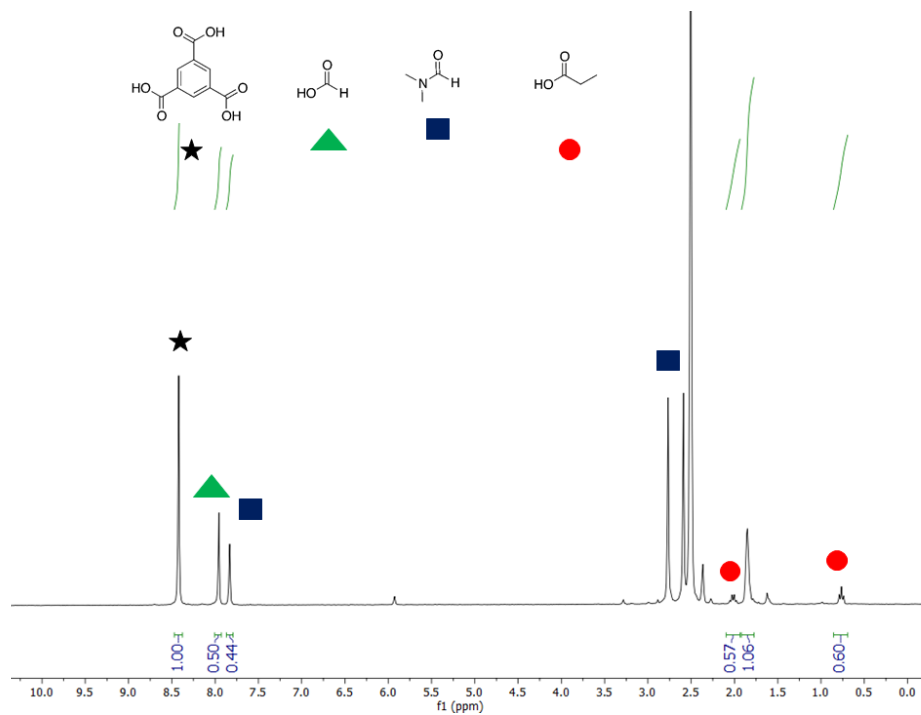


**Figure S14.** <sup>1</sup>H NMR spectrum of digested Hf-MOF-808-HCl-DMF in *d*<sub>6</sub>-DMSO.

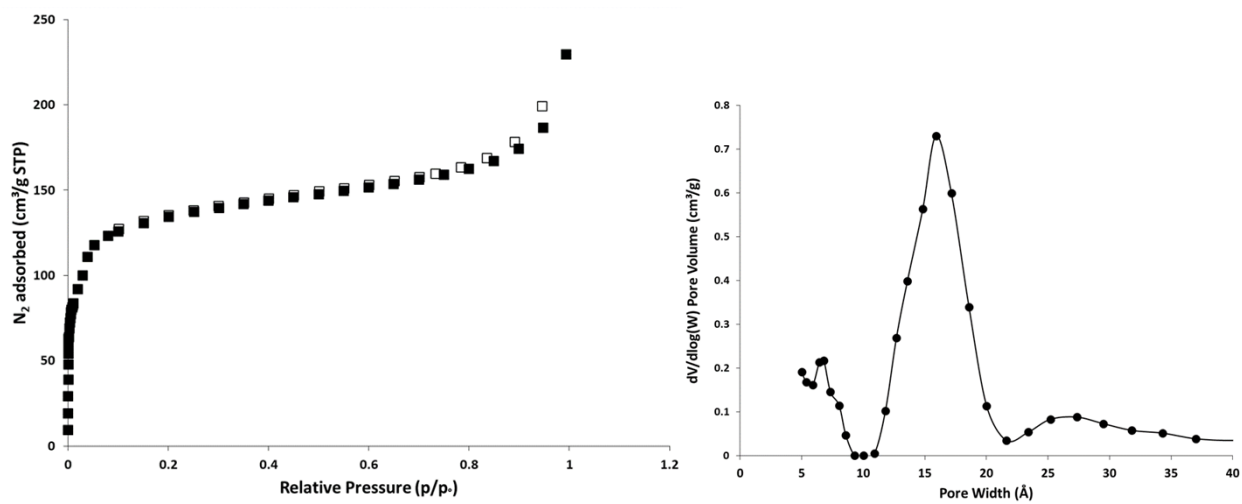


**Figure S15.** N<sub>2</sub> isotherms (left) and pore size distribution (right) of Zr-MOF-808-AA. Adsorption = filled, desorption = empty markers.

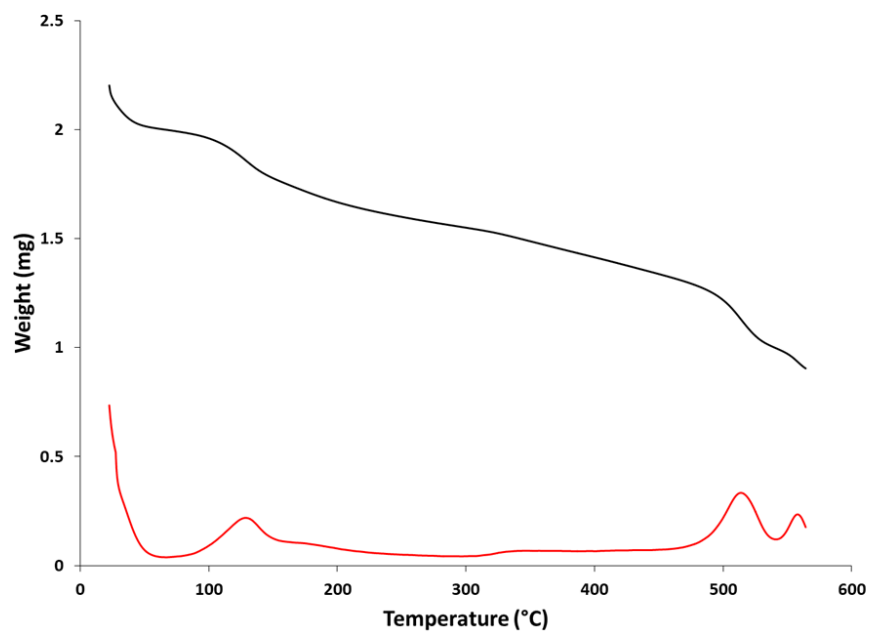


Figure S16. TGA curve (black) and derivative weight in %/°C (red) of Zr-MOF-808-AA.

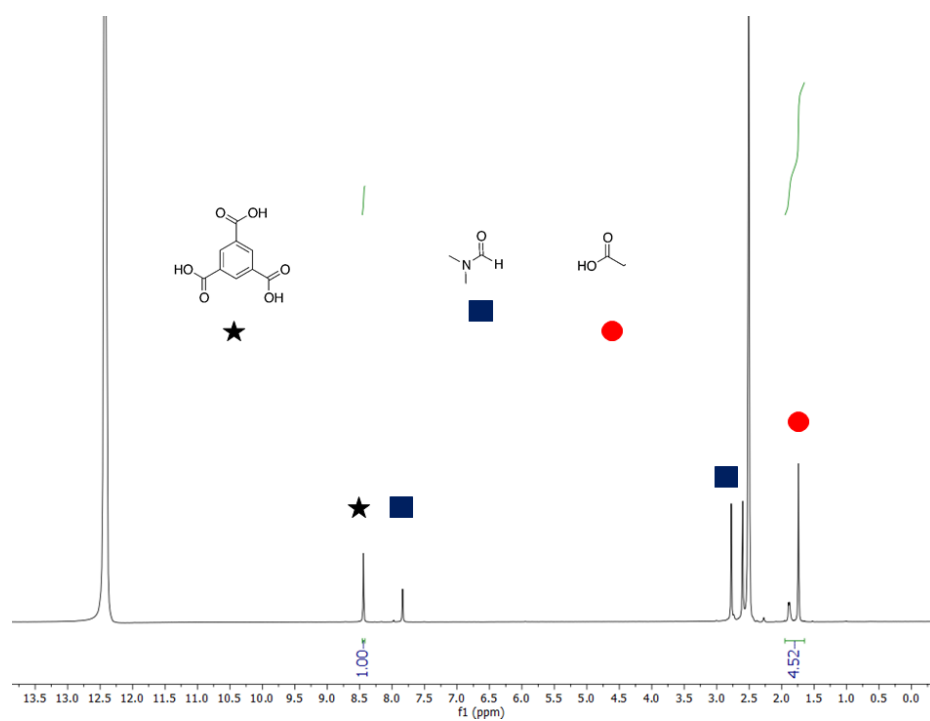
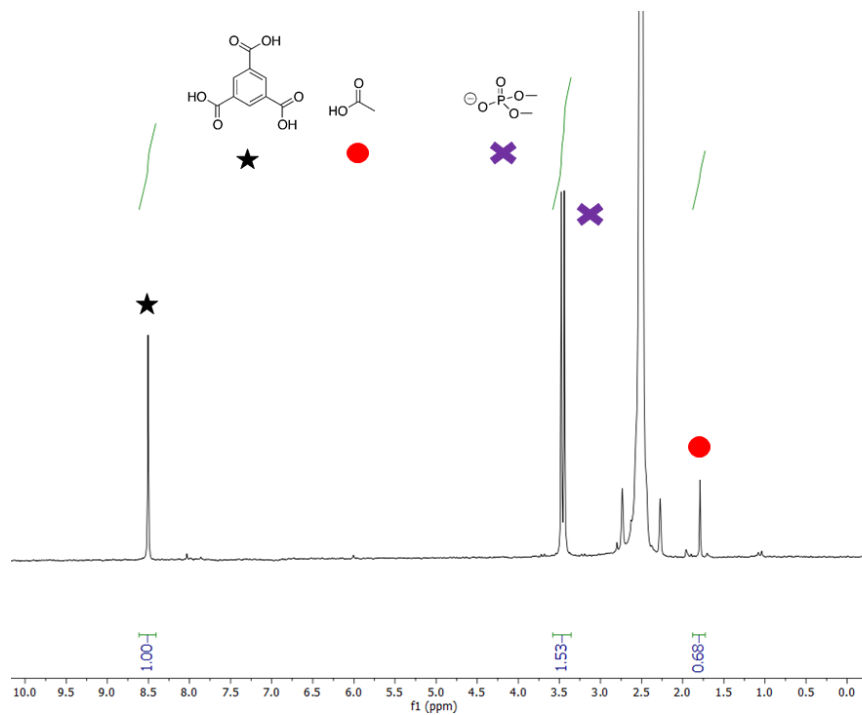
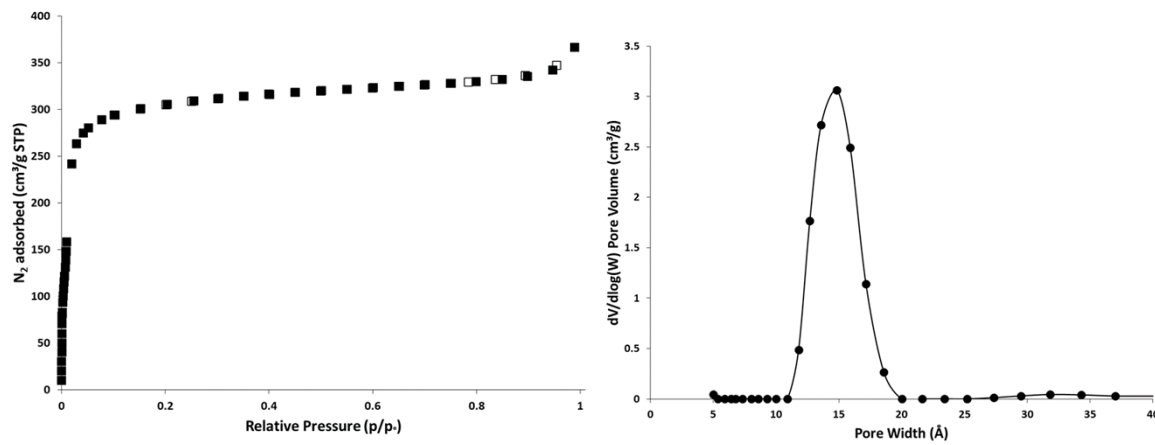


Figure S17. <sup>1</sup>H NMR spectrum of digested Zr-MOF-808-AA in *d*<sub>6</sub>-DMSO.



**Figure S18.**  $^1\text{H}$  NMR spectrum of digested Zr-MOF-808-AA after DMNP hydrolysis in  $d_6$ -DMSO.



**Figure S19.**  $\text{N}_2$  isotherms (left) and pore size distribution (right) of Zr-MOF-808-TFA. Adsorption = filled, desorption = empty markers.

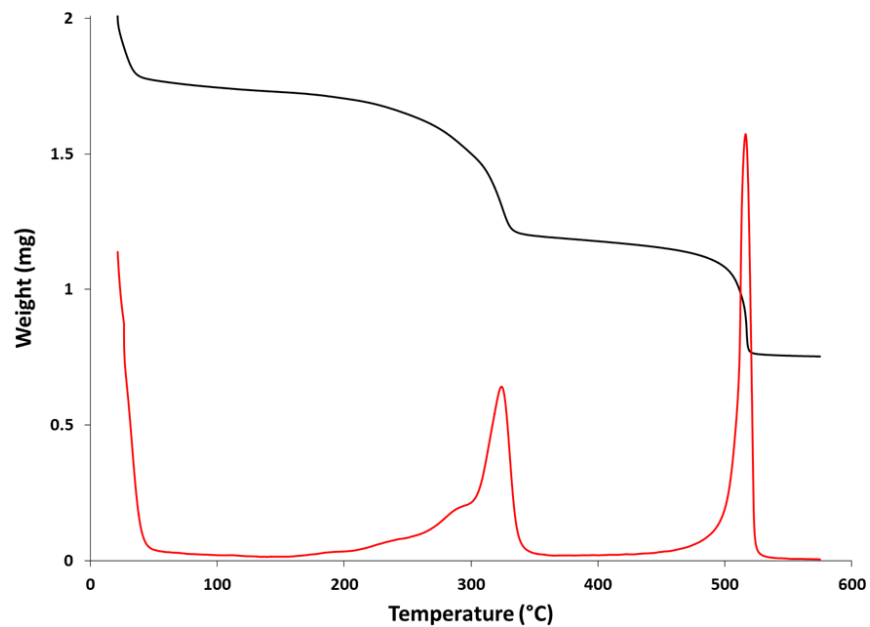


Figure S20. TGA curve (black) and derivative weight in %/°C (red) of Zr-MOF-808-TFA.

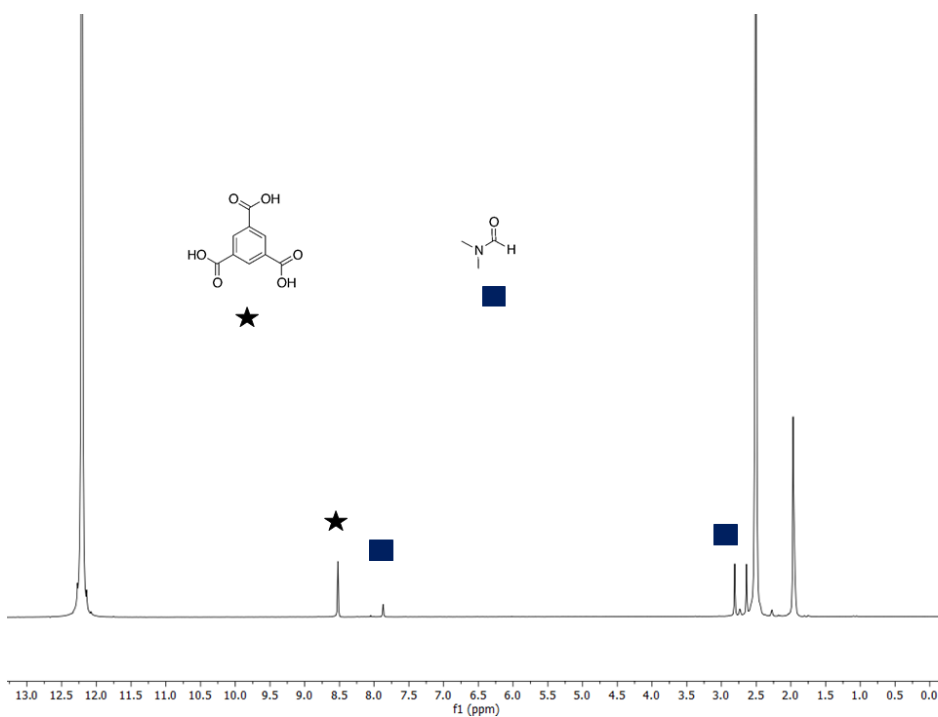


Figure S21. <sup>1</sup>H NMR spectrum of digested Zr-MOF-808-TFA in *d*<sub>6</sub>-DMSO.

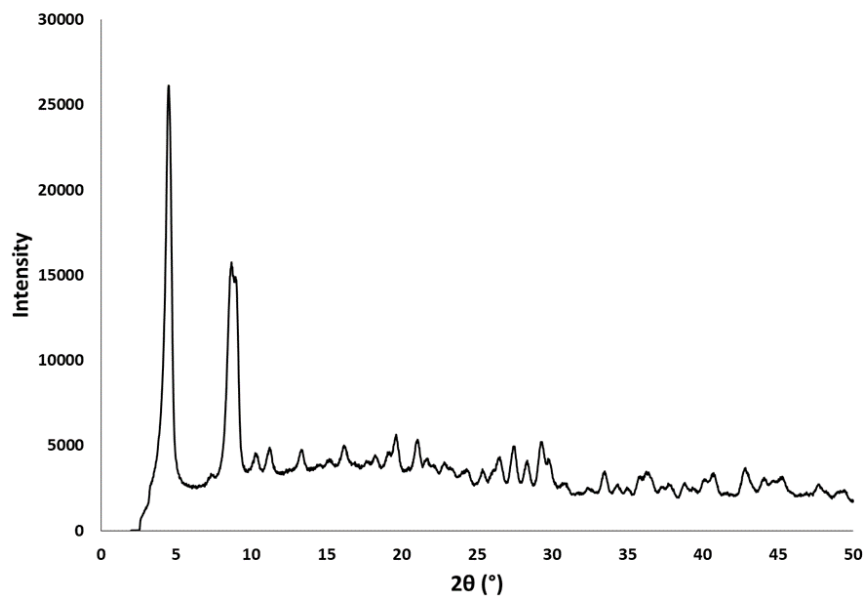


Figure S22. PXRD pattern of Zr-MOF-808-TFA.

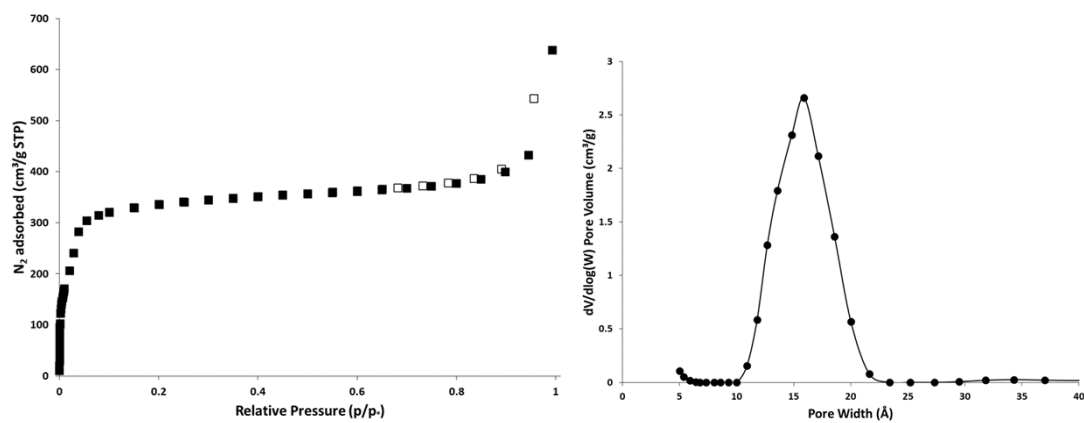


Figure S23. N<sub>2</sub> isotherms (left) and pore size distribution (right) of Hf-MOF-808-HCl-acetone. Adsorption = filled, desorption = empty markers.



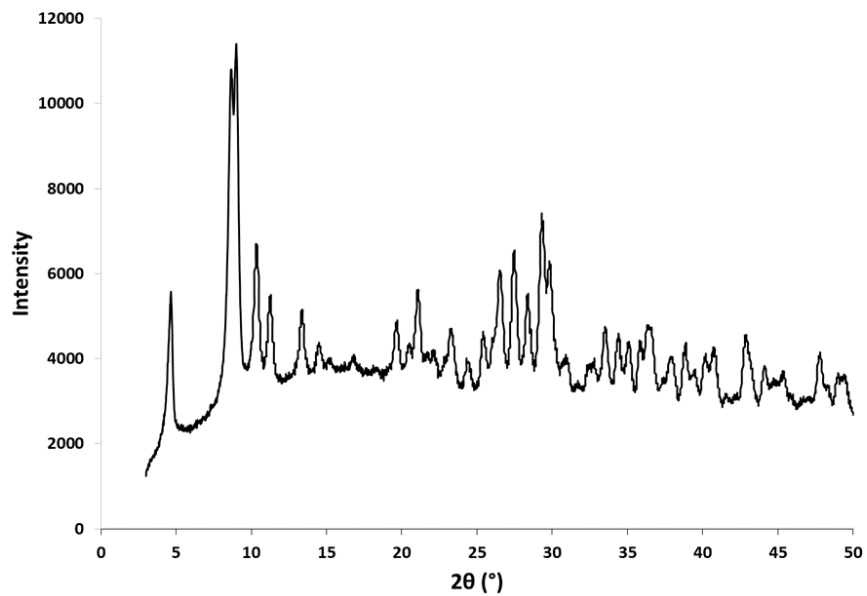


Figure S24. PXRD pattern of Hf-MOF-808-HCl-acetone.

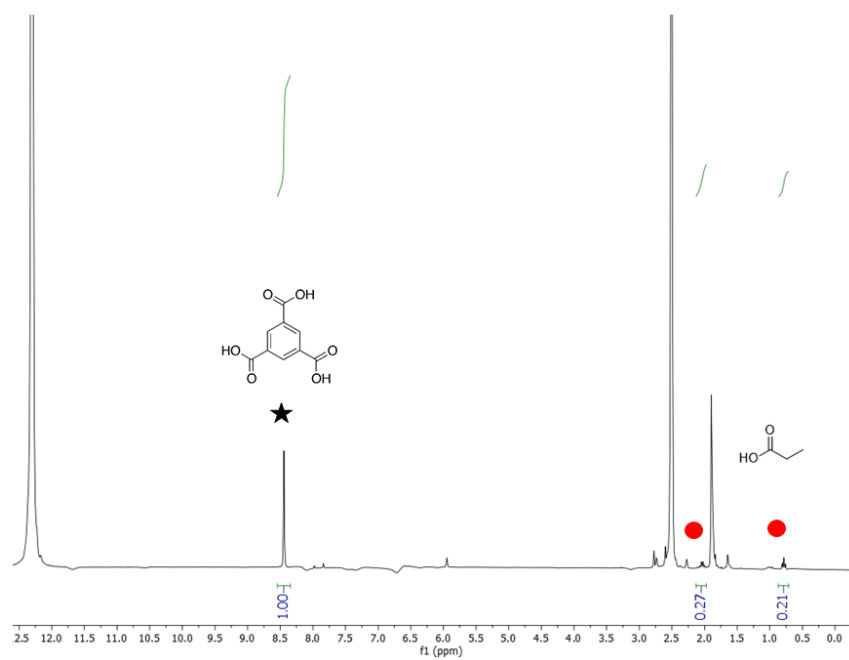
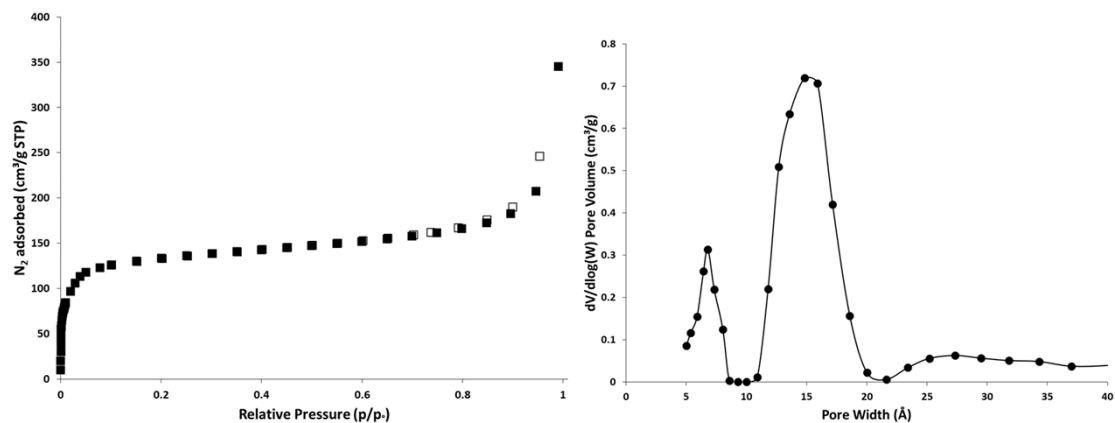
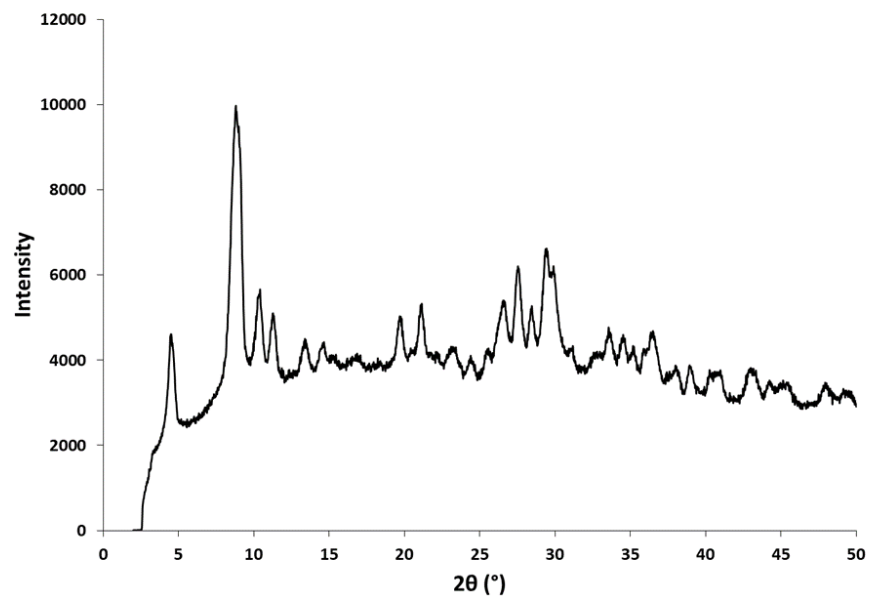


Figure S25.  $^1\text{H}$  NMR spectrum of digested Hf-MOF-808-HCl-acetone in  $d_6$ -DMSO.



**Figure S26.** N<sub>2</sub> isotherms (left) and pore size distribution (right) of Hf-MOF-808-SALI-BA-Morph. Adsorption = filled, desorption = empty markers.



**Figure S27.** PXRD pattern of Hf-MOF-808-SALI-BA-Morph.

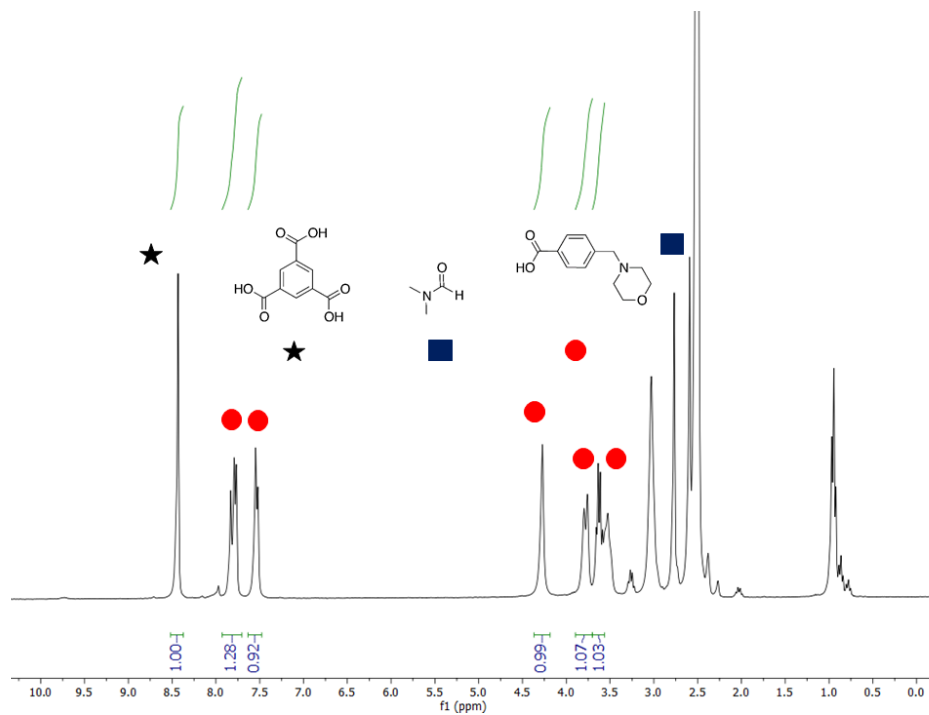


**Figure S28.** <sup>1</sup>H NMR spectrum of digested Hf-MOF-808-SALI-BA-Morph in *d*<sub>6</sub>-DMSO.

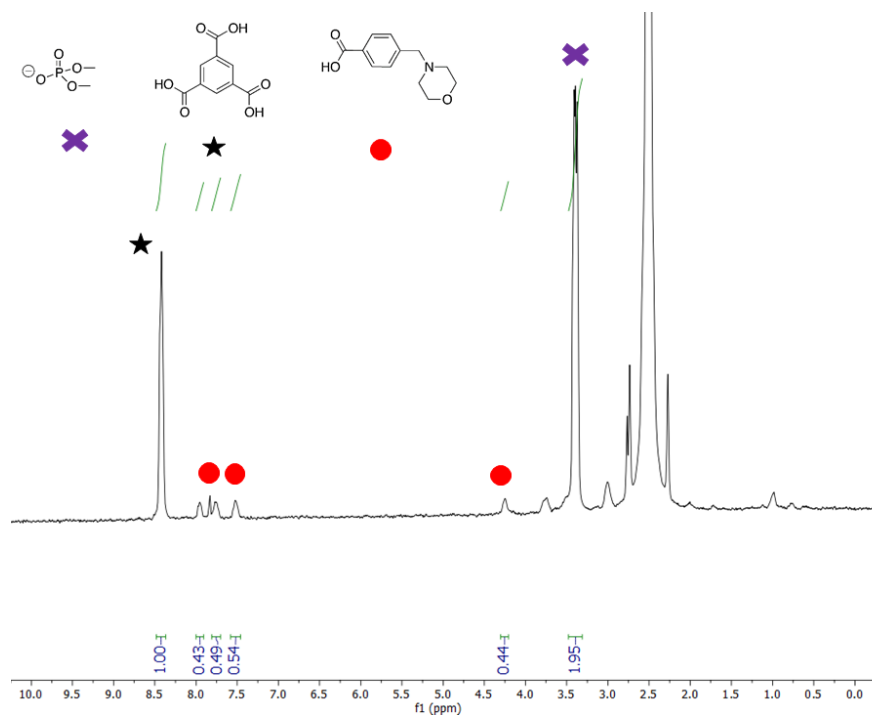


**Figure S29.** <sup>1</sup>H NMR spectrum of digested Hf-MOF-808-SALI-BA-Morph after DMNP hydrolysis in *d*<sub>6</sub>-DMSO.

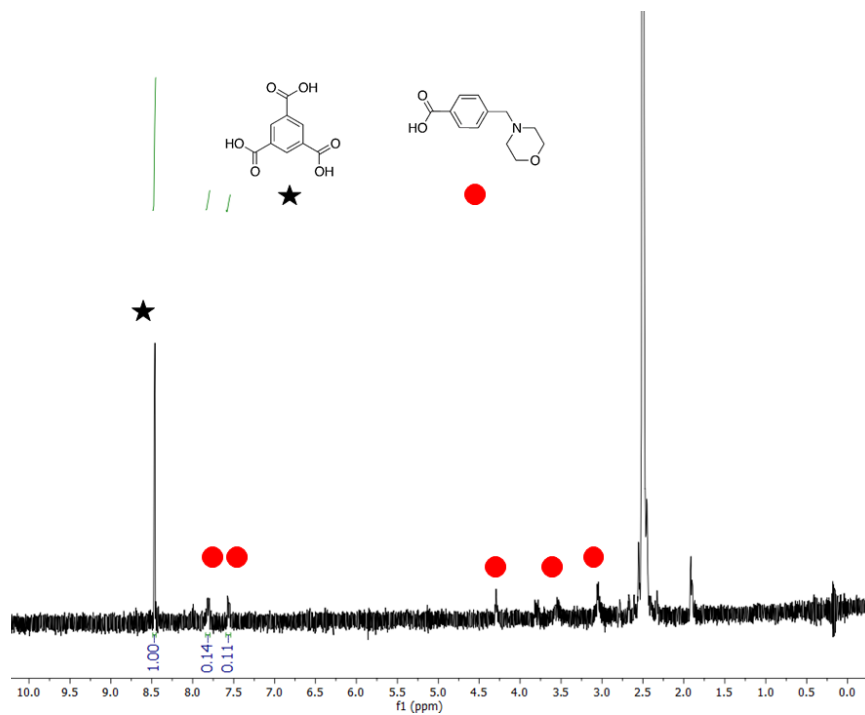


**Figure S30.**  $^1\text{H}$  NMR spectrum of digested Hf-MOF-808-SALI-BA-Morph after 0.013 mM aqueous piperidine treatment in  $d_6$ -DMSO.

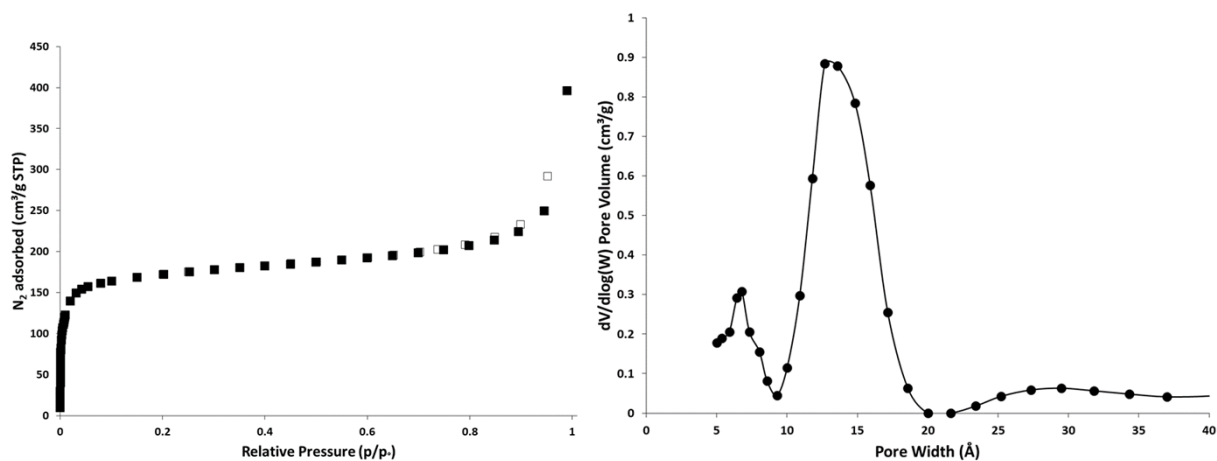


**Figure S31.**  $\text{N}_2$  isotherms (left) and pore size distribution (right) of Hf-MOF-808-SALI-BA-AO. Adsorption = filled, desorption = empty markers.

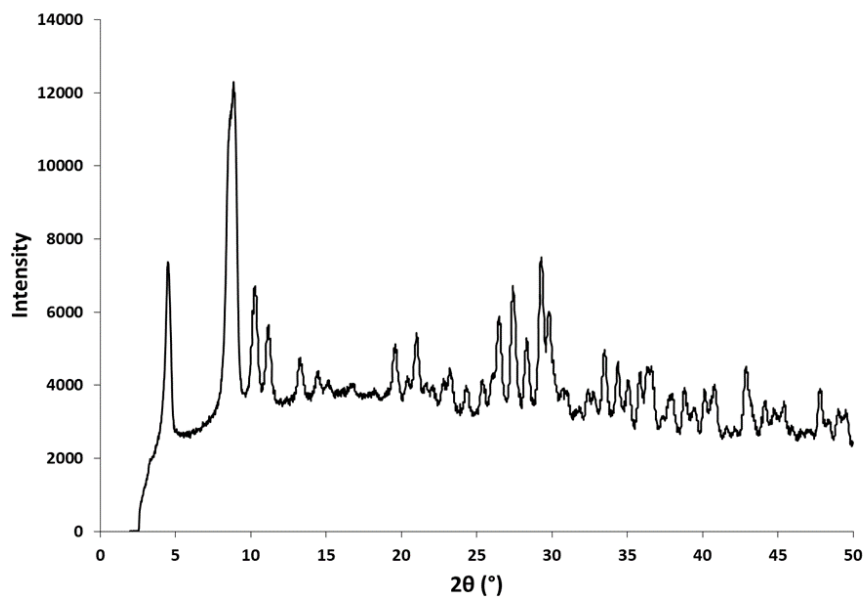


Figure S32. PXRD pattern of Hf-MOF-808-SALI-BA-AO.

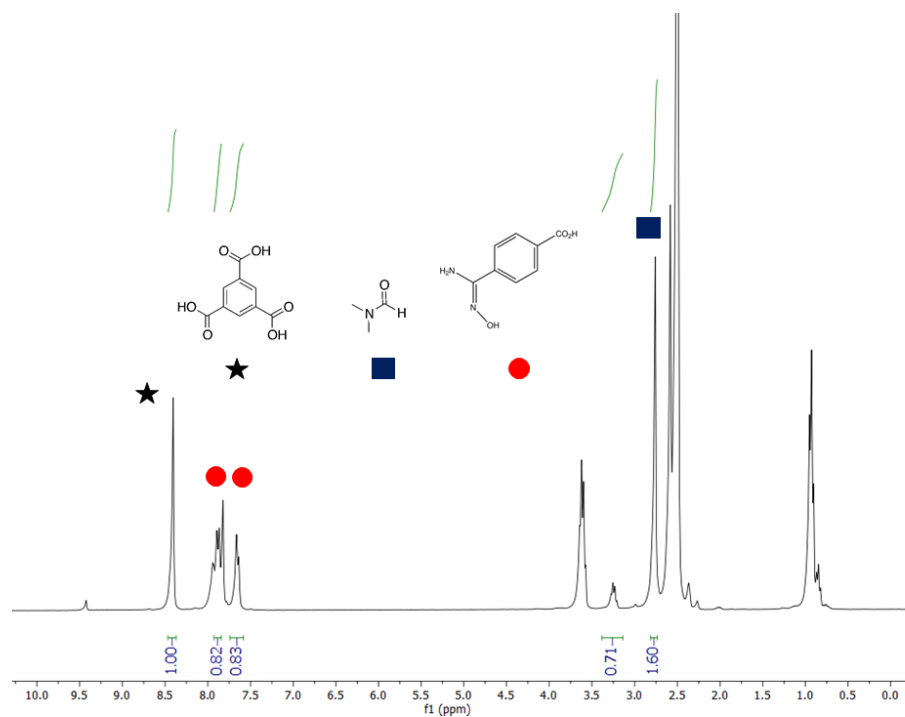
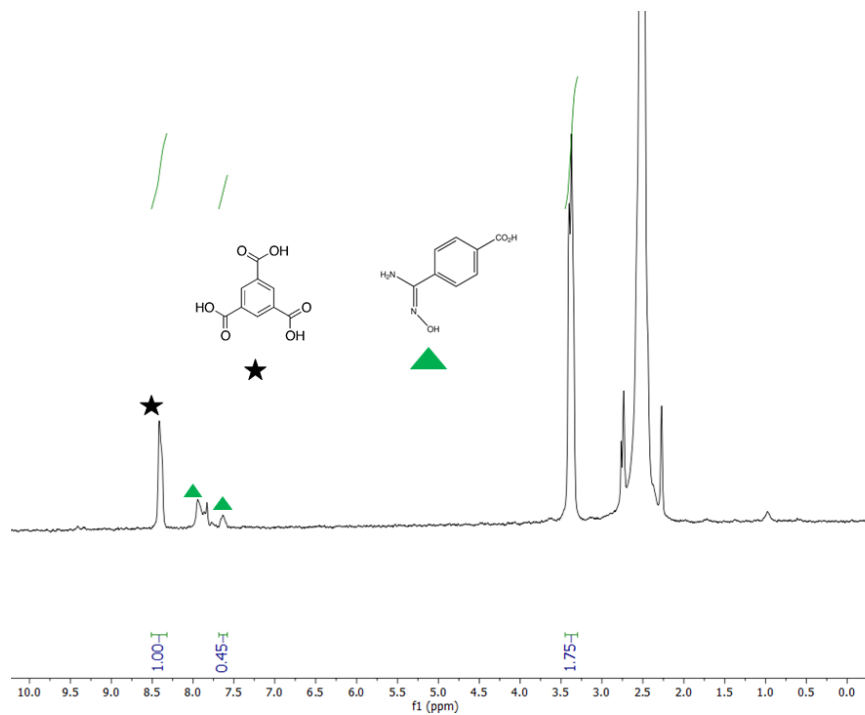
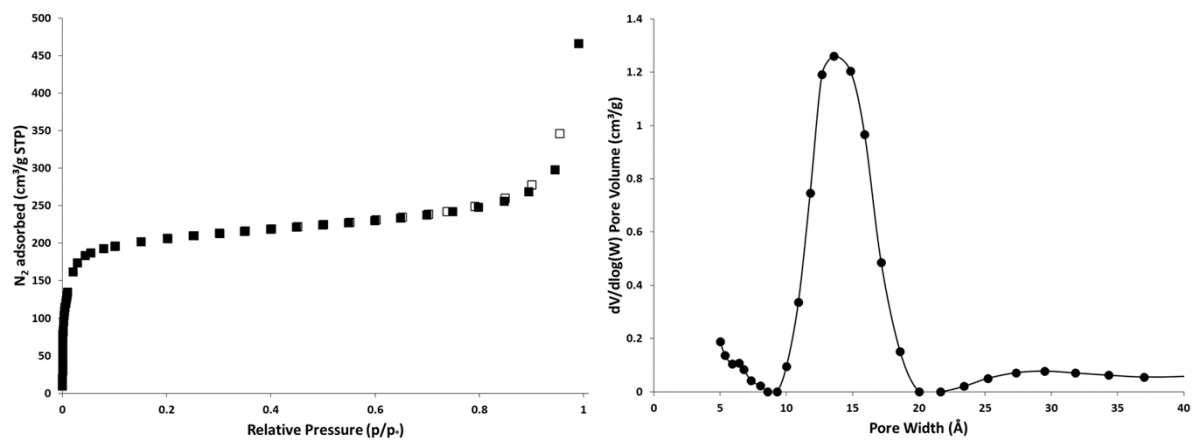


Figure S33.  $^1\text{H}$  NMR spectrum of digested Hf-MOF-808-SALI-BA-AO in  $d_6$ -DMSO.



**Figure S34.** <sup>1</sup>H NMR spectrum of digested Hf-MOF-808-SALI-BA-AO after DMNP hydrolysis in *d*<sub>6</sub>-DMSO.



**Figure S35.** N<sub>2</sub> isotherms (left) and pore size distribution (right) of Hf-MOF-808-SALI-BA-CH<sub>2</sub>NH<sub>2</sub>. Adsorption = filled, desorption = empty markers.

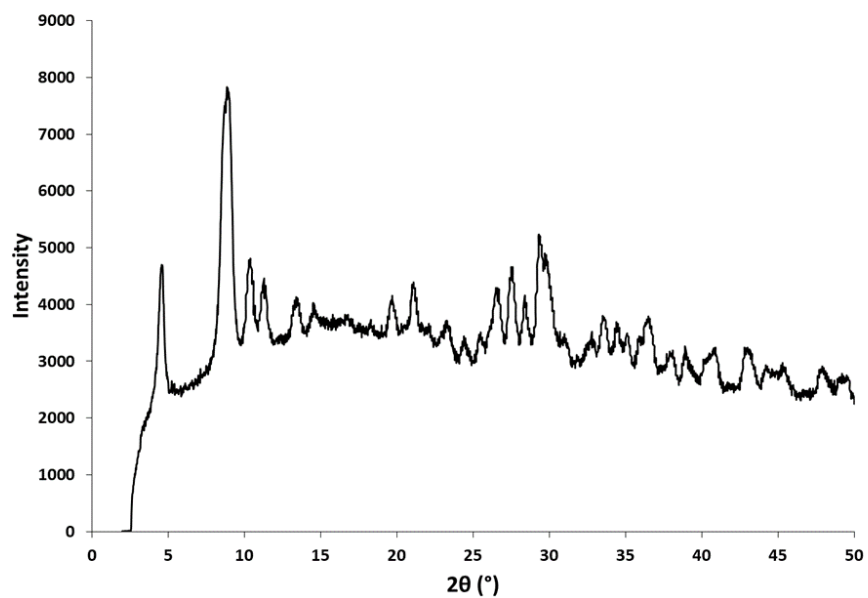


Figure S36. PXRD pattern of Hf-MOF-808-SALI-BA-CH<sub>2</sub>NH<sub>2</sub>.

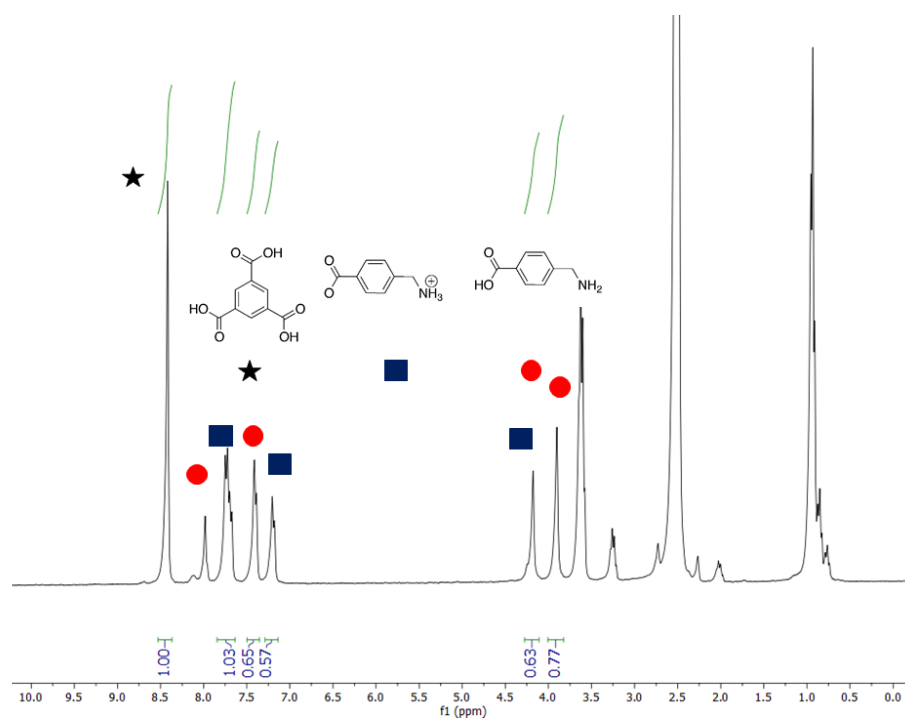
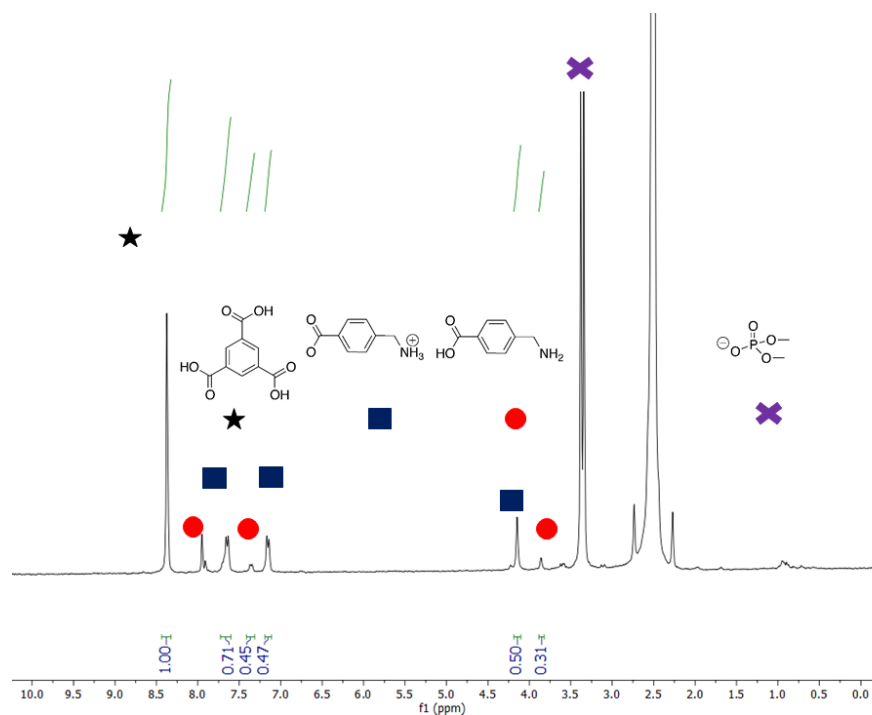
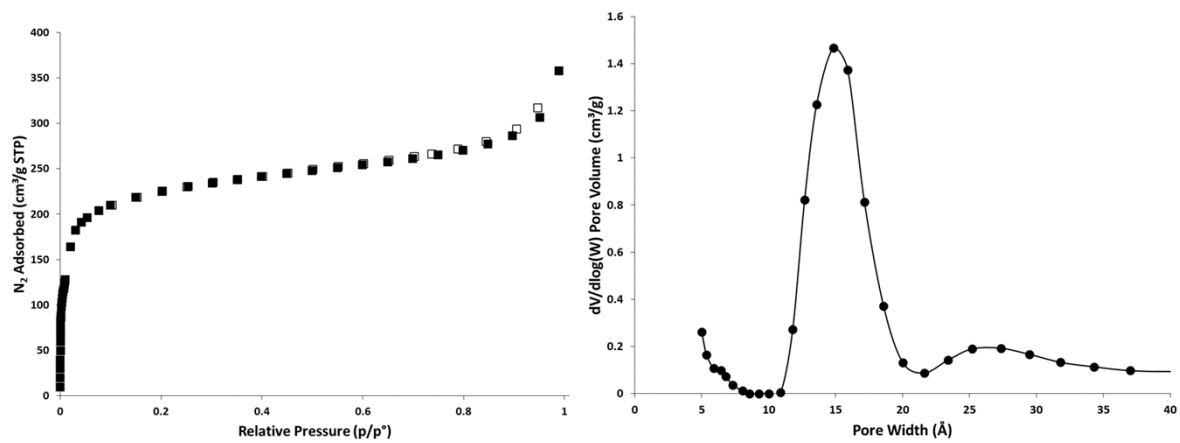


Figure S37. <sup>1</sup>H NMR spectrum of digested Hf-MOF-808-SALI-BA-CH<sub>2</sub>NH<sub>2</sub> in *d*<sub>6</sub>-DMSO.



**Figure S38.**  $^1\text{H}$  NMR spectrum of digested Hf-MOF-808-SALI-BA- $\text{CH}_2\text{NH}_2$  after DMNP hydrolysis in  $d_6$ -DMSO.



**Figure S39.**  $\text{N}_2$  isotherms (left) and pore size distribution (right) of Zr-MOF-808-PA. Adsorption = filled, desorption = empty markers.



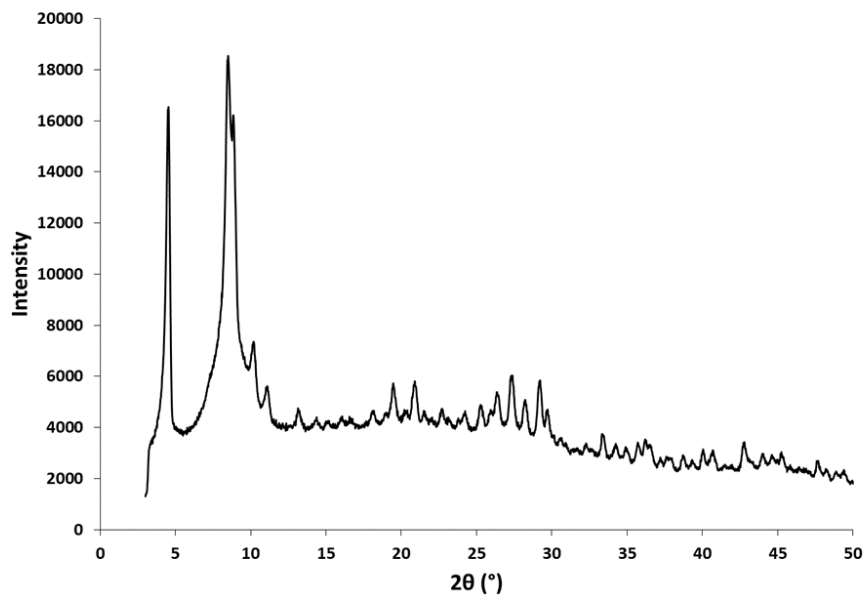


Figure S40. PXRD pattern of Zr-MOF-808-PA.

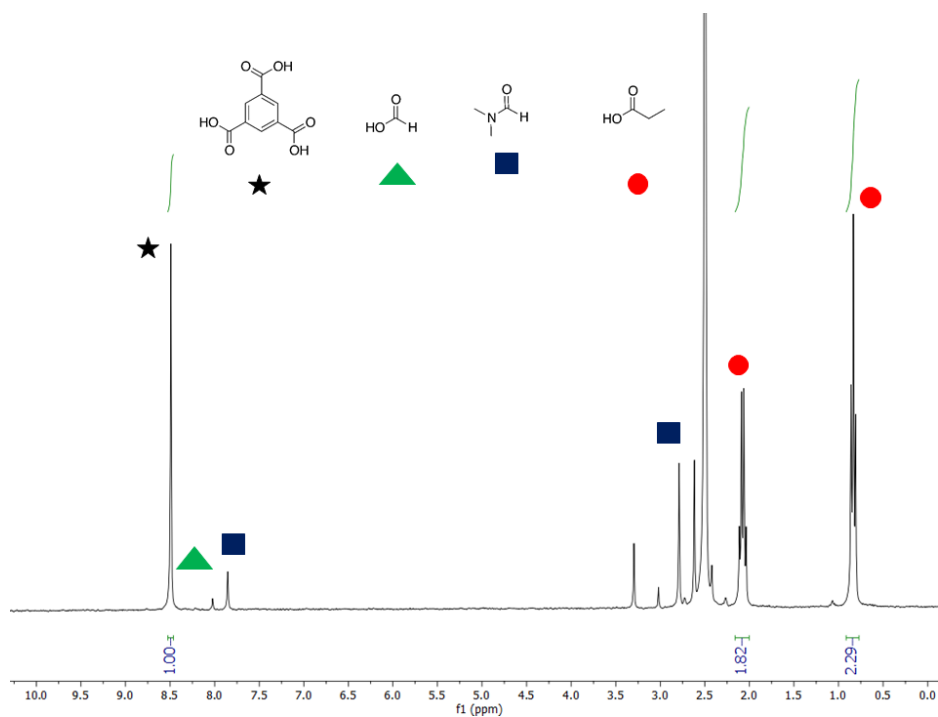
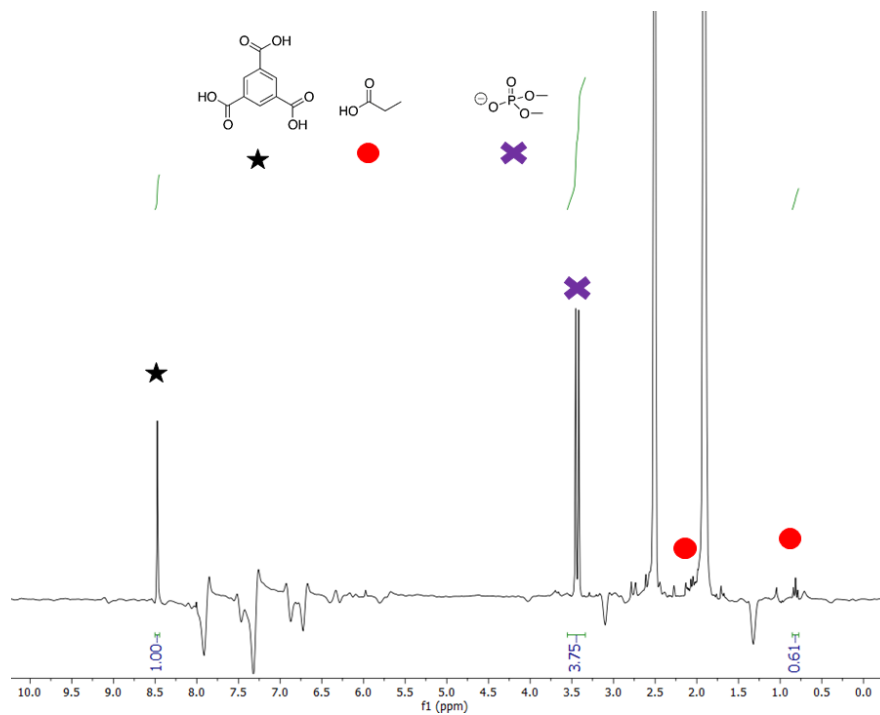
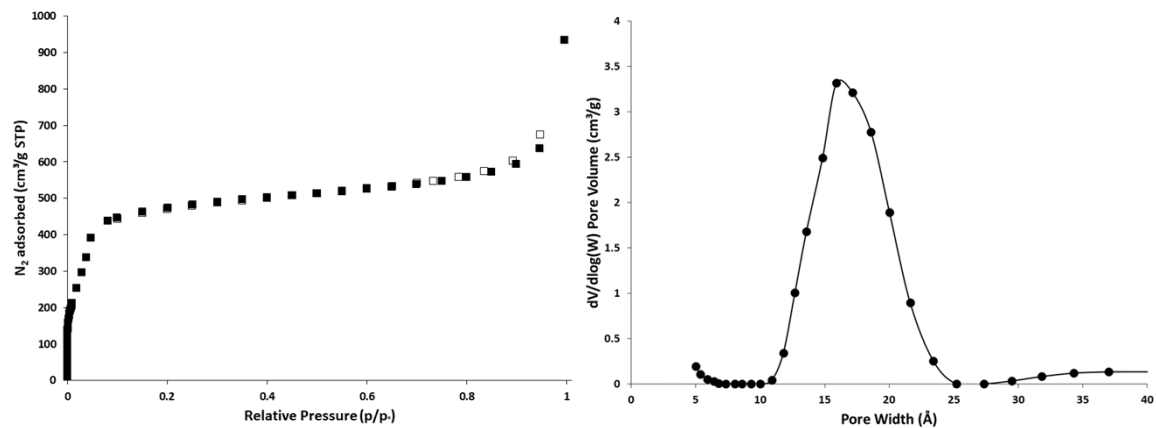


Figure S41.  $^1\text{H}$  NMR spectrum of digested Zr-MOF-808-PA in  $d_6$ -DMSO.



**Figure S42.**  $^1\text{H}$  NMR spectrum of digested Zr-MOF-808-PA after DMNP hydrolysis in  $d_6$ -DMSO.



**Figure S43.**  $\text{N}_2$  isotherms (left) and pore size distribution (right) of Zr-MOF-808-HCl-DMF. Adsorption = filled, desorption = empty markers.

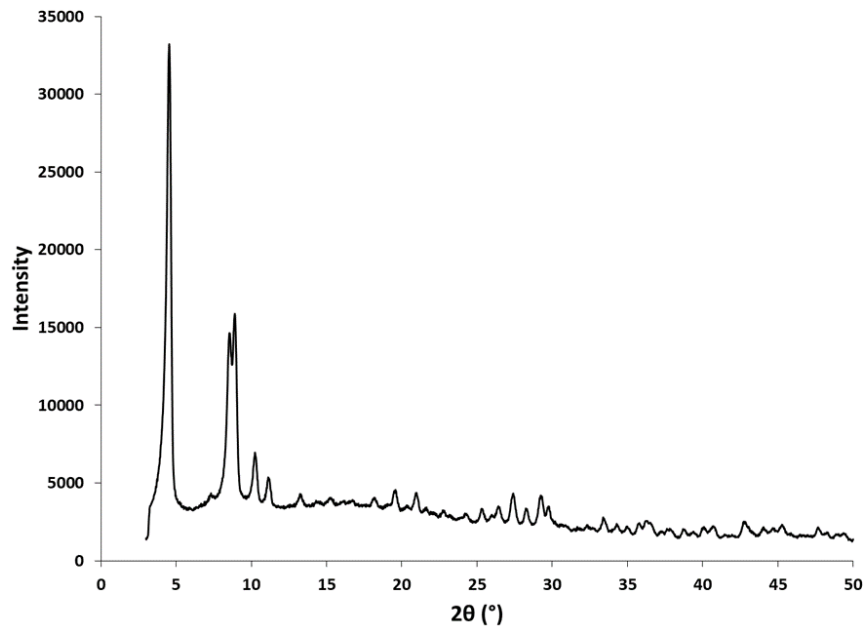


Figure S44. PXRD pattern of Zr-MOF-808-HCl-DMF.

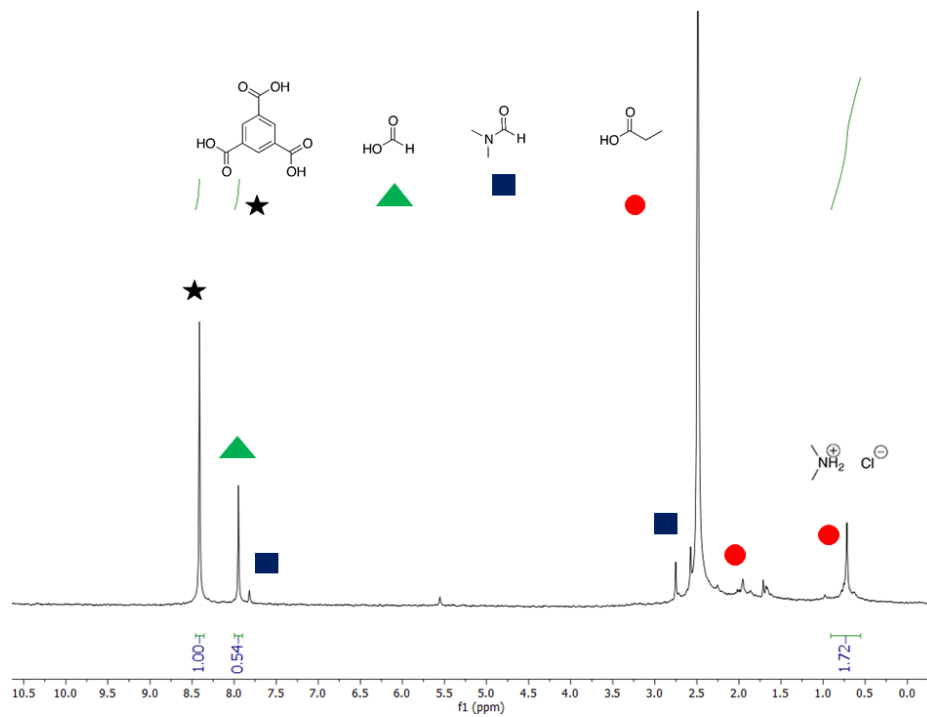
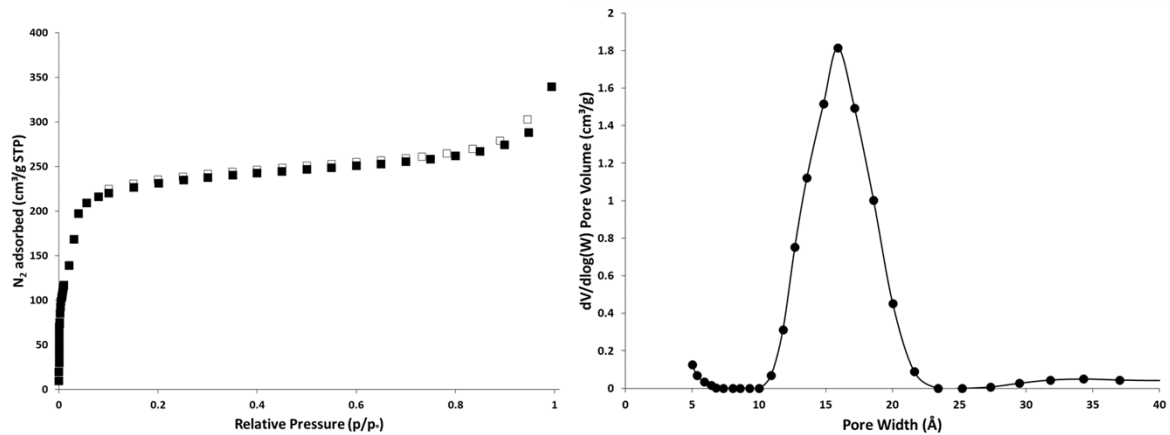
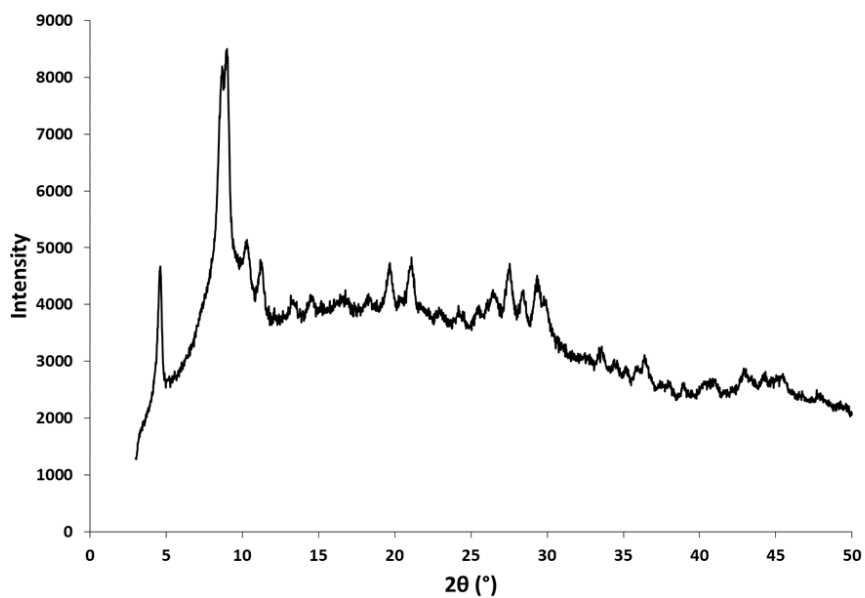


Figure S45.  $^1\text{H}$  NMR spectrum of digested Zr-MOF-808-HCl-DMF in  $d_6$ -DMSO.



**Figure S46.** N<sub>2</sub> isotherms (left) and pore size distribution (right) of Zr-MOF-808-HCl-acetone. Adsorption = filled, desorption = empty markers.



**Figure S47.** PXRD pattern of Zr-MOF-808-HCl-acetone.

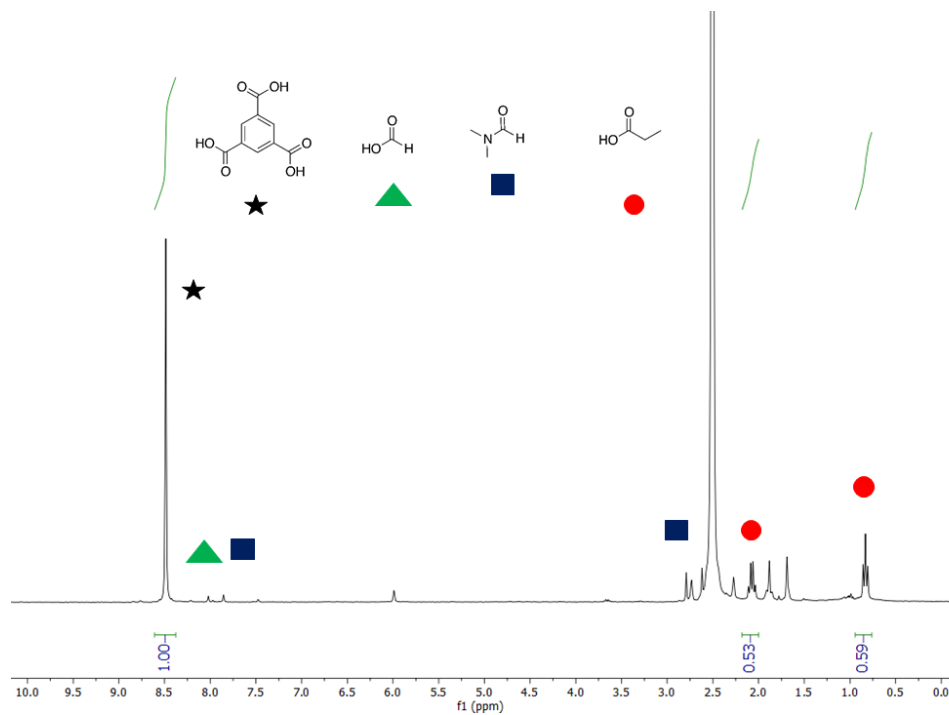


**Figure S48.** <sup>1</sup>H NMR spectrum of digested Zr-MOF-808-HCl-acetone in *d*<sub>6</sub>-DMSO.

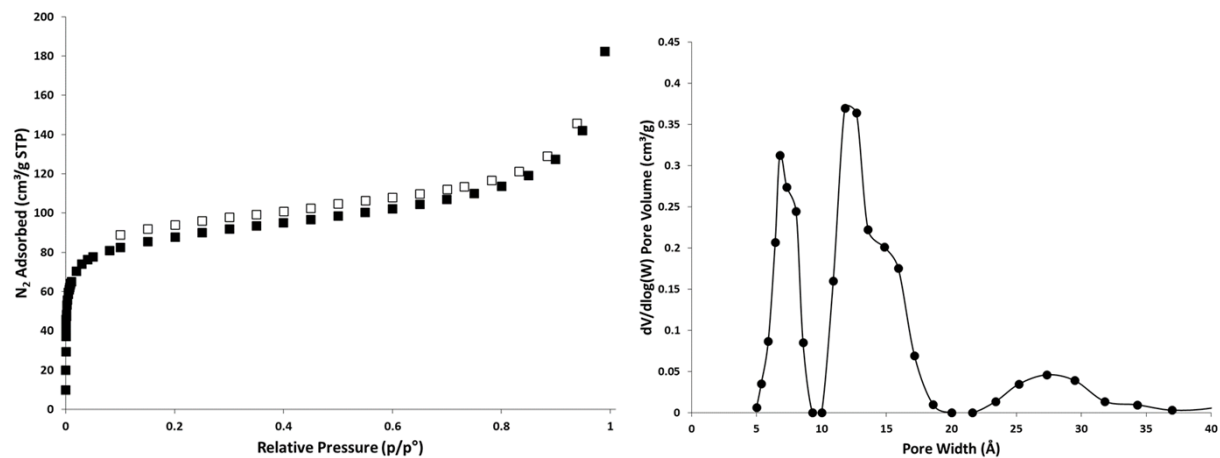


**Figure S49.** N<sub>2</sub> isotherms (left) and pore size distribution (right) of Zr-MOF-808-SALI-BA-Morph. Adsorption = filled, desorption = empty markers.

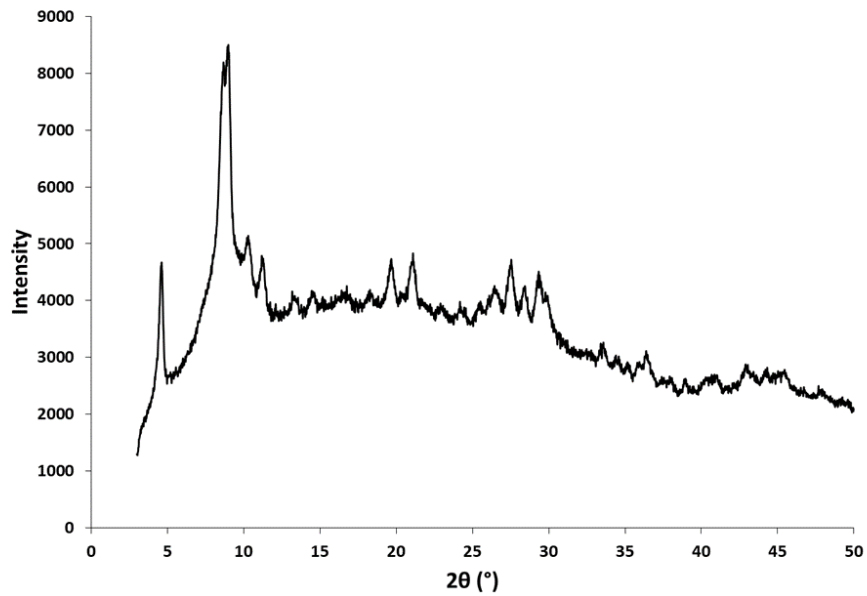


Figure S50. PXRD pattern of Zr-MOF-808-SALI-BA-Morph.

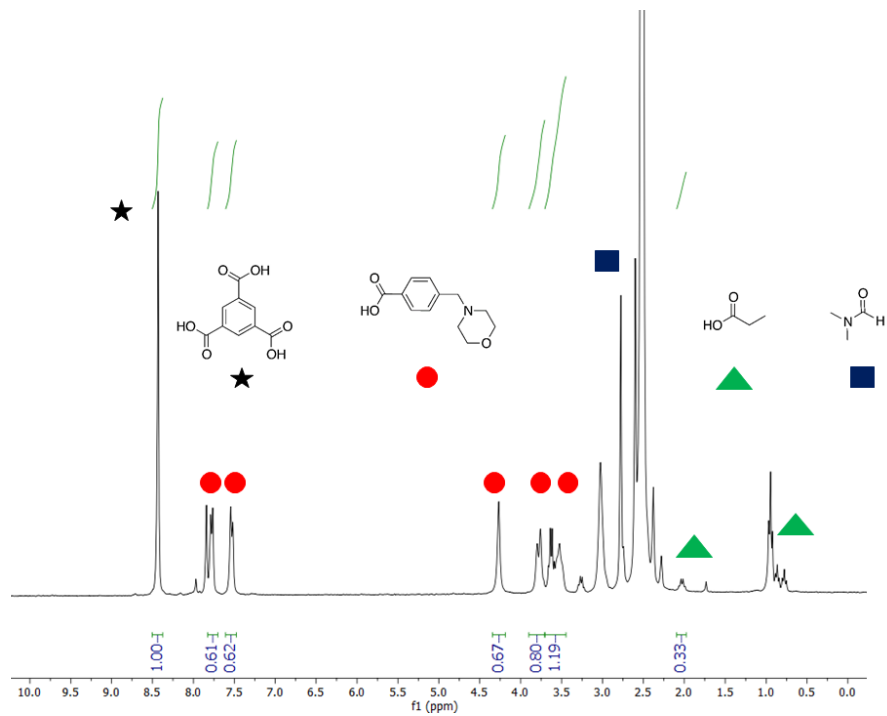
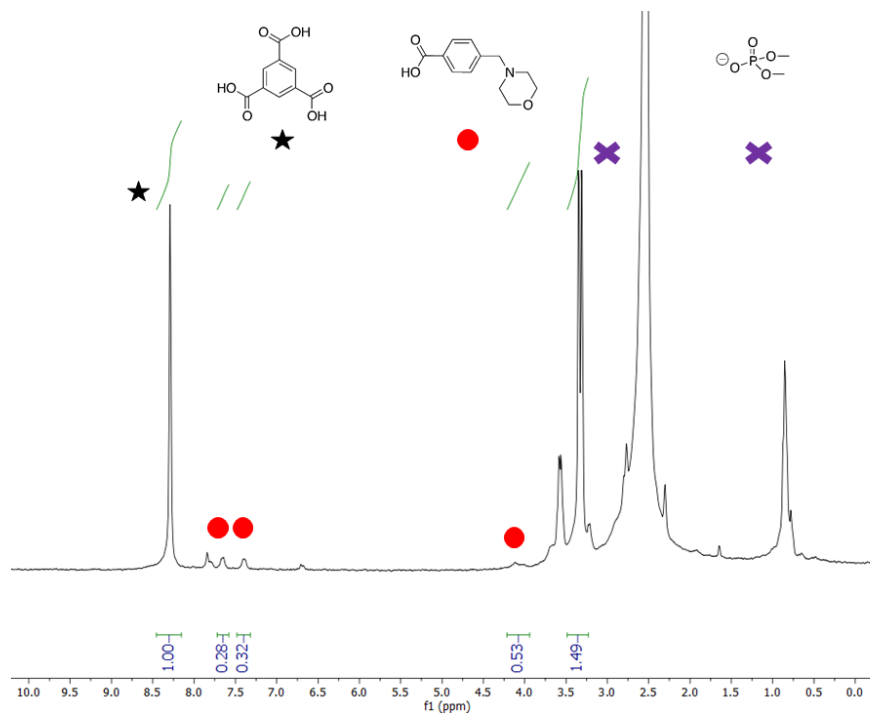
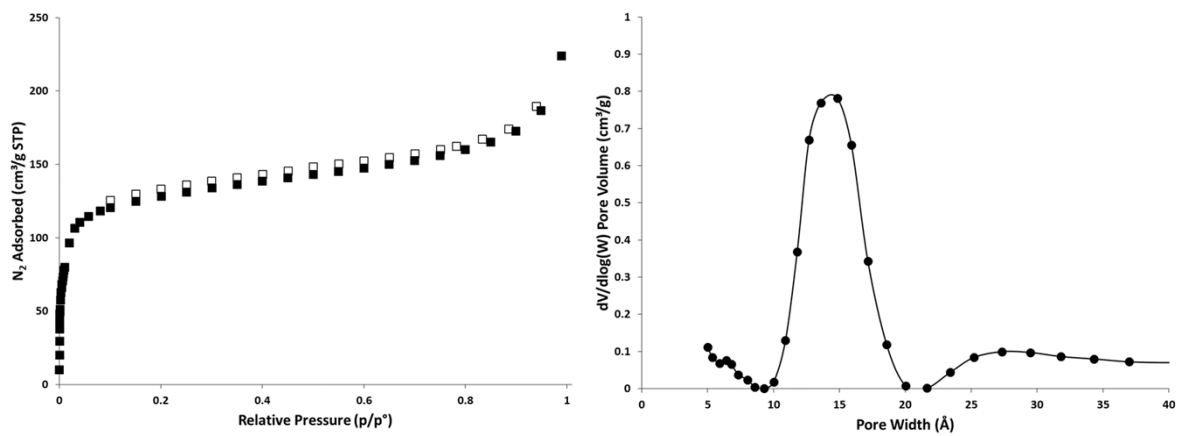


Figure S51. <sup>1</sup>H NMR spectrum of digested Zr-MOF-808-SALI-BA-Morph in *d*<sub>6</sub>-DMSO.



**Figure S52.**  $^1\text{H}$  NMR spectrum of digested Zr-MOF-808-SALI-BA-Morph after DMNP hydrolysis in  $d_6$ -DMSO.



**Figure S53.**  $\text{N}_2$  isotherms (left) and pore size distribution (right) of Zr-MOF-808-SALI-BA-AO. Adsorption = filled, desorption = empty markers.

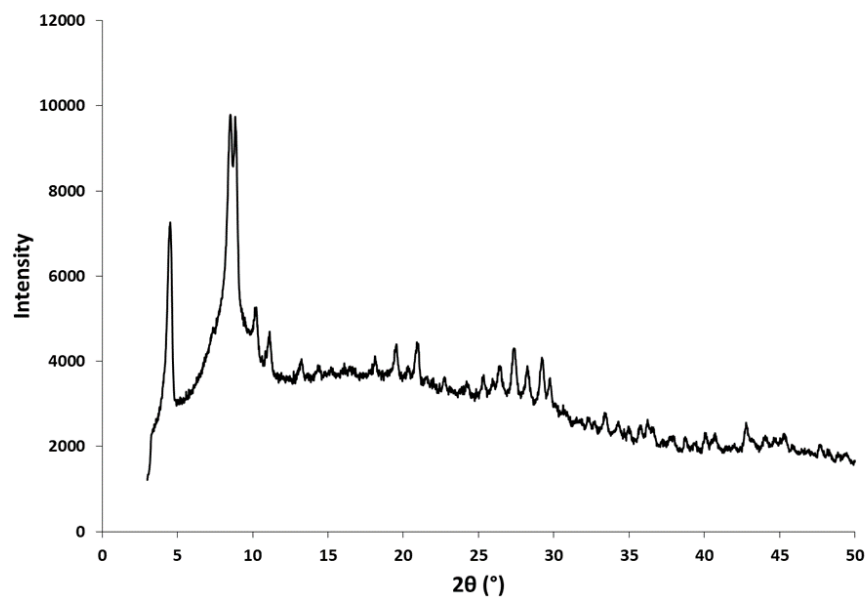


Figure S54. PXRD pattern of Zr-MOF-808-SALI-BA-AO.

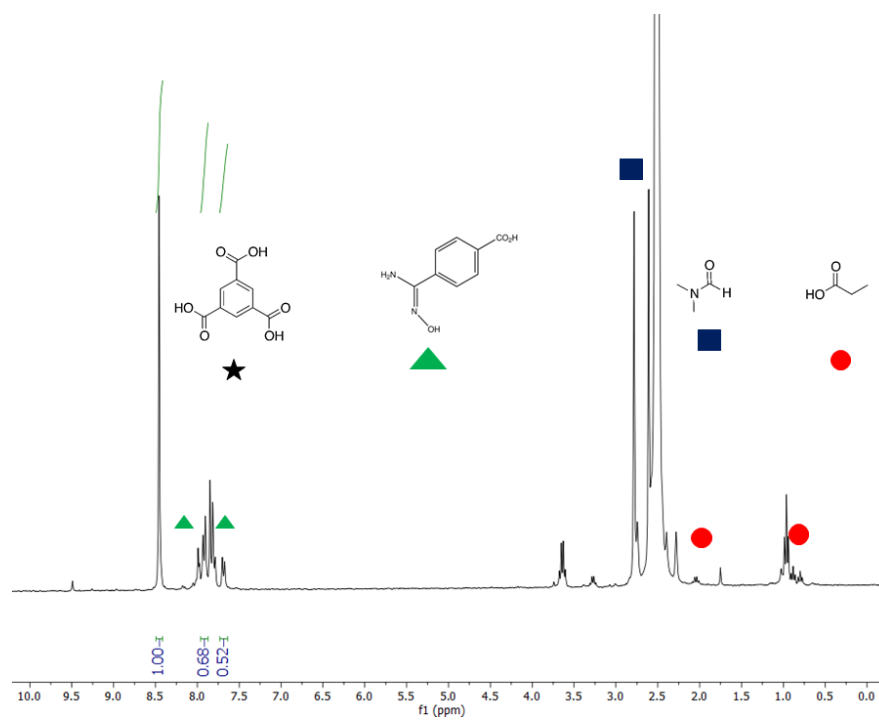
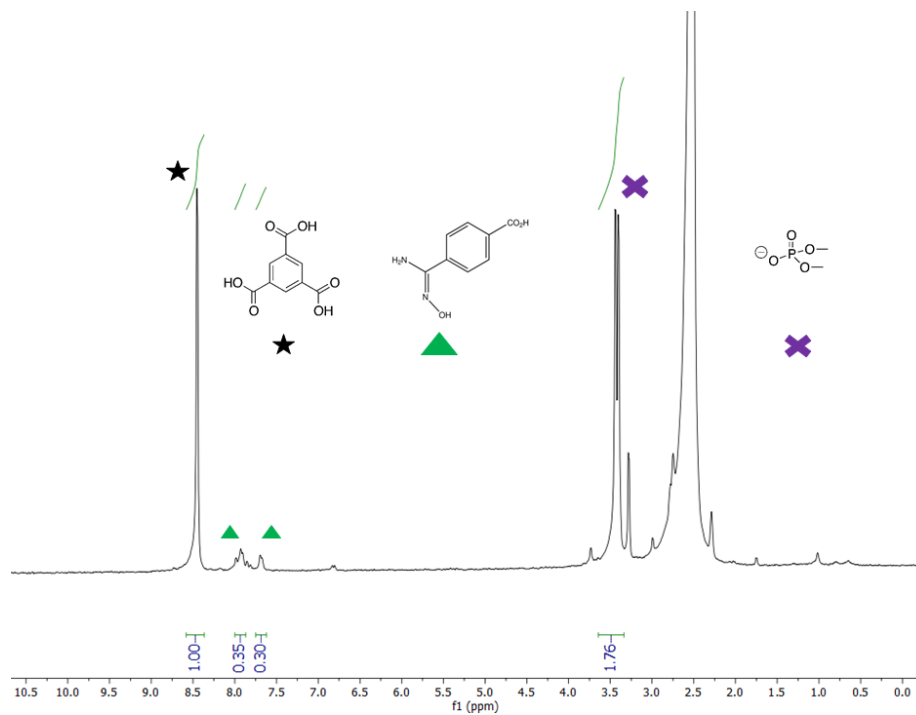
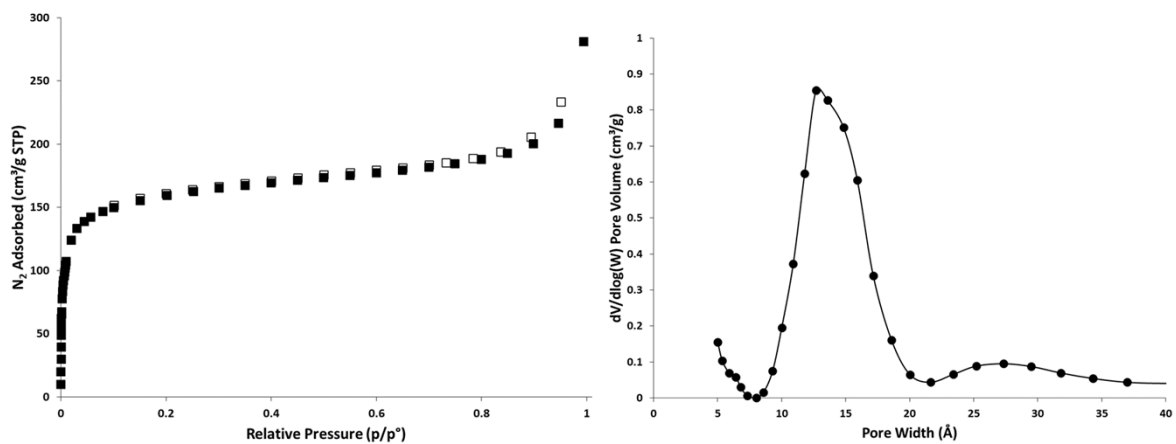


Figure S55.  $^1\text{H}$  NMR spectrum of digested Zr-MOF-808-SALI-BA-AO in  $d_6$ -DMSO.





**Figure S56.**  $^1\text{H}$  NMR spectrum of digested Zr-MOF-808-SALI-BA-AO after DMNP hydrolysis in  $d_6$ -DMSO.



**Figure S57.**  $\text{N}_2$  isotherms (left) and pore size distribution (right) of Zr-MOF-808-SALI-BA- $\text{CH}_2\text{NH}_2$ . Adsorption = filled, desorption = empty markers.

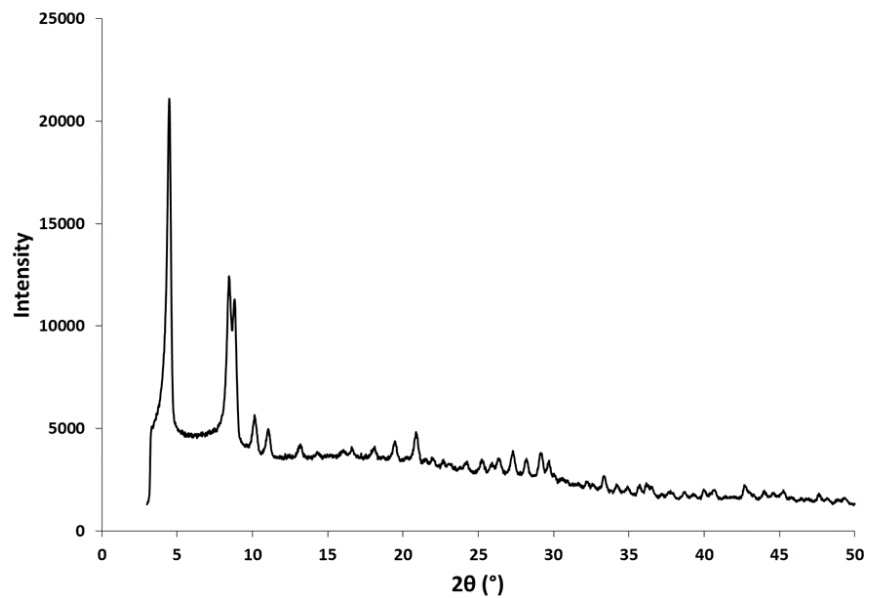


Figure S58. PXRD pattern of Zr-MOF-808-SALI-BA-CH<sub>2</sub>NH<sub>2</sub>.

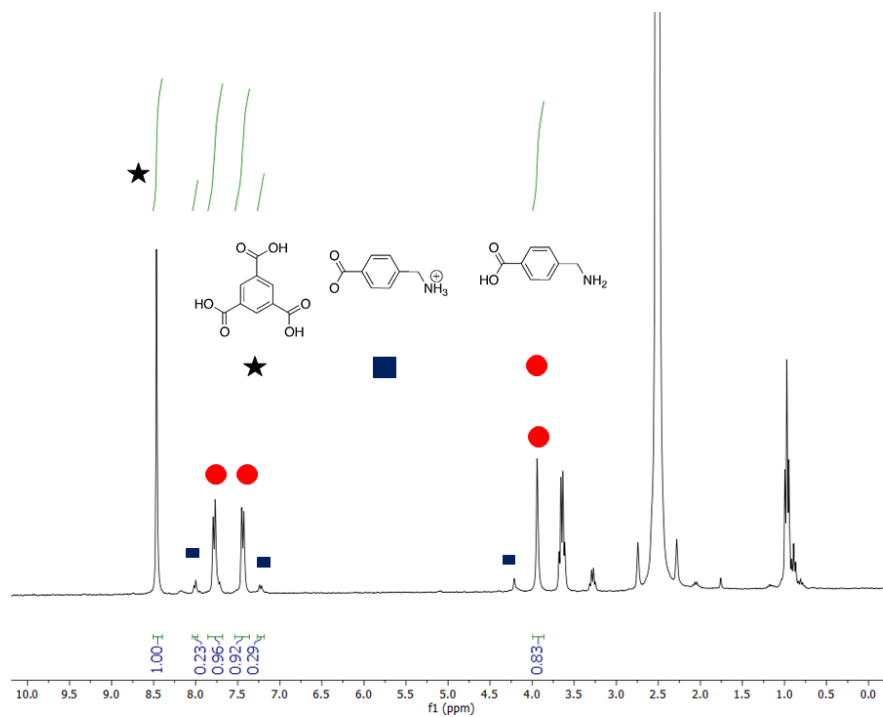
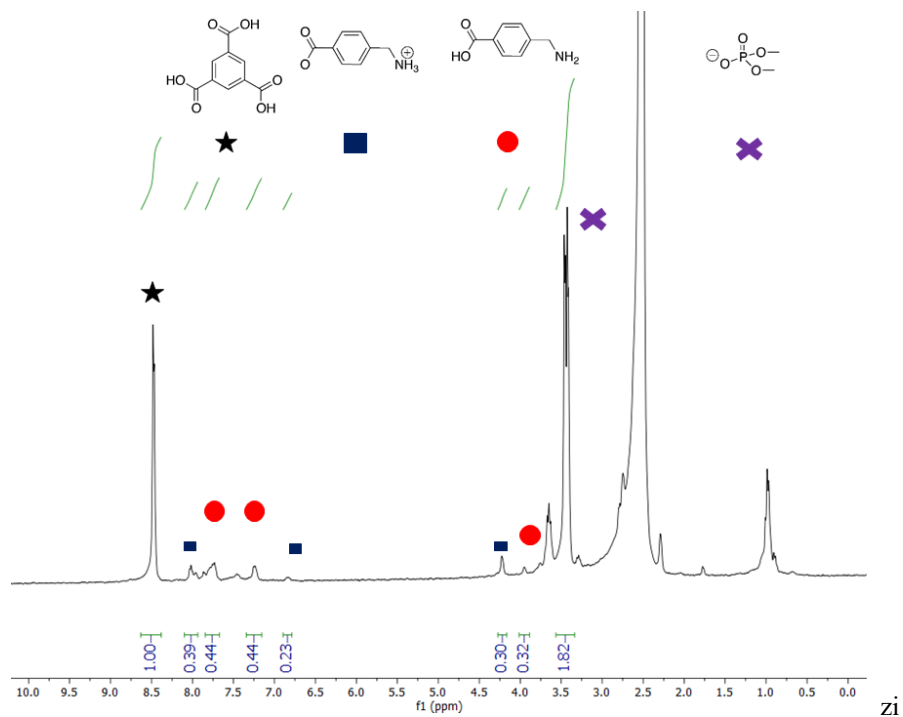
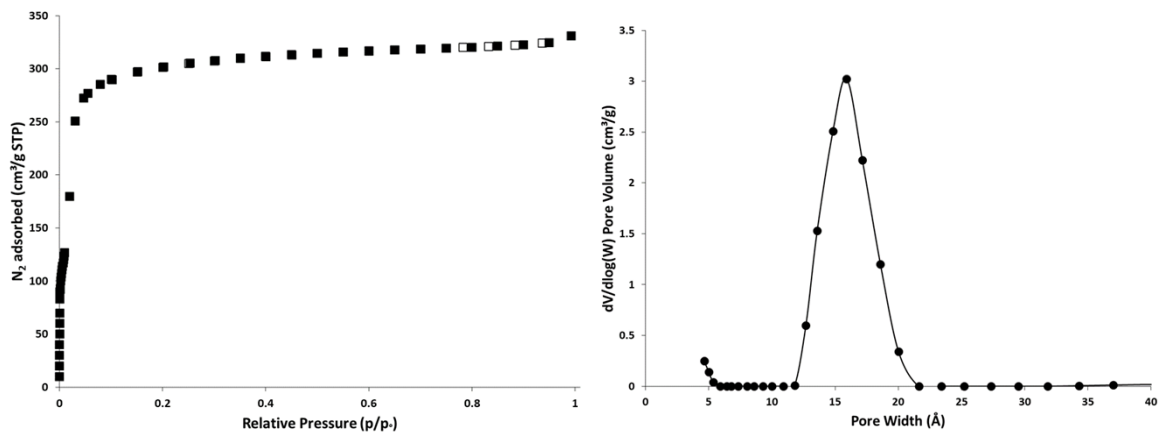


Figure S59. <sup>1</sup>H NMR spectrum of digested Zr-MOF-808-SALI-BA-CH<sub>2</sub>NH<sub>2</sub> in *d*<sub>6</sub>-DMSO.



**Figure S60.**  $^1\text{H}$  NMR spectrum of digested Zr-MOF-808-SALI-BA- $\text{CH}_2\text{NH}_2$  after DMNP hydrolysis in  $d_6$ -DMSO.



**Figure S61.**  $\text{N}_2$  isotherms (left) and pore size distribution (right) of Zr-MOF-808-NH-TFA. Adsorption = filled, desorption = empty markers.

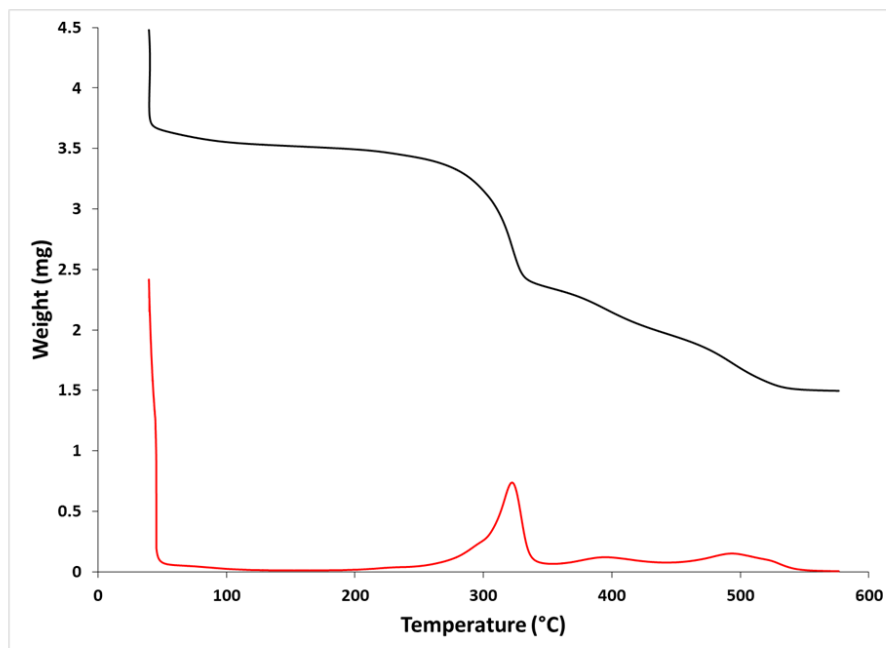
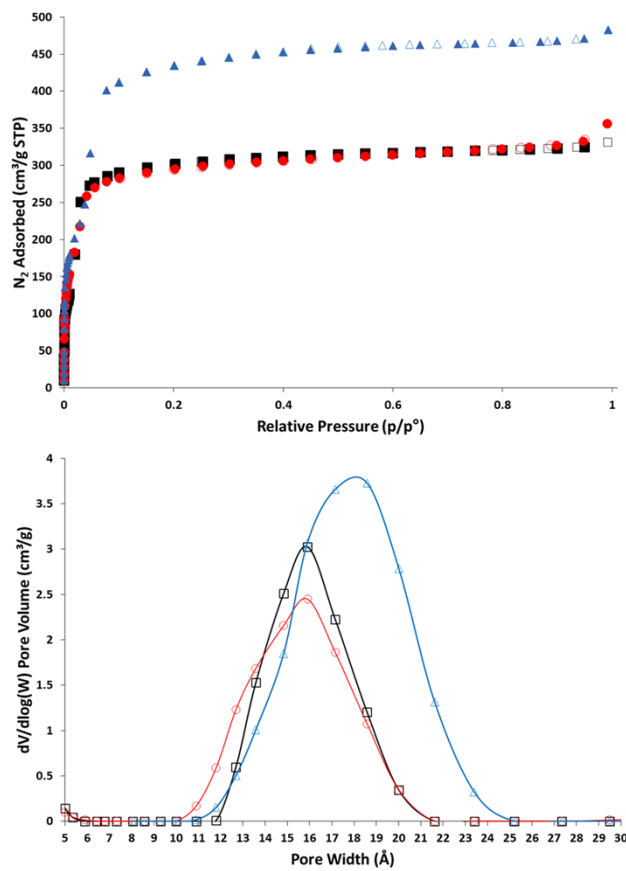
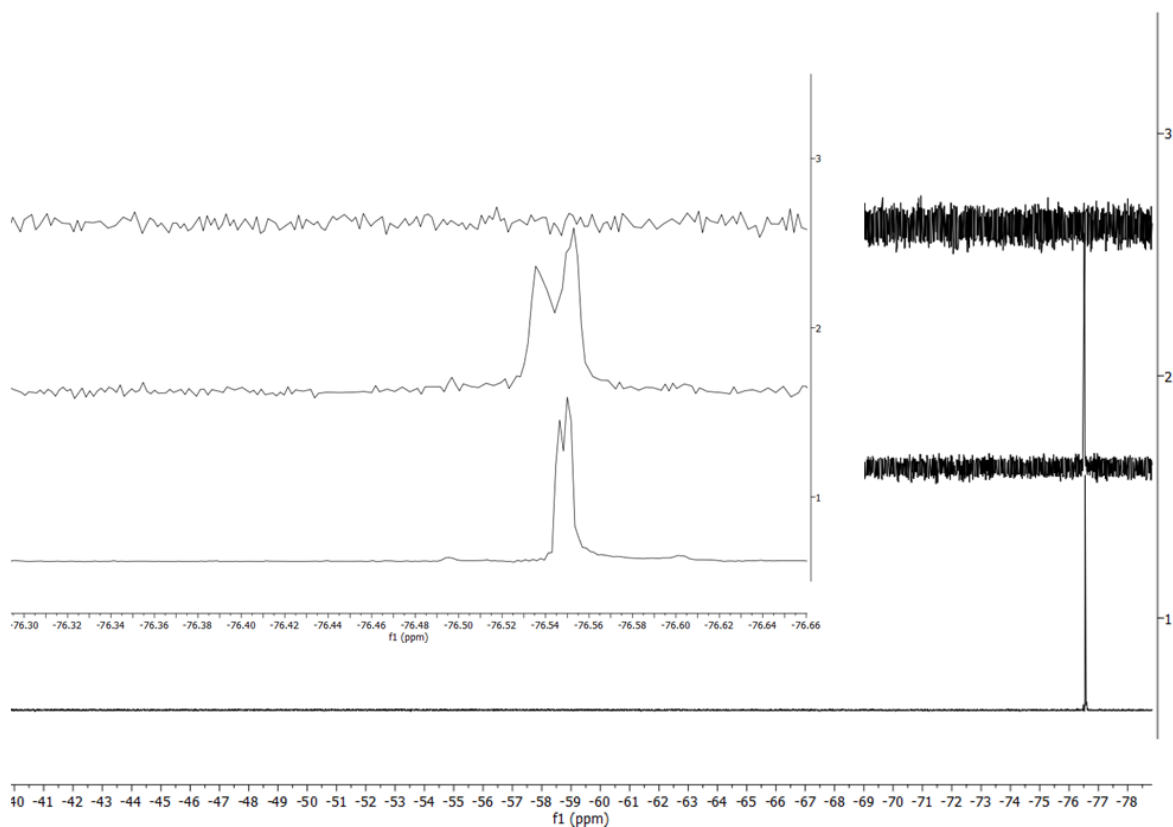


Figure S62. TGA curve (black) and derivative weight in %/°C (red) of Zr-MOF-808-NH-TFA.



**Figure S63.** N<sub>2</sub> isotherms (left) and pore size distribution (right) of Zr-MOF-808-NH-TFA (black squares) activated with acetone-HCl (red circles), aqueous K<sub>2</sub>CO<sub>3</sub> (blue triangles). Adsorption = filled, desorption = empty markers.



**Figure S64.** <sup>19</sup>F NMR spectrum of digested as synthesized Zr-MOF-808-NH-TFA (1), after acetone-HCl activation (2), and after aqueous K<sub>2</sub>CO<sub>3</sub> activation (3) in *d*<sub>6</sub>-DMSO. Inset graph is the zoom in region of the <sup>19</sup>F NMR spectra.

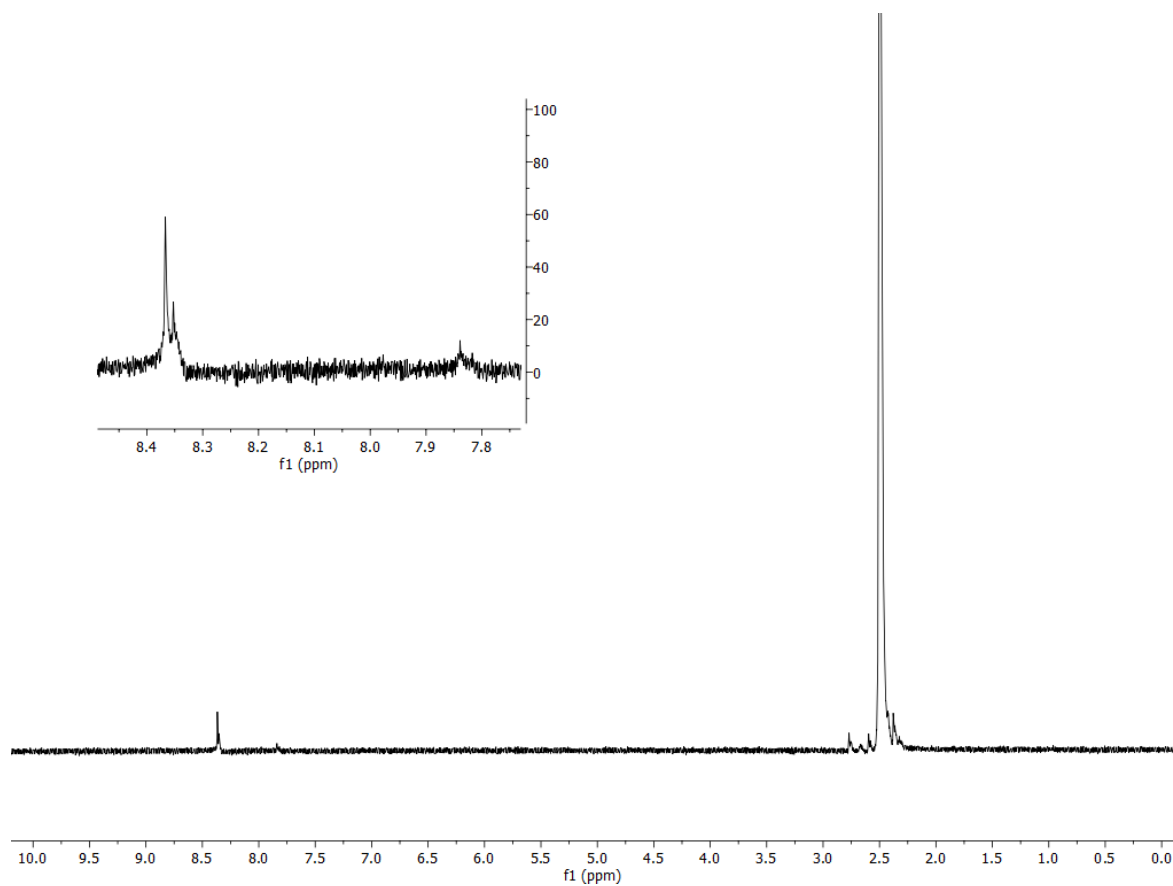


Figure S65.  $^1\text{H}$  NMR spectrum of digested Zr-MOF-808-NH-TFA in  $d_6$ -DMSO.

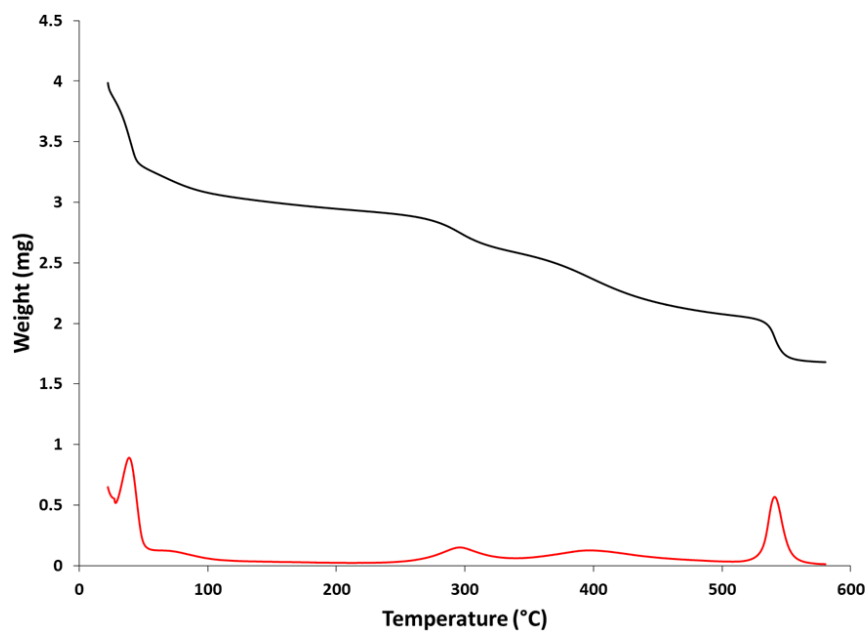
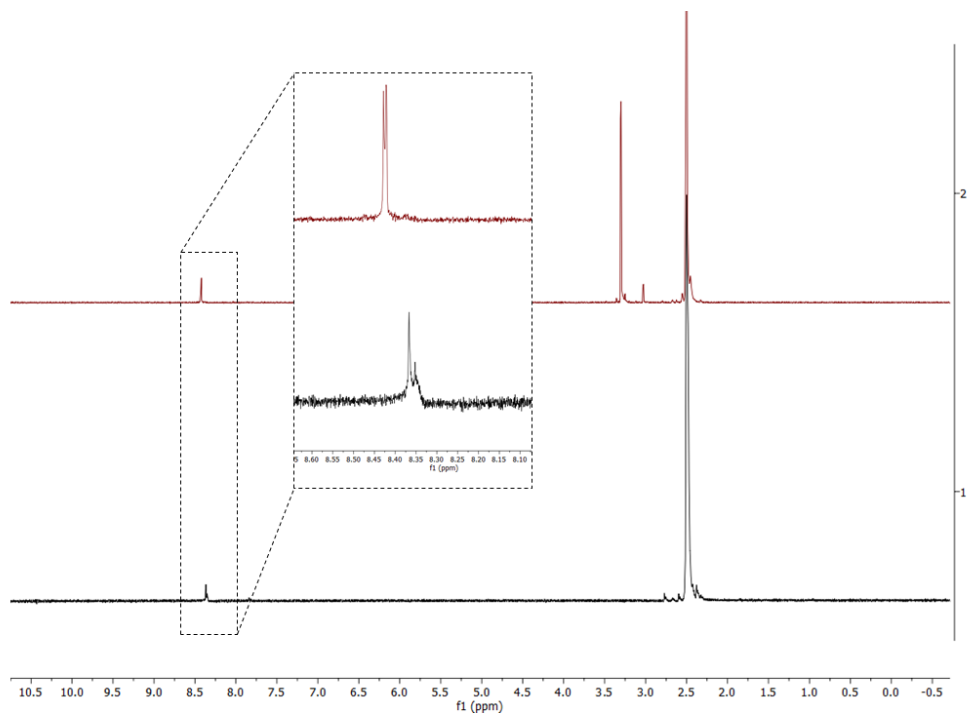
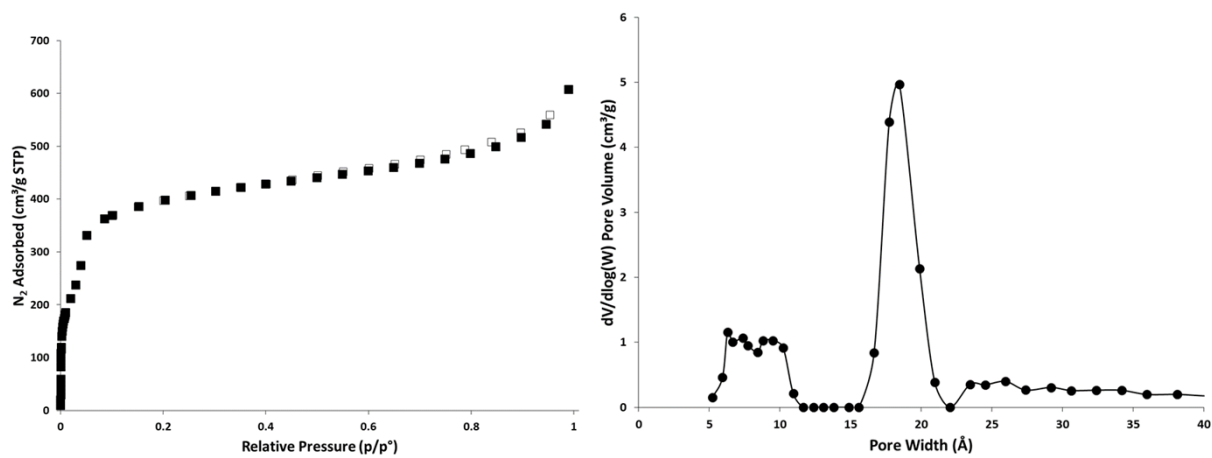


Figure S66. TGA curve (black) and derivative weight in  $\%/\text{°C}$  (red) of Zr-MOF-808-NH-TFA after aqueous  $\text{K}_2\text{CO}_3$  activation at  $90\text{ °C}$  for 2 hours.



**Figure S67.**  $^1\text{H}$  NMR spectrum of digested Zr-MOF-808-NH-TFA (bottom), and after  $\text{K}_2\text{CO}_3$  activation (top) in  $d_6$ -DMSO.



**Figure S68.**  $\text{N}_2$  isotherms (left) and pore size distribution (right) of Zr-MOF-808-NH-Morph. Adsorption = filled, desorption = empty markers.

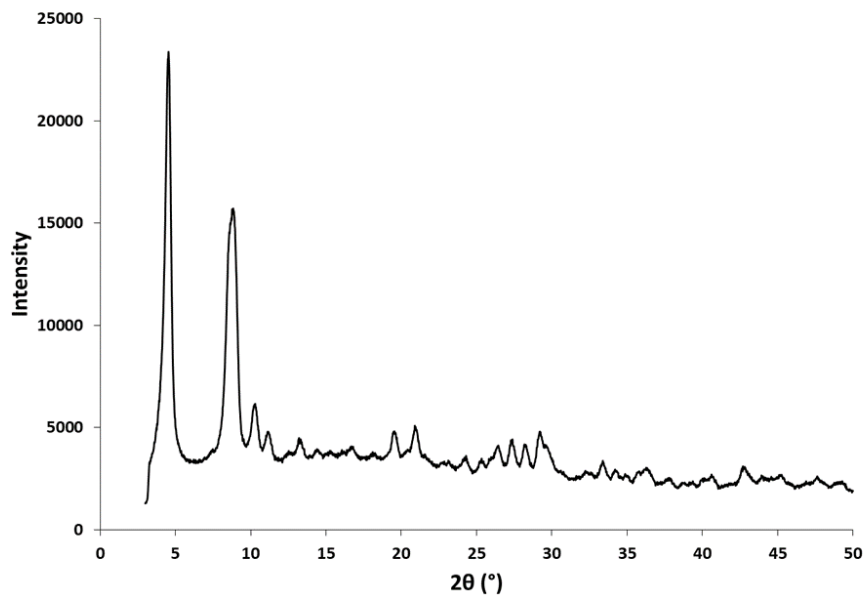


Figure S69. PXRD pattern of Zr-MOF-808-NH-Morph.

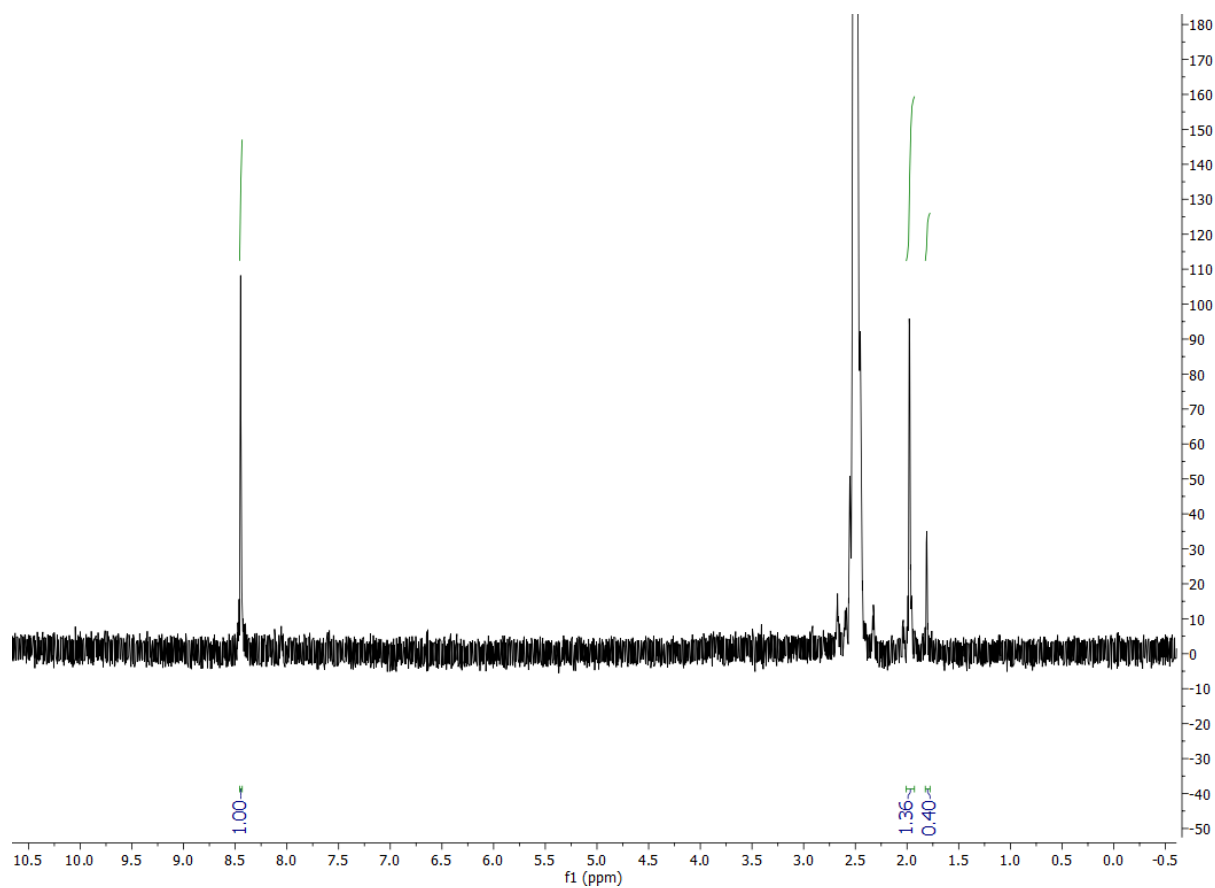
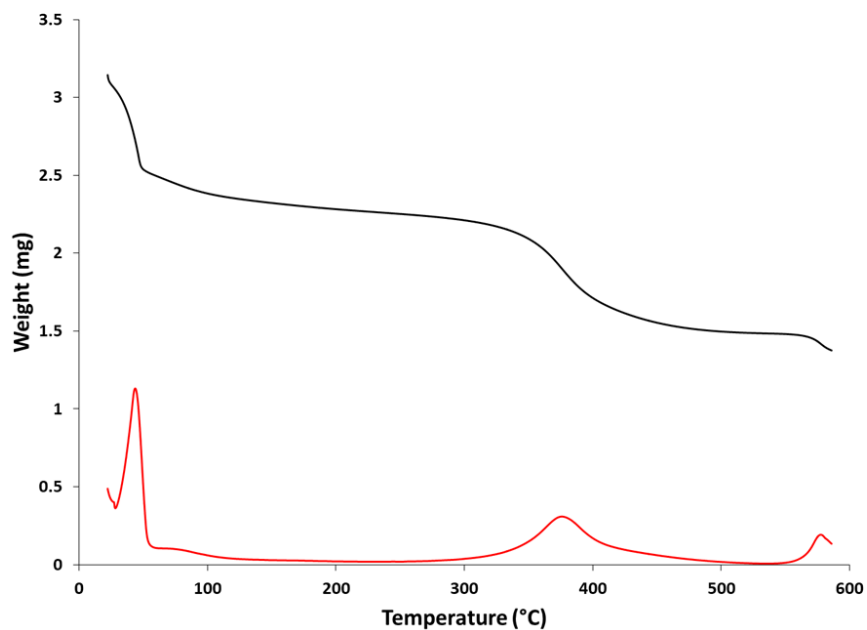
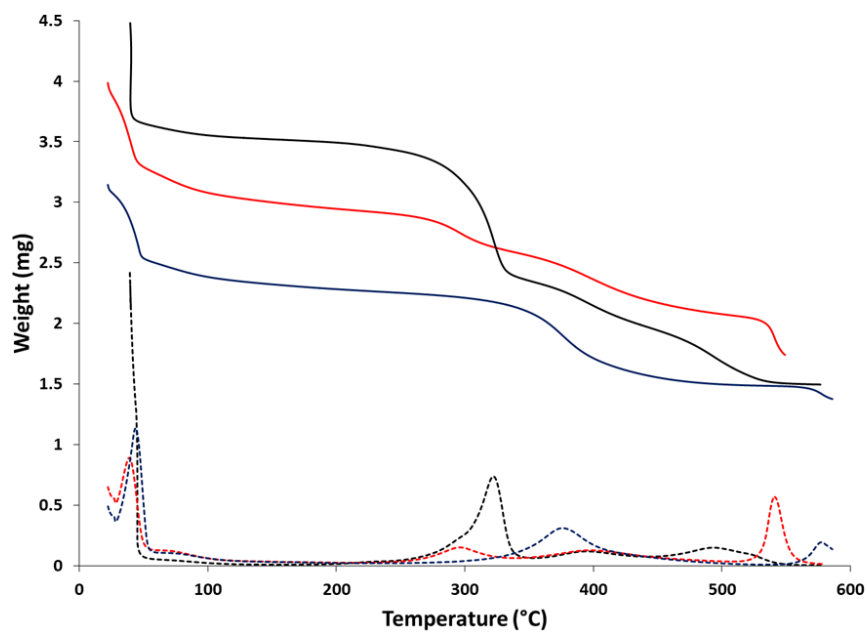


Figure S70. <sup>1</sup>H NMR spectrum of digested Zr-MOF-808-NH-Morph in *d*<sub>6</sub>-DMSO.





**Figure S71.** TGA curve (black) and derivative weight in %/°C (red) of Zr-MOF-808-NH-Morph.



**Figure S72.** Comparison of the TGA curves and derivatives weight in %/°C (dashed lines) of as synthesized Zr-MOF-808-NH-TFA (black), Zr-MOF-808-NH-TFA after K<sub>2</sub>CO<sub>3</sub> activation (red), and Zr-MOF-808-NH-Morph (blue).

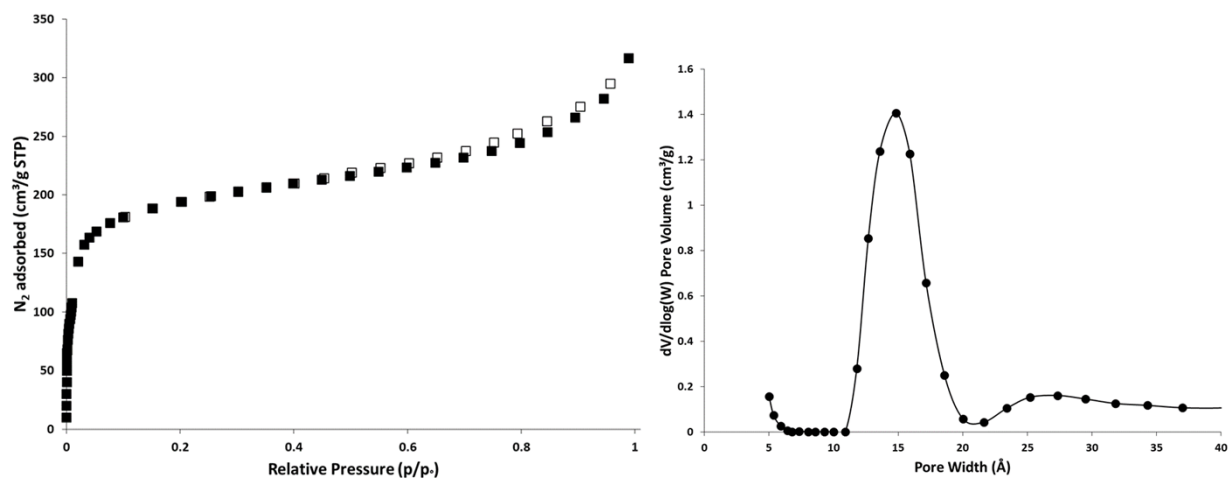


**Figure S73.** N<sub>2</sub> isotherms (left) and pore size distribution (right) of Hf-MOF-808-NH-TFA. Adsorption = filled, desorption = empty markers.

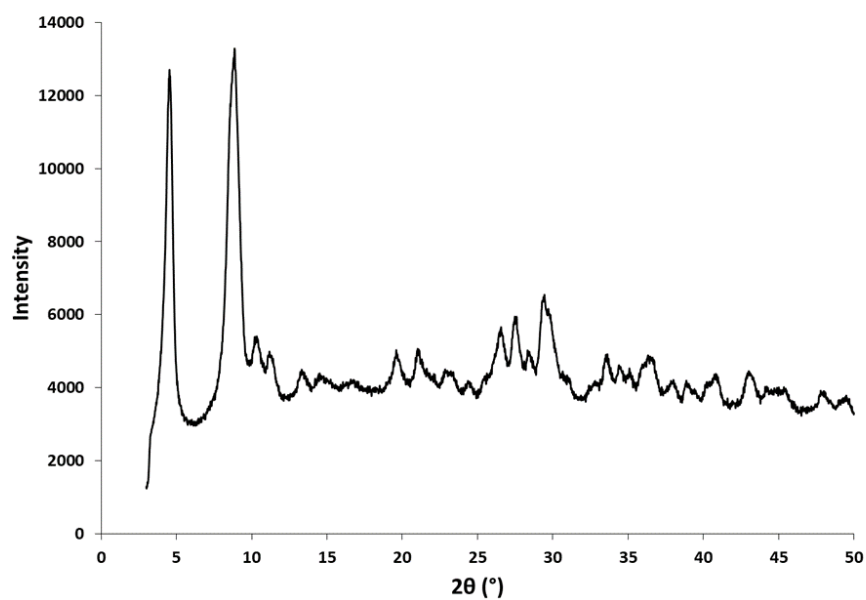


**Figure S74.** PXRD pattern of Hf-MOF-808-NH-TFA.

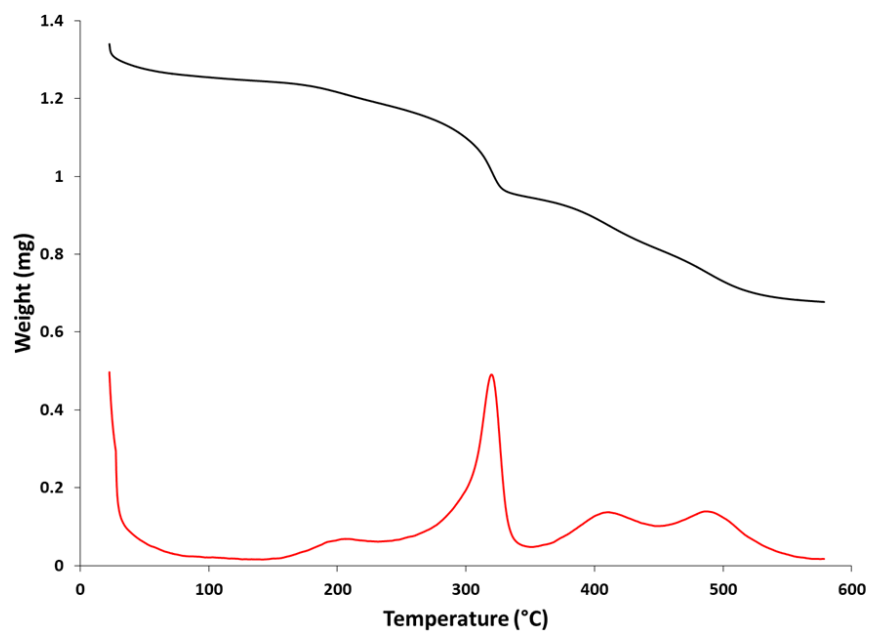


**Figure S75.** TGA curve (black) and derivative weight in %/°C (red) of Hf-MOF-808-NH-TFA.

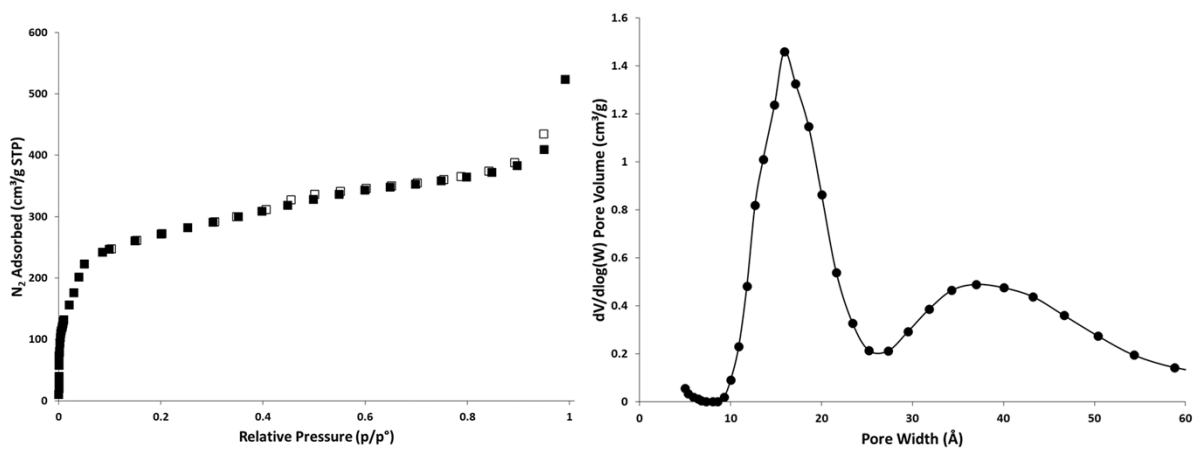


**Figure S76.** N<sub>2</sub> isotherms (left) and pore size distribution (right) of Hf-MOF-808-NH-TFA after K<sub>2</sub>CO<sub>3</sub> activation. Adsorption = filled, desorption = empty markers.

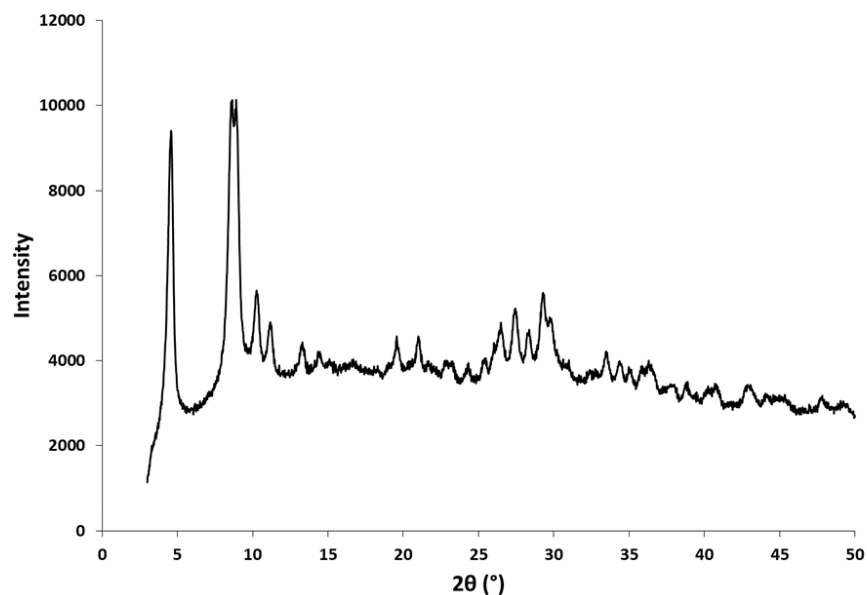


**Figure S77.** PXRD pattern of Hf-MOF-808-NH-TFA after  $K_2CO_3$  activation.

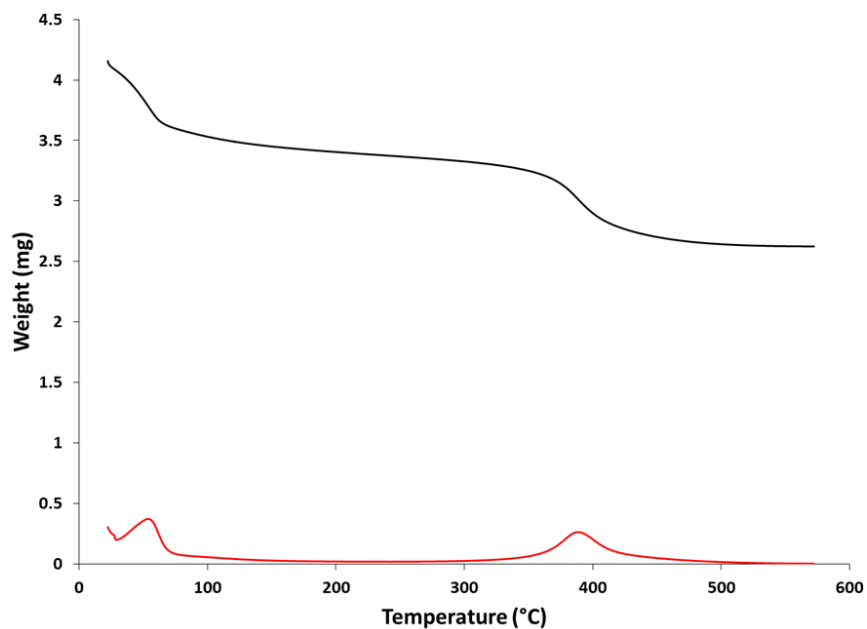


**Figure S78.** TGA curve (black) and derivative weight in  $\%/^{\circ}C$  (red) of Hf-MOF-808-NH-TFA after  $K_2CO_3$  activation.

**DMNP hydrolysis with MOFs:** MOF catalyst 12 mol% (3  $\mu$ mol) was added to a 1 dram vial. 1 mL of a 10% v/v  $D_2O/H_2O$  (0.1 mL  $D_2O$ , 0.9 mL DI  $H_2O$ ) solution was added to the MOF. The vial was capped and sonicated briefly (~1 min) to disperse the MOF. The mixture was then transferred to an NMR tube via pipette. DMNP (25

$\mu\text{mol}$ ,  $4 \mu\text{L}$ ) was added to the inside of the tube via pipetter and capped. The NMR tube was quickly inverted thrice and placed into an NMR instrument. The hydrolysis was monitored by  $^{31}\text{P}$  NMR as described above.

**Reactivation of spent MOFs and DMNP hydrolysis:** The NMR tubes containing previously utilized MOF catalyst 12 mol% and 1 mL of a 10% v/v  $\text{D}_2\text{O}/\text{H}_2\text{O}$  (0.1 mL  $\text{D}_2\text{O}$ , 0.9 mL DI  $\text{H}_2\text{O}$ ) solution were removed from the NMR instrument and MOF particles were allowed to settle on the bottom of the tube. The solution was carefully removed via pipette and 1 mL of 0.013M aqueous piperidine solution or an aqueous  $\text{K}_2\text{CO}_3$  solution (9.2 mM, 10 mL) was added to the MOF within the tube. For  $\text{K}_2\text{CO}_3$  activation, the NMR tube was capped and placed in a  $90^\circ\text{C}$  oven for  $\sim 18$  hours at room temperature. For piperidine activation, the NMR tube was capped and allowed to react with the MOF for  $\sim 18$  hours. After removing the tube from the oven and allowing it to cool to room temperature, the solution was carefully removed via pipette and solvent exchanged with fresh  $\text{H}_2\text{O}$  ( $3 \times 2\text{mL}$ ). The reactivated MOF was then added 1 mL of a 10% v/v  $\text{D}_2\text{O}/\text{H}_2\text{O}$  (0.1 mL  $\text{D}_2\text{O}$ , 0.9 mL DI  $\text{H}_2\text{O}$ ) solution. DMNP ( $25 \mu\text{mol}$ ,  $4 \mu\text{L}$ ) was added to the inside of the tube via pipetter and capped. The NMR tube was quickly inverted thrice and placed into an NMR instrument. The hydrolysis was monitored by  $^{31}\text{P}$  NMR as described above.

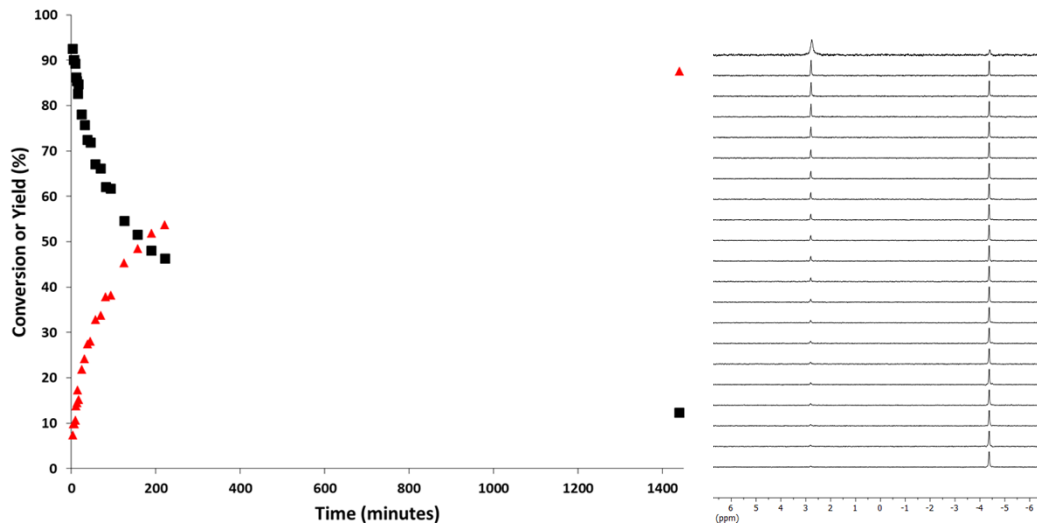


**Figure S79.** (Left) Plots of DMNP hydrolysis with Zr-MOF-808-PA at 12 mol% MOF loading. (Right) Corresponding  $^{31}\text{P}$  NMR spectra of DMNP hydrolysis with Zr-MOF-808-PA at 12 mol% MOF loading.

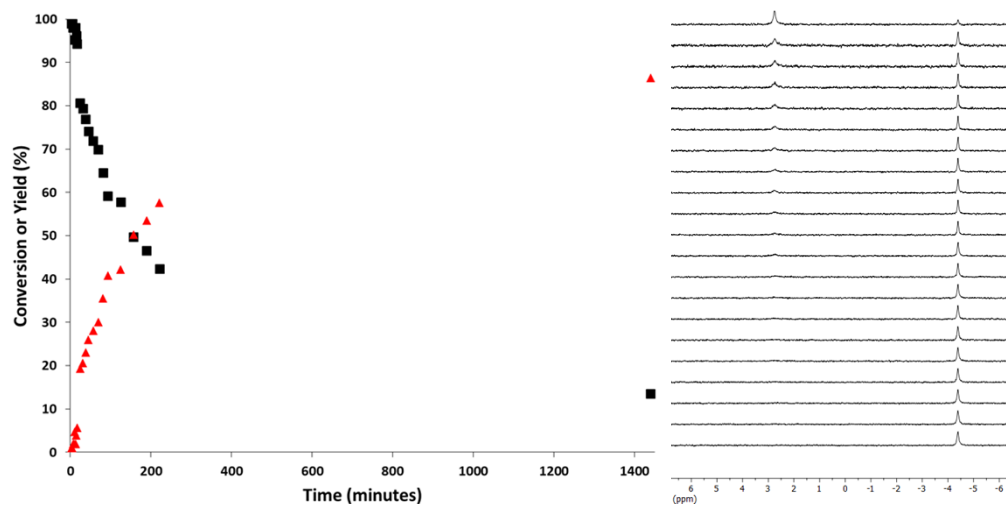


**Figure S80.** (Left) Plots of DMNP hydrolysis with Hf-MOF-808-PA at 12 mol% MOF loading. (Right) Corresponding  $^{31}\text{P}$  NMR spectra of DMNP hydrolysis with Hf-MOF-808-PA at 12 mol% MOF loading..

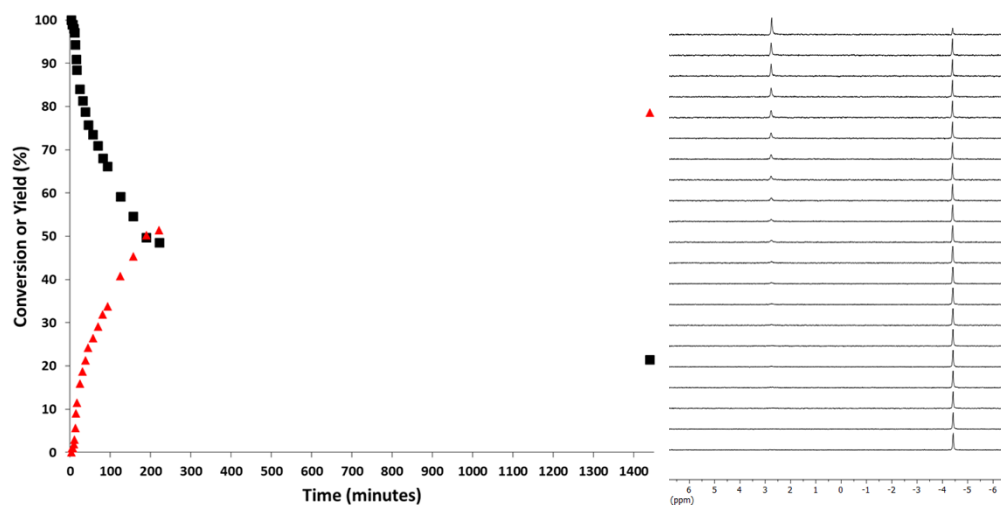


**Figure S81.** (Left) Plots of DMNP hydrolysis with Zr-MOF-808-AA at 12 mol% MOF loading. (Right) Corresponding  $^{31}\text{P}$  NMR spectra of DMNP hydrolysis with Zr-MOF-808-AA at 12 mol% MOF loading.

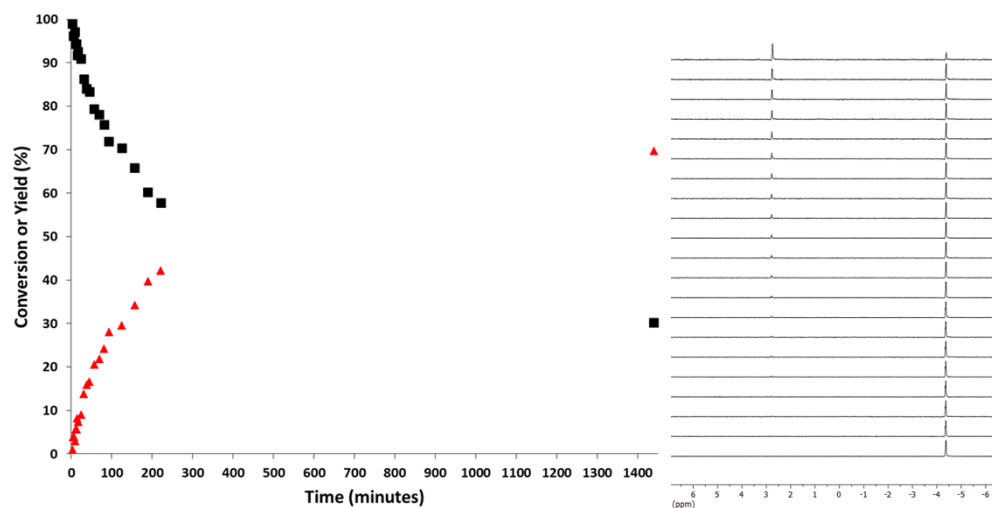


**Figure S82.** (Left) Plots of DMNP hydrolysis with Zr-MOF-808-TFA at 12 mol% MOF loading. (Right) Corresponding  $^{31}\text{P}$  NMR spectra of DMNP hydrolysis with Zr-MOF-808-TFA at 12 mol% MOF loading.

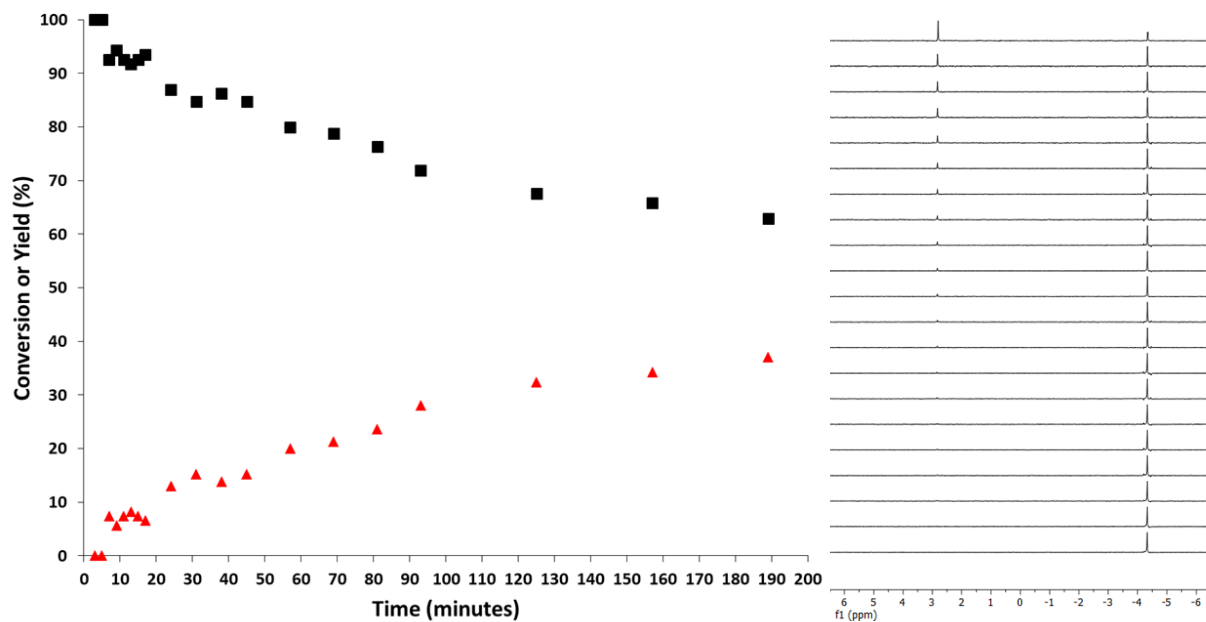


**Figure S83.** (Left) Plots of DMNP hydrolysis with HCl-DMF activated Zr-MOF-808 at 12 mol% MOF loading. (Right) Corresponding  $^{31}\text{P}$  NMR spectra of DMNP hydrolysis with HCl-DMF activated Zr-MOF-808 at 12 mol% MOF loading.

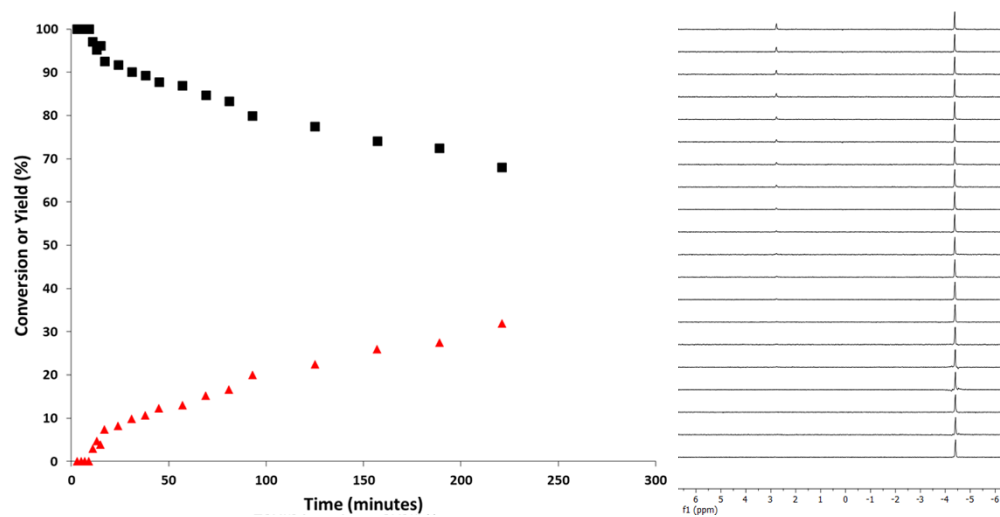


**Figure S84.** (Left) Plots of DMNP hydrolysis with HCl-acetone activated Zr-MOF-808 at 12 mol% MOF loading. (Right) Corresponding  $^{31}\text{P}$  NMR spectra of DMNP hydrolysis with HCl-acetone activated Zr-MOF-808 at 12 mol% MOF loading.

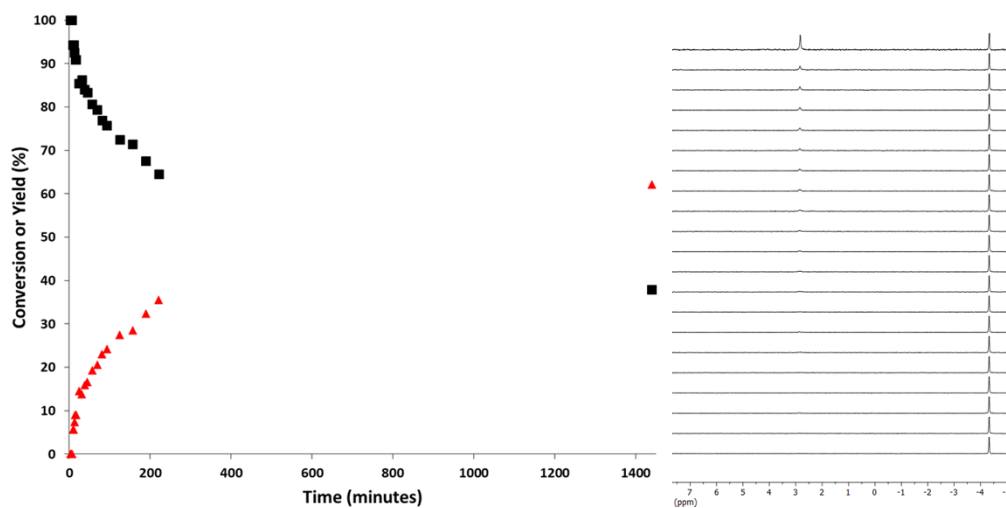


**Figure S85.** (Left) Plots of DMNP hydrolysis with HCl-DMF activated Hf-MOF-808 at 12 mol% MOF loading. (Right) Corresponding  $^{31}\text{P}$  NMR spectra of DMNP hydrolysis with HCl-DMF activated Hf-MOF-808 at 12 mol% MOF loading.



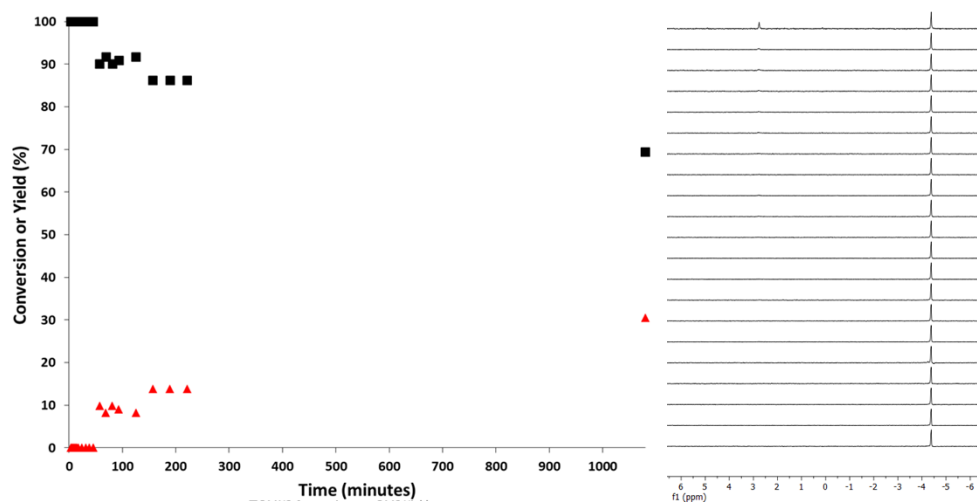


**Figure S86.** (Left) Plots of DMNP hydrolysis with HCl-acetone activated Hf-MOF-808 at 12 mol% MOF loading. (Right) Corresponding <sup>31</sup>P NMR spectra of DMNP hydrolysis with HCl-acetone activated Hf-MOF-808 at 12 mol% MOF loading.

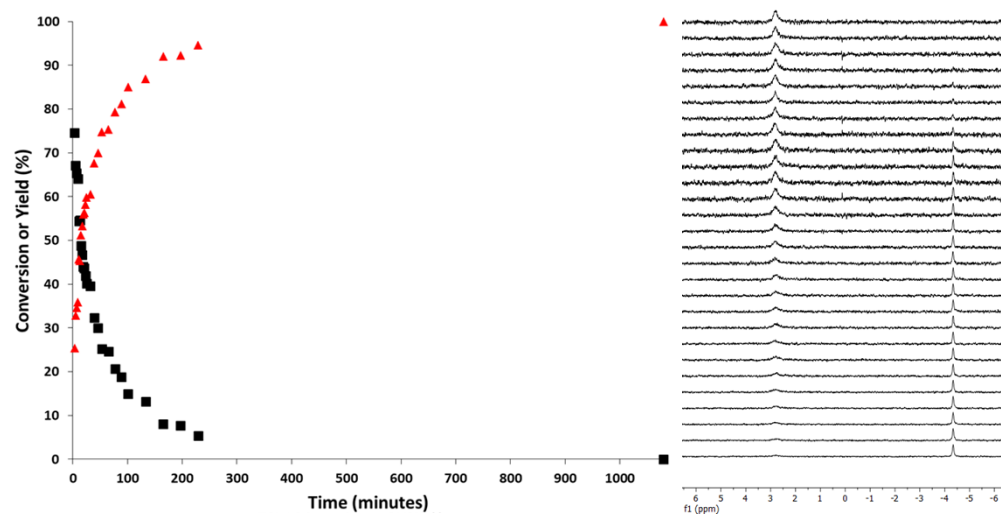


**Figure S87.** (Left) Reaction profile of DMNP hydrolysis with Hf-MOF-808-SALI-[BA-Morph]<sub>2</sub> at 12 mol% MOF loading. (Right) Corresponding <sup>31</sup>P NMR spectra of DMNP hydrolysis with Hf-MOF-808-SALI-[BA-Morph]<sub>2</sub>.

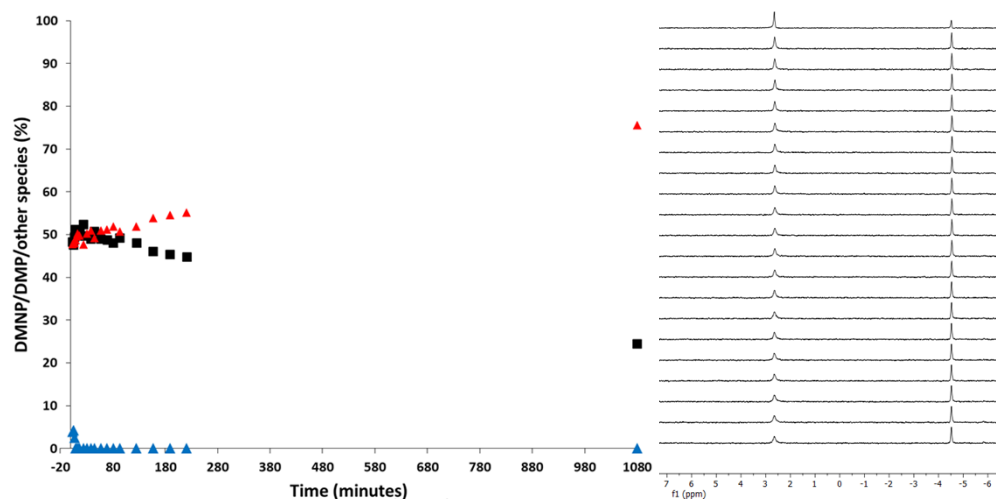


**Figure S88.** (Left) Reaction profile of DMNP hydrolysis with spent Hf-MOF-808-SALI-[BA-Morph]<sub>2</sub> at 12 mol% MOF loading. (Right) Corresponding <sup>31</sup>P NMR spectra of DMNP hydrolysis with Hf-MOF-808-SALI-[BA-Morph]<sub>2</sub>.

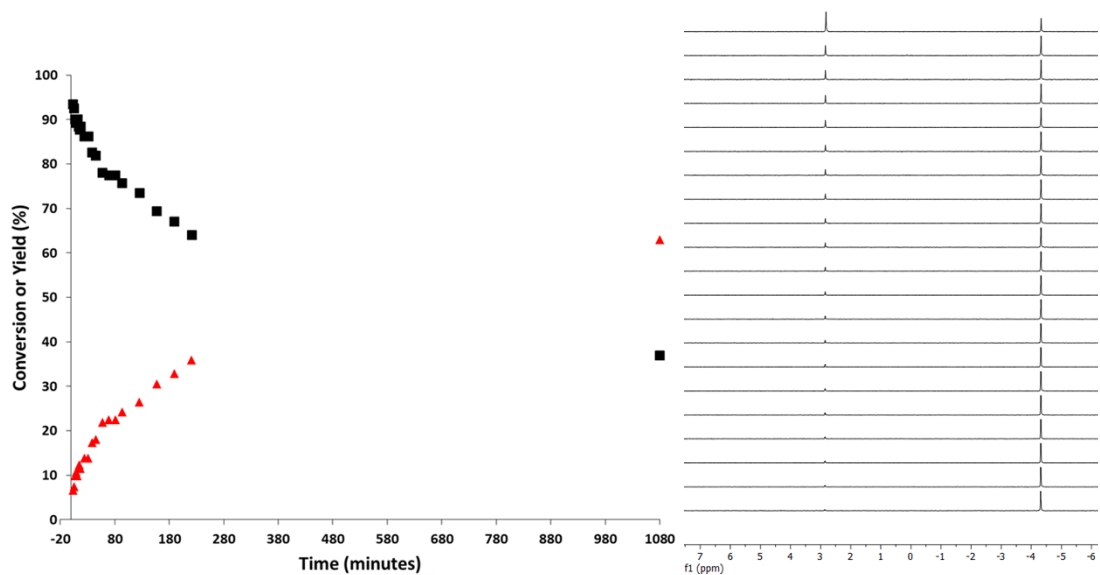


**Figure S89.** (Left) Reaction profile of DMNP hydrolysis with reactivated Hf-MOF-808-SALI-[BA-Morph]<sub>2</sub> at 12 mol% MOF loading. (Right) Corresponding <sup>31</sup>P NMR spectra of DMNP hydrolysis with piperidine treated Hf-MOF-808-SALI-[BA-Morph]<sub>2</sub>.

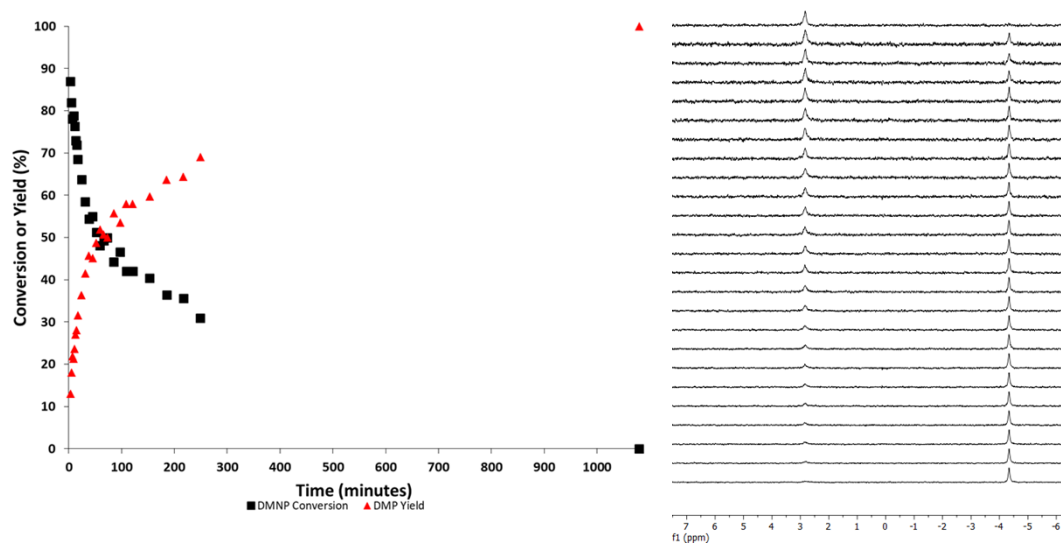


**Figure S90.** (Left) Reaction profile of DMNP hydrolysis with Hf-MOF-808-SALI-[BA-CH<sub>2</sub>NH<sub>2</sub>]<sub>2</sub> at 12 mol% MOF loading. (Right) Corresponding <sup>31</sup>P NMR spectra of DMNP hydrolysis with Hf-MOF-808-SALI-[BA-CH<sub>2</sub>NH<sub>2</sub>]<sub>2</sub>.

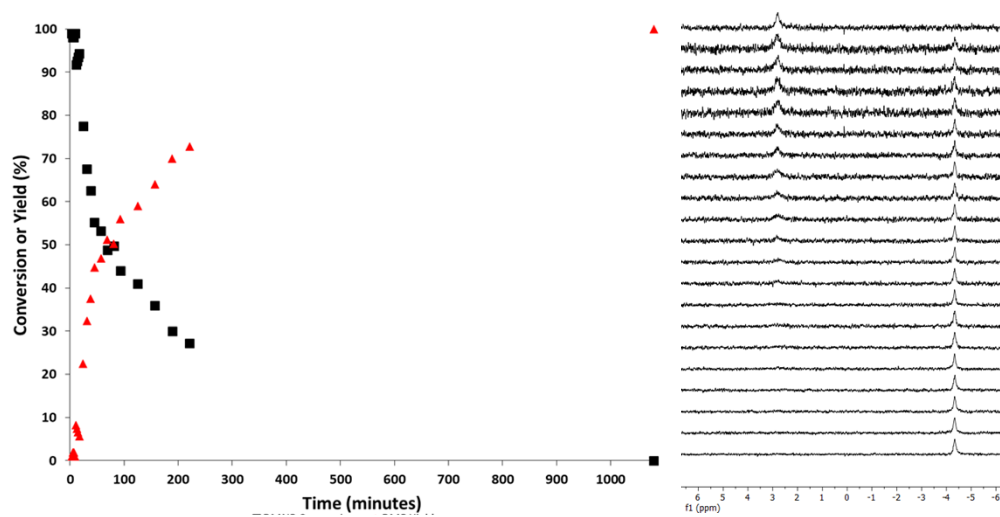


**Figure S91.** (Left) Reaction profile of DMNP hydrolysis with Hf-MOF-808-SALI-[BA-AO]<sub>2</sub> at 12 mol% MOF loading. (Right) Corresponding <sup>31</sup>P NMR spectra of DMNP hydrolysis with Hf-MOF-808-SALI-[BA-AO]<sub>2</sub>.

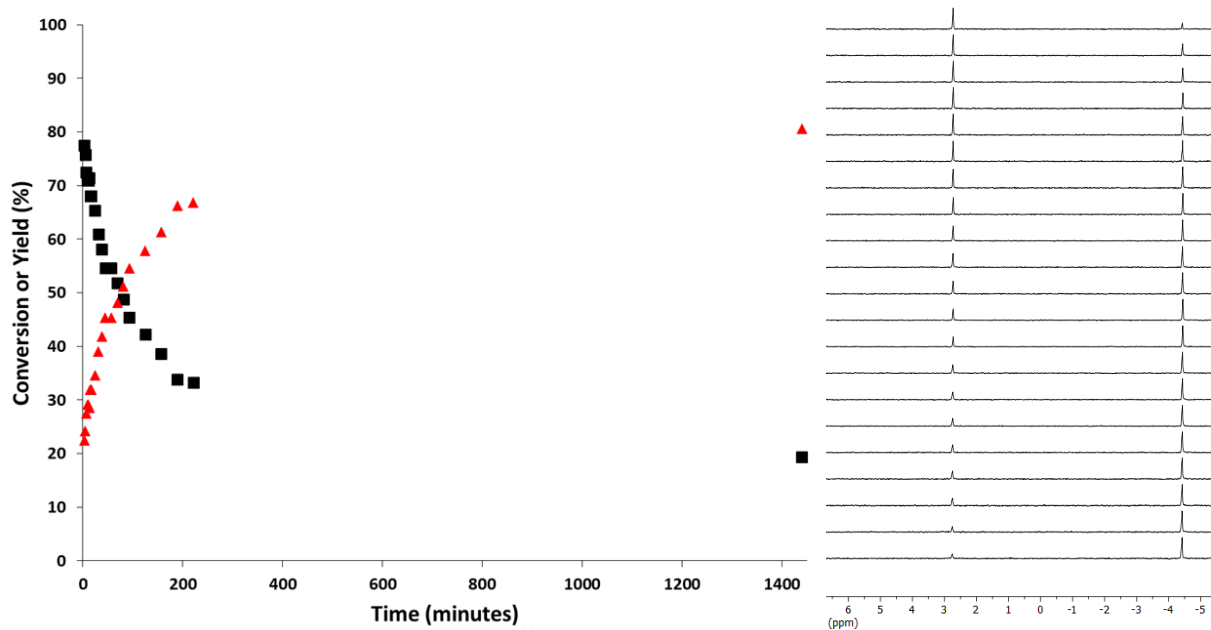


**Figure S92.** (Left) Reaction profile of DMNP hydrolysis with Zr-MOF-808-SALI-[BA-Morph]<sub>2</sub> at 12 mol% MOF loading. (Right) Corresponding <sup>31</sup>P NMR spectra of DMNP hydrolysis with Zr-MOF-808-SALI-[BA-Morph]<sub>2</sub>.

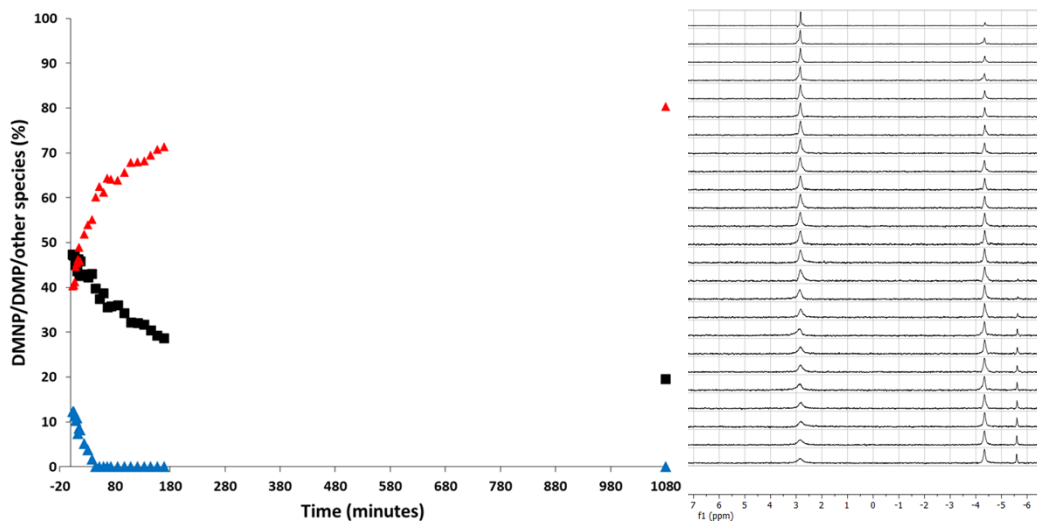


**Figure S93.** (Left) Reaction profile of DMNP hydrolysis with spent Zr-MOF-808-SALI-[BA-Morph]<sub>2</sub> at 12 mol% MOF loading. (Right) Corresponding <sup>31</sup>P NMR spectra of DMNP hydrolysis with Zr-MOF-808-SALI-[BA-Morph]<sub>2</sub>.

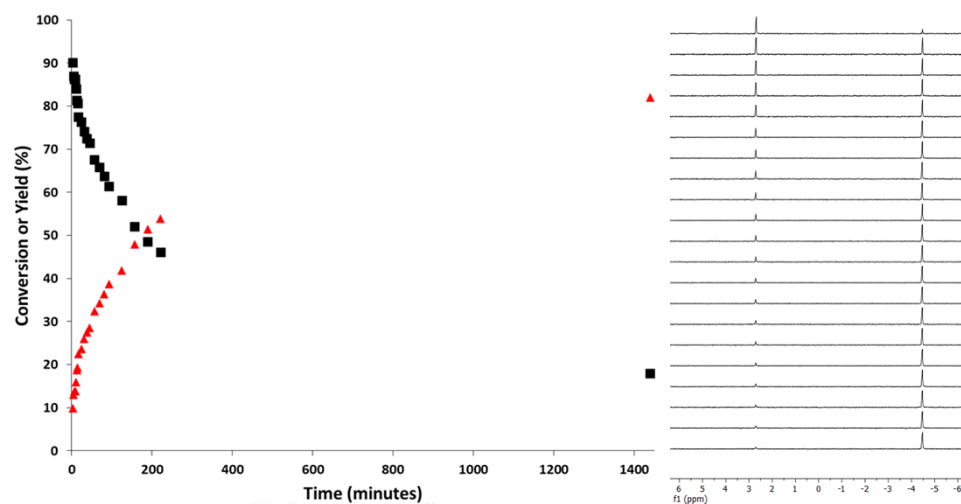


**Figure S94.** (Left) Reaction profile of DMNP hydrolysis with Zr-MOF-808-SALI-[BA-CH<sub>2</sub>NH<sub>2</sub>]<sub>2</sub> at 12 mol% MOF loading. (Right) Corresponding <sup>31</sup>P NMR spectra of DMNP hydrolysis with Zr-MOF-808-SALI-[BA-CH<sub>2</sub>NH<sub>2</sub>]<sub>2</sub>.

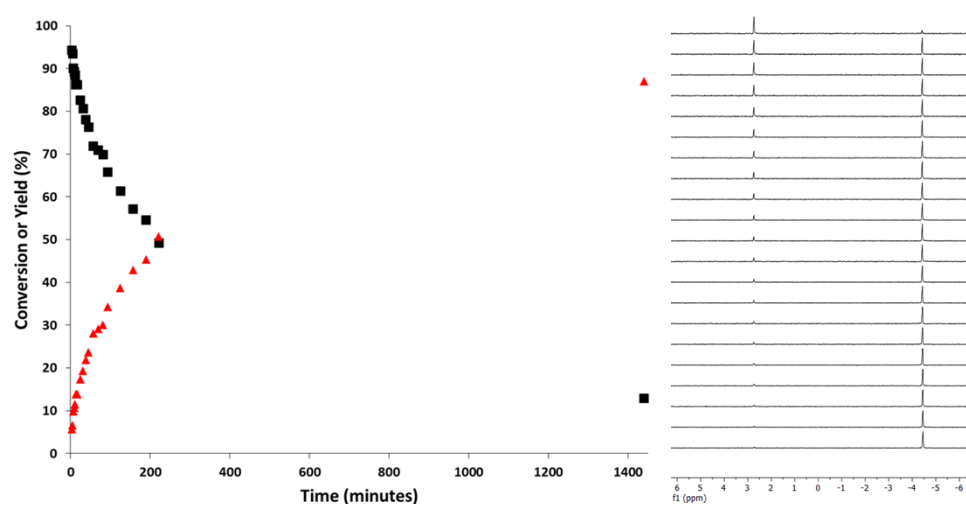


**Figure S95.** (Left) Reaction profile of DMNP hydrolysis with Zr-MOF-808-SALI-[BA-AO]<sub>2</sub> at 12 mol% MOF loading. (Right) Corresponding <sup>31</sup>P NMR spectra of DMNP hydrolysis with Zr-MOF-808-SALI-[BA-AO]<sub>2</sub>.

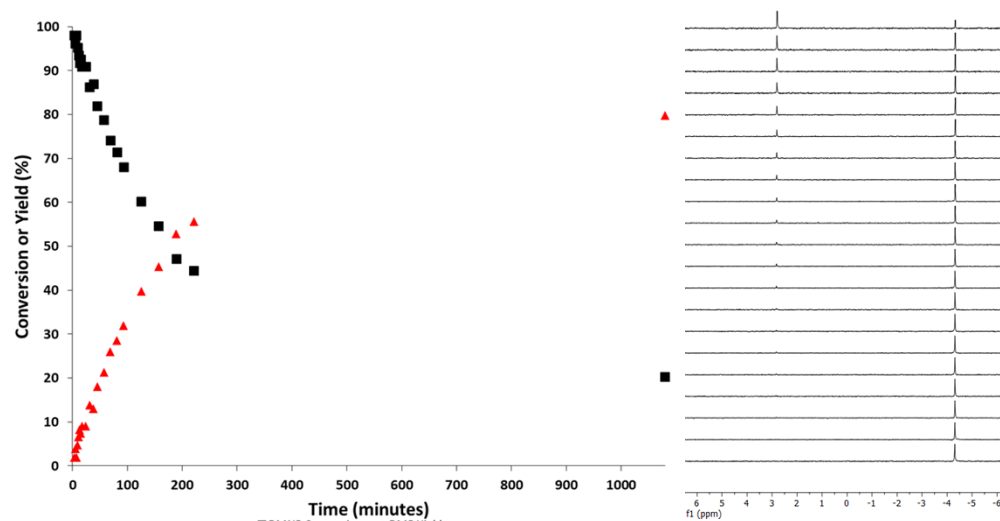


**Figure S96.** (Left) Reaction profile of DMNP hydrolysis with Zr-MOF-808-NH-TFA at 12 mol% MOF loading. (Right) Corresponding <sup>31</sup>P NMR spectra of DMNP hydrolysis with Zr-MOF-808-NH-TFA.

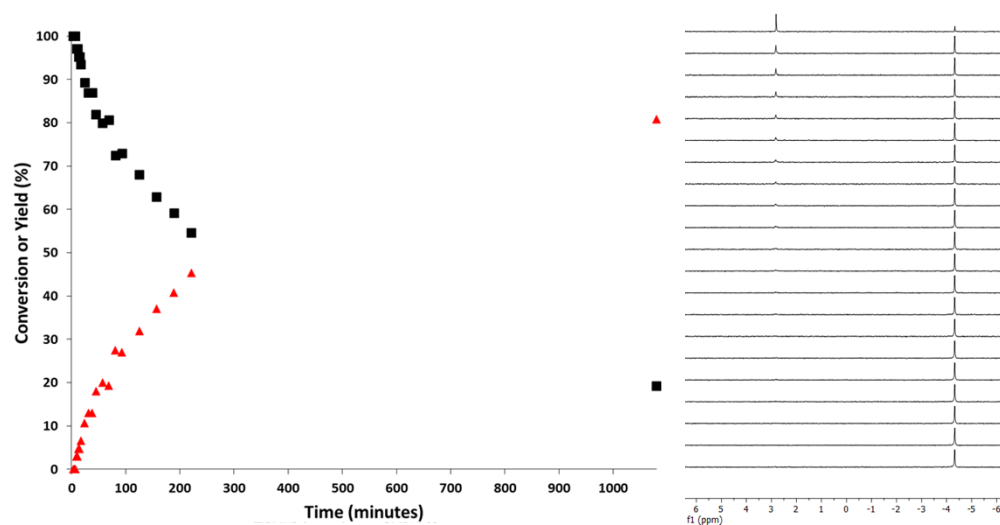


**Figure S97.** (Left) Reaction profile of DMNP hydrolysis with Zr-MOF-808-NH-TFA after HCl activation at 12 mol% MOF loading. (Right) Corresponding <sup>31</sup>P NMR spectra of DMNP hydrolysis with Zr-MOF-808-NH-TFA after HCl activation.

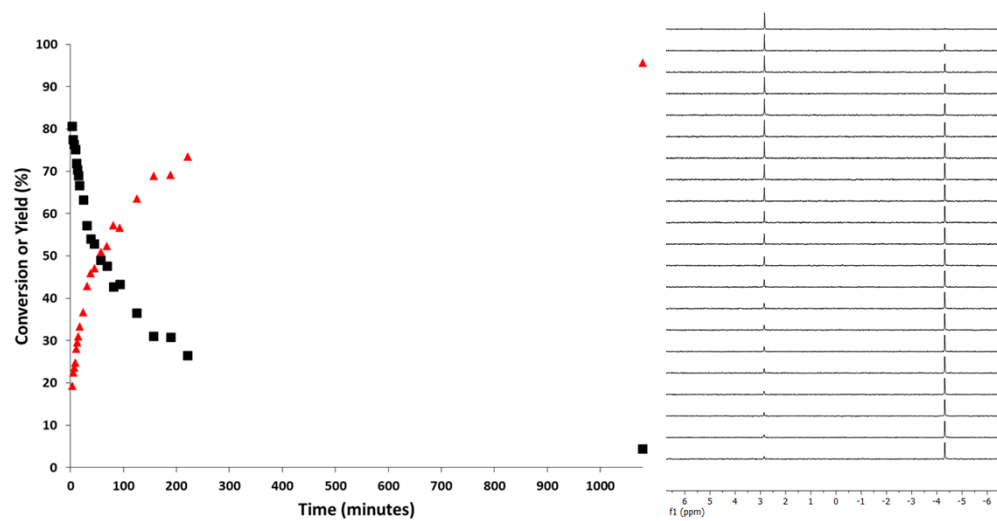


**Figure S98.** (Left) Reaction profile of DMNP hydrolysis with Zr-MOF-808-NH-TFA after  $K_2CO_3$  activation at 12 mol% MOF loading. (Right) Corresponding  $^{31}P$  NMR spectra of DMNP hydrolysis with Zr-MOF-808-NH-TFA after  $K_2CO_3$  activation.

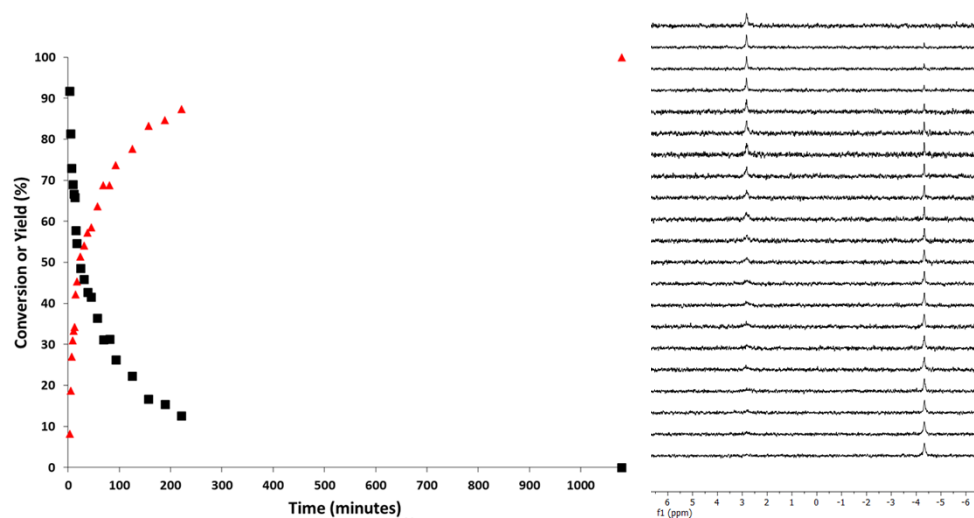


**Figure S99.** (Left) Reaction profile of DMNP hydrolysis with Zr-MOF-808-NH-Morph after at 12 mol% MOF loading. (Right) Corresponding  $^{31}P$  NMR spectra of DMNP hydrolysis with Zr-MOF-808-NH-Morph.

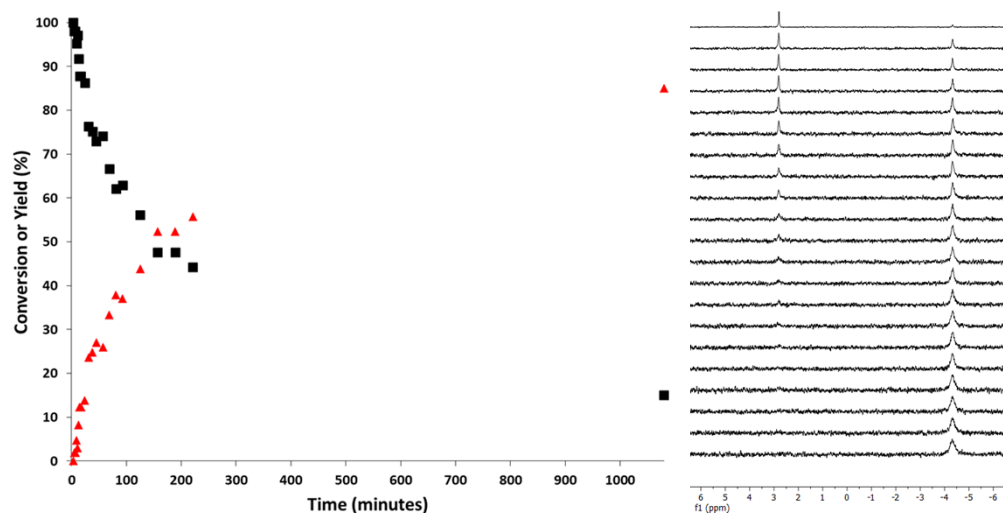


**Figure S100.** (Left) Reaction profile of DMNP hydrolysis with Hf-MOF-808-NH-TFA at 12 mol% MOF loading. (Right) Corresponding <sup>31</sup>P NMR spectra of DMNP hydrolysis with Hf-MOF-808-NH-TFA.

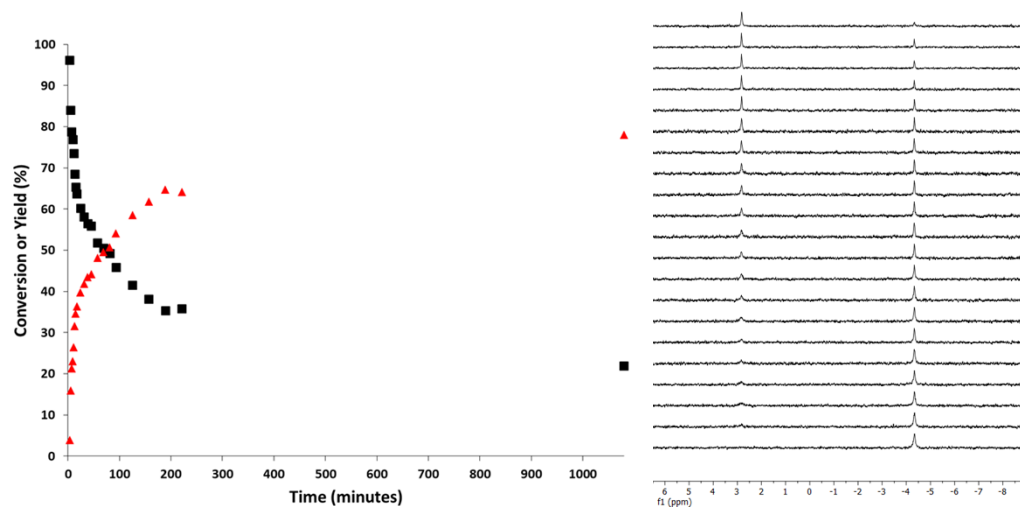


**Figure S101.** (Left) Reaction profile of DMNP hydrolysis with Hf-MOF-808-NH-TFA after K<sub>2</sub>CO<sub>3</sub> activation at 12 mol% MOF loading. (Right) Corresponding <sup>31</sup>P NMR spectra of DMNP hydrolysis with Hf-MOF-808-NH-TFA after K<sub>2</sub>CO<sub>3</sub> activation.



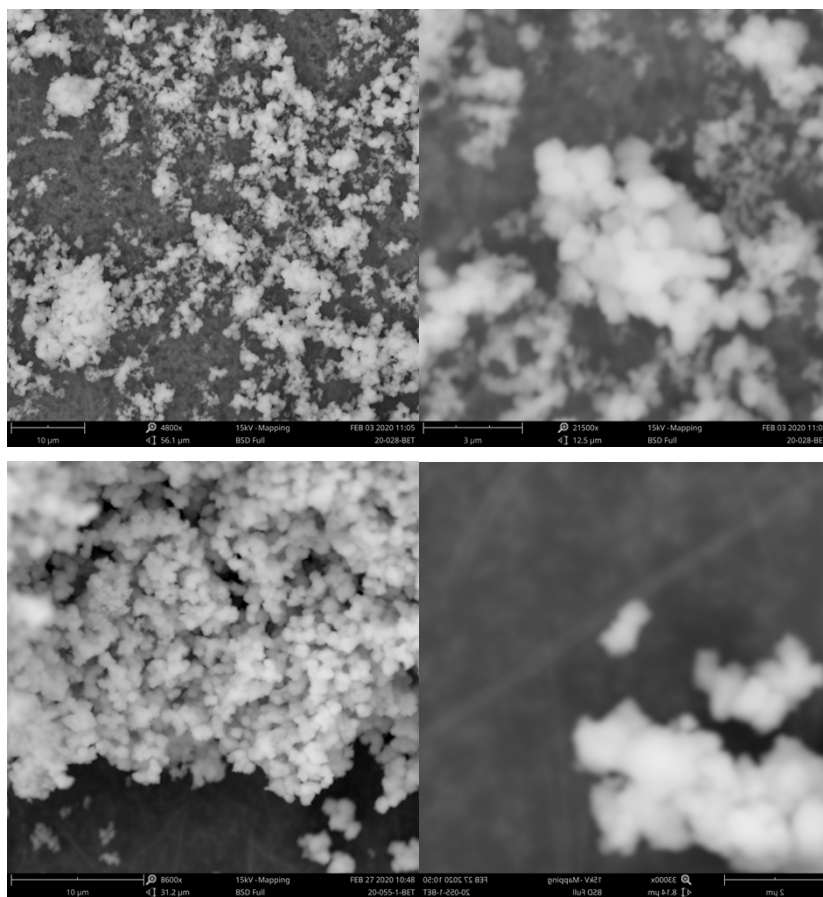


**Figure S102.** (Top Left) SEM image of as synthesized amine functionalized Zr-MOF-808 at 10  $\mu\text{m}$  magnification. (Top Right) SEM image of as synthesized amine functionalized Zr-MOF-808 at 3  $\mu\text{m}$  magnification. (Bottom Left) SEM image of as synthesized amine functionalized Zr-MOF-808 after  $\text{K}_2\text{CO}_3$  activation at 10  $\mu\text{m}$  magnification. (BottomRight) SEM image of as synthesized amine functionalized Zr-MOF-808 after  $\text{K}_2\text{CO}_3$  activation at 3  $\mu\text{m}$  magnification

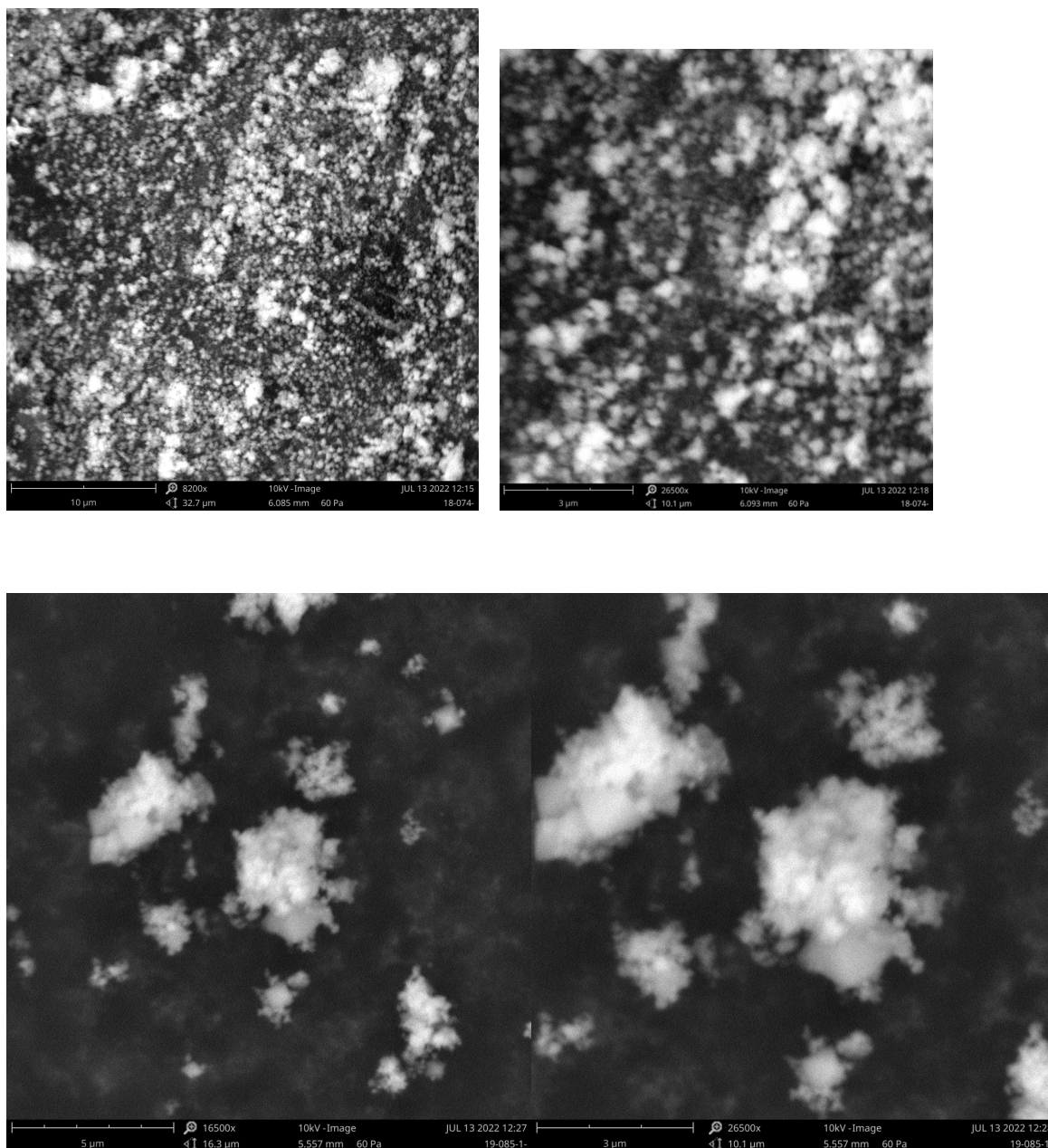


**Figure S103.** (Top Left) SEM image of Zr-MOF-808-PA at 10 µm magnification. (Top Right) SEM image of Zr-MOF-808 at 3 µm magnification. (Bottom Left) SEM image of Zr-MOF-808-5X at 5 µm magnification. (Bottom Right) SEM image of Zr-MOF-808-5x at 3 µm magnification

**Schiff-base test:** The MOFs (50 mg) were added to a 8 dram vial and 10 mL of acetone was added to the MOF. The vial was capped and allowed to stand at room temperature for ~18 hours. The acetone was carefully removed from the vial via pipette and the uncapped vial was heated briefly ~80 C.

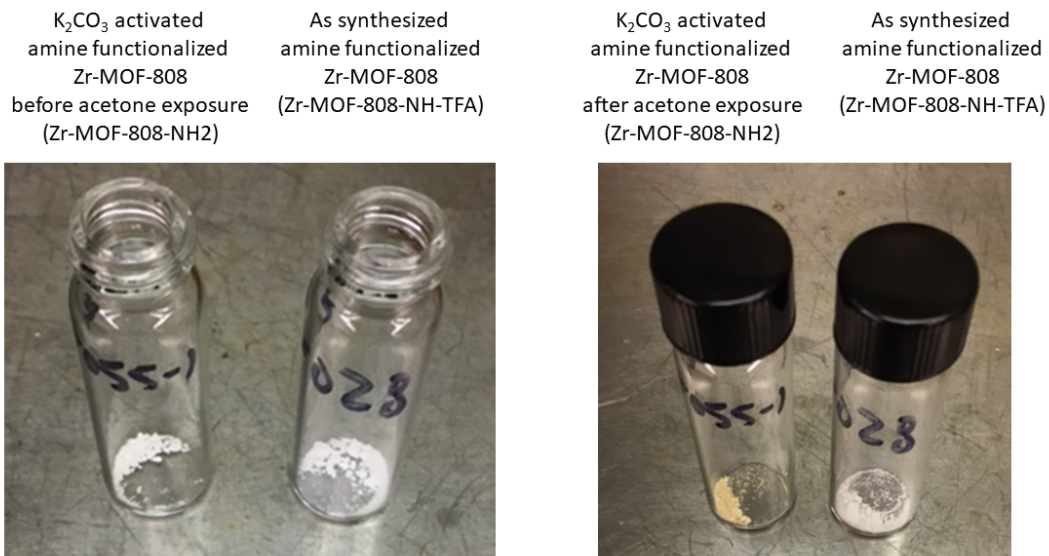
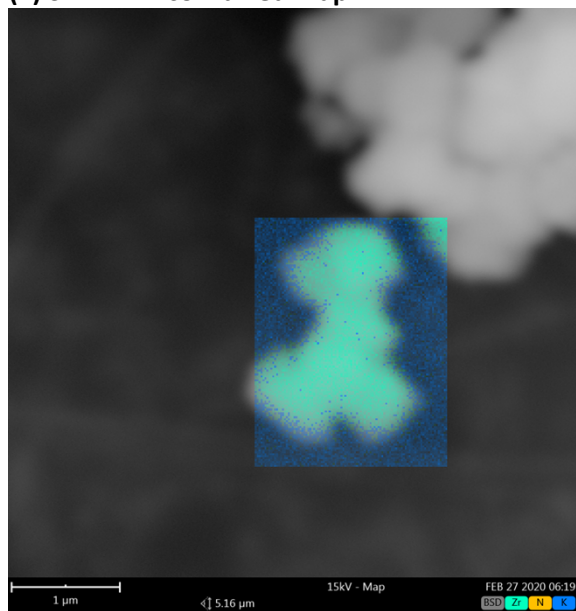


**Figure S104.** (Left)  $K_2CO_3$  activated Zr-MOF-808-NH-TFA (055-1) and as synthesized Zr-MOF-808-NH-TFA (028). (Right)  $K_2CO_3$  activated Zr-MOF-808-NH-TFA and as synthesized Zr-MOF-808-NH-TFA after acetone treatment.

**(1) SEM-EDX combined map**



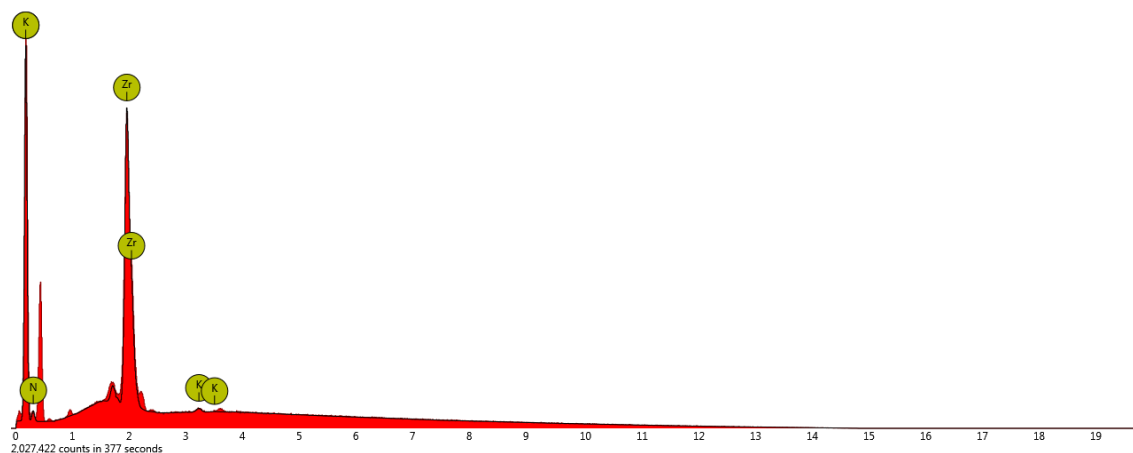
FOV: 5.16  $\mu$ m, Mode: 15kV - Map, Detector: BSD Full, Time: FEB 27 2020 06:19

**(2)**

Element Number	Element Symbol	Element Name	Atomic Conc.	Weight Conc.
40	Zr	Zirconium	39.81	80.72

7	N	Nitrogen	59.21	18.43
19	K	Potassium	0.98	0.85

(3)



Disabled elements: C, O

**Figure S105.** (1) Combined SEM-EDX mapping of  $K_2CO_3$  activated amine functionalized Zr-MOF-808. (2) Chemical composition analysis of  $K_2CO_3$  activated amine functionalized Zr-MOF-808. (3) EDX spectrum of  $K_2CO_3$  activated amine functionalized Zr-MOF-808.

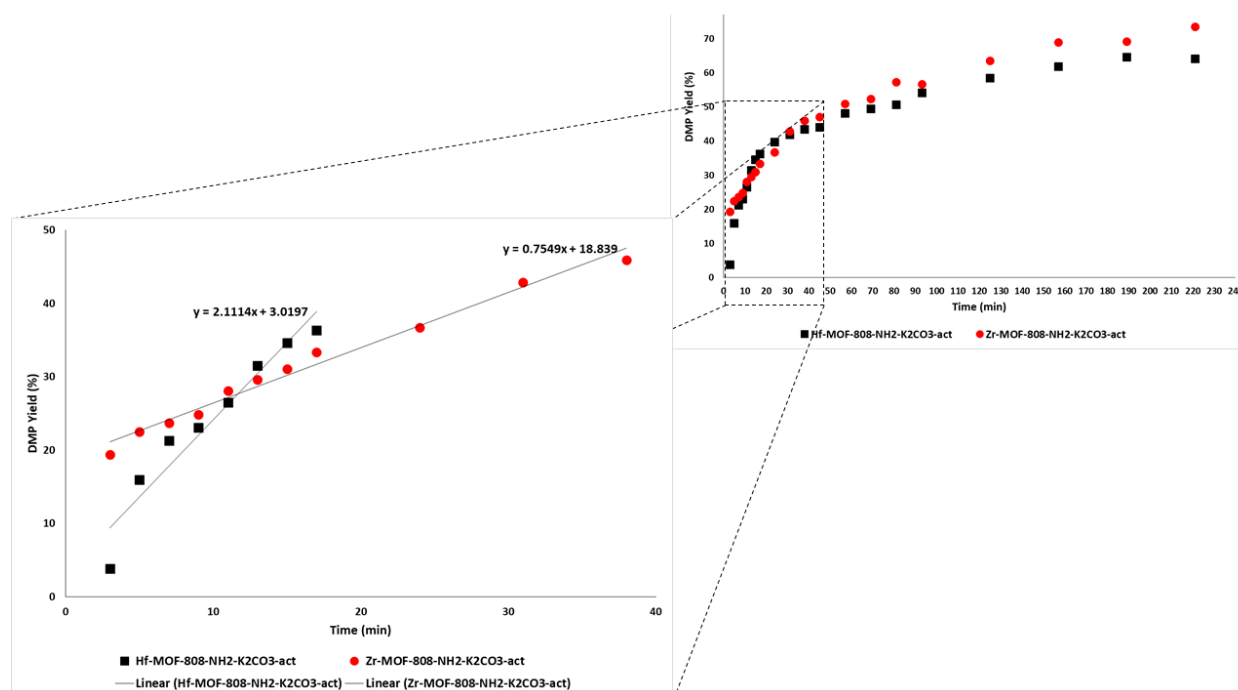


**Figure S106.** (Left) Comparison of the reaction profiles of DMNP hydrolysis with Zr-MOF-808-NH-TFA (red) and Hf-MOF-808-NH-TFA (black) after  $K_2CO_3$  activation at 12 mol% MOF loading. (Right) Zoom in on the initial reaction profile of DMNP hydrolysis with Zr-MOF-808-NH-TFA (red) and Hf-MOF-808-NH-TFA (black) after  $K_2CO_3$  activation at 12 mol% MOF loading.

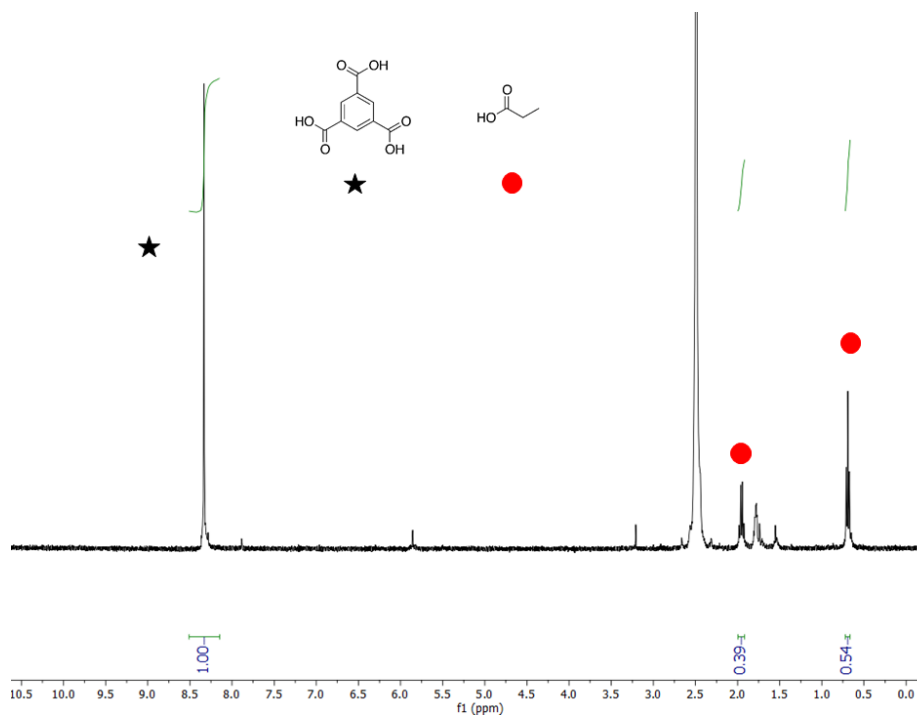


**Figure S107.**  $^1H$  NMR spectrum of digested  $K_2CO_3$  activated Zr-MOF-808-PA(5X) in  $d_6$ -DMSO.

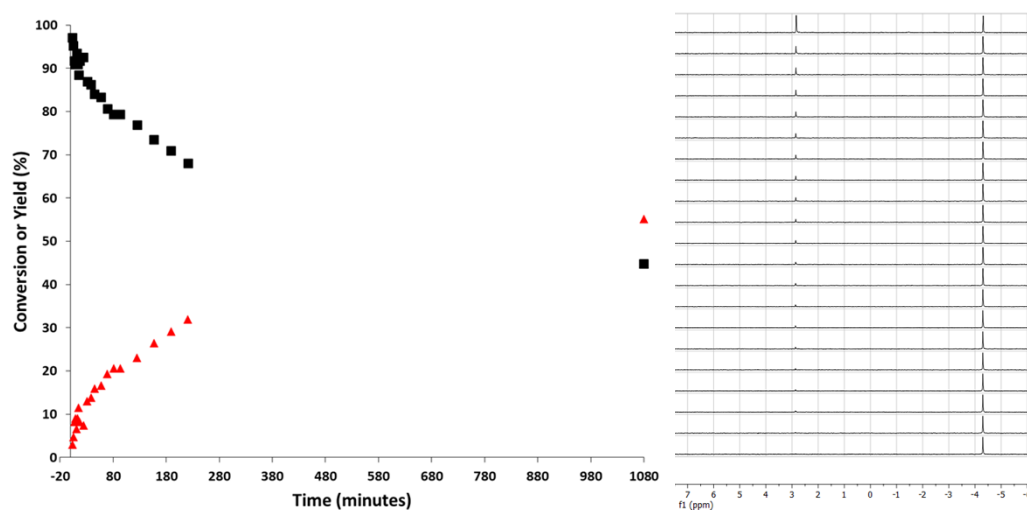


**Figure S108.** (Left) Reaction profile of DMNP hydrolysis with Zr-MOF-808-PA(5X) after  $K_2CO_3$  activation (red). (Right) Corresponding  $^{31}P$  NMR spectra of DMNP hydrolysis with Zr-MOF-808-PA(5X) after  $K_2CO_3$  activation.

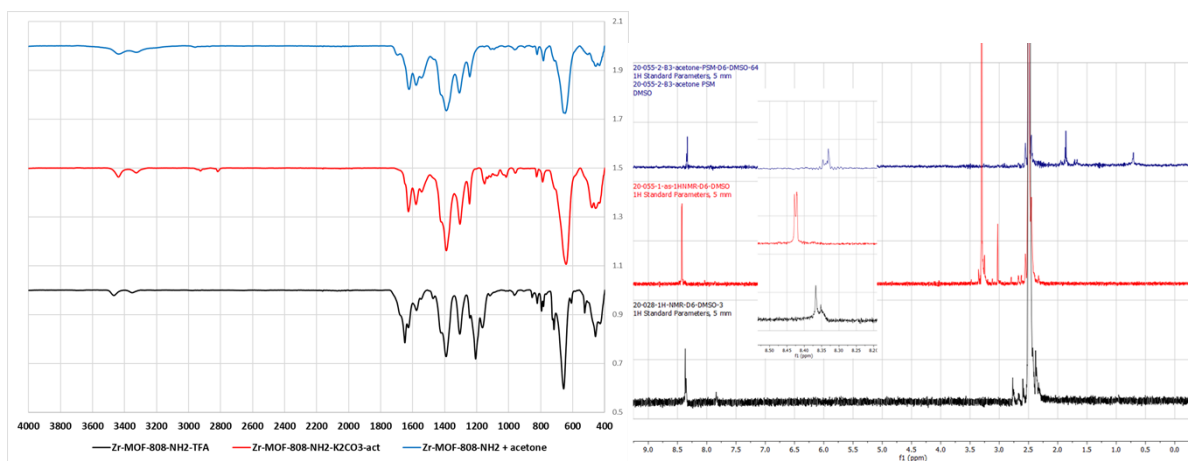


**Figure S109.** (Left) Transmittance ATF-IR spectra of Zr-MOF-808-NH-TFA (black), Zr-MOF-808-NH-TFA K<sub>2</sub>CO<sub>3</sub>-activated (red), and Zr-MOF-808-NH<sub>2</sub> after acetone treatment (blue). (Right) <sup>1</sup>H NMR spectrum of digested Zr-MOF-808-NH-TFA (black), Zr-MOF-808-NH-TFA K<sub>2</sub>CO<sub>3</sub>-activated (red), and Zr-MOF-808-NH<sub>2</sub> after acetone treatment (blue).

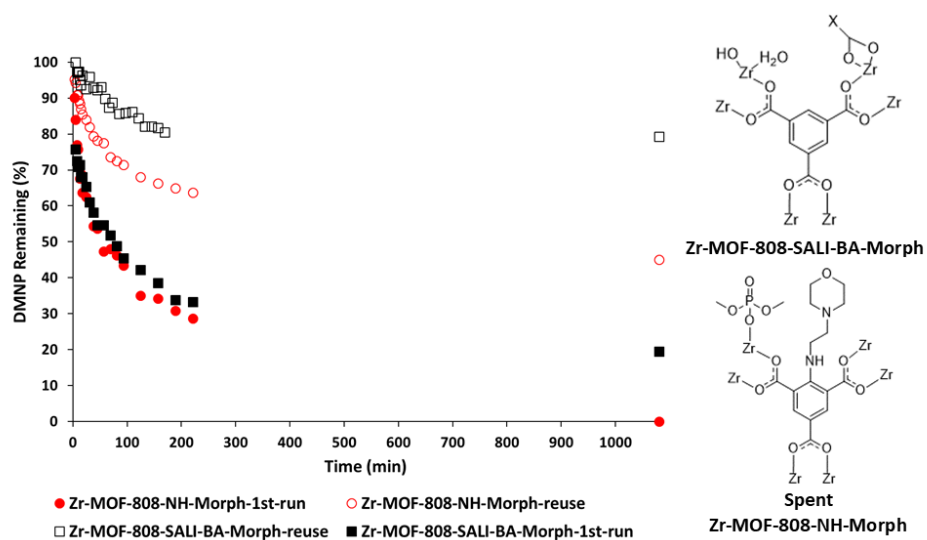


**Figure S110.** (Left) Initial DMNP hydrolysis conversion with Zr-MOF-808-NH-Morph (red solid squares), spent Zr-MOF-808-NH-Morph (red unfilled squares), Zr-MOF-808-SALI-BA-Morph (black solid squares), and spent Zr-MOF-808-SALI-BA-Morph (black unfilled squares) at 12 mol% MOF loading.

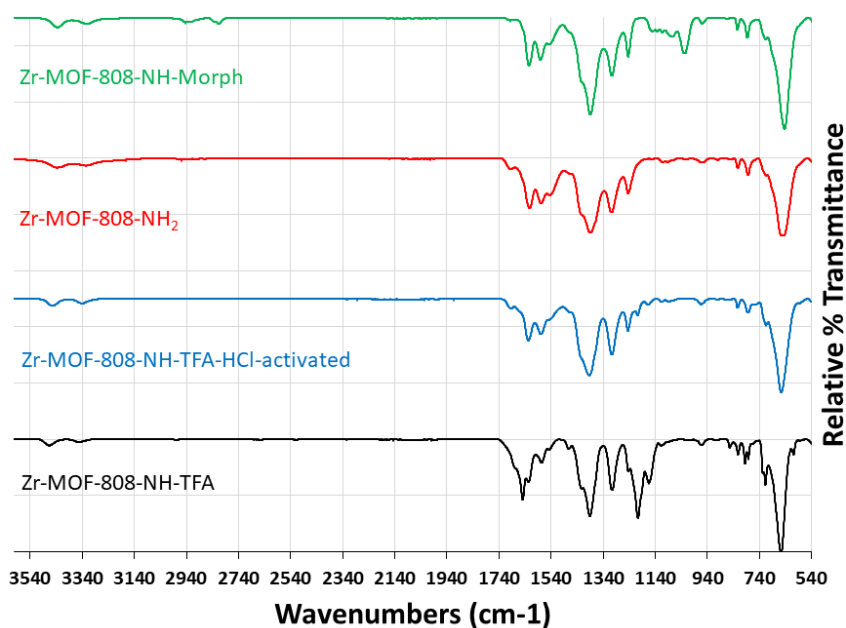


**Figure S111.** % Transmittance ATF-IR spectra of Zr-MOF-808-NH-TFA (black), Zr-MOF-808-NH-TFA HCl-activated (blue), Zr-MOF-808-NH-TFA  $K_2CO_3$ -activated (red), and Zr-MOF-808-NH-Morph (green).

### Computational Modeling

Given that there is no reported synthesis of Zr-MOF-808-NH<sub>2</sub>, computational modeling was utilized to construct a simulated single X-ray structure. The structure was then utilized to generate a simulated PXRD pattern as seen in Figure 2. Ab-initio DFT calculations were performed using the PBE functional and plane-wave basis sets as implemented in the Quantum Espresso 6.4 software package (P. Giannozzi et. al., J.Phys.: Condens.Matter 29, 465901 (2017)). Energy cutoffs were set at 50 Ry for the wavefunction and 400 Ry for density. The calculations used the primitive cell of MOF-808, with hydroxyl termination of the 6 open sites at each SBU. Following is the .cif file of the geometry optimised structure (Total energy is -8308.3829395732 Ry):

```

data_
loop_
_symmetry_equiv_pos_as_xyz
x,y,z
_cell_length_a 24.732090
_cell_length_b 24.732082
_cell_length_c 24.732098
_cell_angle_alpha 60.000035
_cell_angle_beta 60.000031
_cell_angle_gamma 60.000010
loop_
_atom_site_label
_atom_site_fract_x
_atom_site_fract_y
_atom_site_fract_z

```

O	0.472898	0.184351	0.282812
O	0.190109	0.479561	0.055222
O	0.279118	0.059391	0.472930
O	0.066396	0.276957	0.185249
O	0.273449	0.477389	0.186361
O	0.067020	0.182615	0.470159
O	0.466804	0.276243	0.076588
O	0.182713	0.065141	0.281374
O	0.184645	0.274567	0.469494
O	0.477499	0.061663	0.188491
O	0.059899	0.479299	0.271066
O	0.277298	0.180242	0.073527
O	0.778474	0.064640	0.186777
O	0.066394	0.779245	0.967189
O	0.971719	0.183977	0.065394
O	0.188445	0.968606	0.776769
O	0.971510	0.782155	0.176446
O	0.186087	0.062524	0.978485
O	0.774801	0.978954	0.063102
O	0.070145	0.177482	0.779703
O	0.058700	0.974708	0.196482
O	0.770133	0.194154	0.976205
O	0.180808	0.780670	0.064095
O	0.974488	0.064146	0.777293
O	0.780088	0.070516	0.972314
O	0.062006	0.774164	0.185477
O	0.978966	0.182795	0.774319
O	0.176665	0.971785	0.069738
O	0.975214	0.770881	0.058074
O	0.194245	0.060572	0.769433
O	0.778930	0.974071	0.183536
O	0.065159	0.180349	0.975138
O	0.065450	0.971202	0.778298
O	0.778573	0.186710	0.066778
O	0.185611	0.779290	0.970539
O	0.967711	0.066035	0.188764
O	0.469424	0.184635	0.073453
O	0.181542	0.470919	0.276513
O	0.273530	0.056619	0.190087
O	0.062942	0.272883	0.476302
O	0.280084	0.472587	0.064350
O	0.062433	0.186687	0.278750
O	0.480273	0.275595	0.191735
O	0.186851	0.060701	0.472197
O	0.186980	0.271977	0.065117
O	0.471850	0.064268	0.281305
O	0.069747	0.470177	0.179793
O	0.277308	0.183309	0.467391
C	0.351759	0.352621	0.249587
N	0.386150	0.387318	0.191686
C	0.343889	0.346328	0.061602
H	0.367429	0.370964	0.065333



C	0.252267	0.050854	0.347268
H	0.200587	0.053769	0.371512
C	0.057157	0.250717	0.346659
H	0.060979	0.198774	0.370955
C	0.248782	0.346547	0.343548
H	0.196046	0.369709	0.366042
C	0.050504	0.351522	0.349661
N	0.044003	0.384888	0.382787
C	0.342820	0.247696	0.065876
H	0.365568	0.194951	0.073011
C	0.352390	0.046167	0.249232
N	0.385482	0.040452	0.188864
C	0.347171	0.250980	0.345637
H	0.371651	0.199211	0.369714
C	0.348995	0.051695	0.347265
H	0.373002	0.055318	0.371534
C	0.056716	0.347765	0.249397
H	0.059890	0.371947	0.197643
C	0.249054	0.350463	0.049657
N	0.191900	0.384741	0.037035
C	0.904198	0.903550	0.192345
H	0.881237	0.880785	0.185393
C	0.898012	0.899876	-0.000083
N	0.863755	0.865968	0.058645
C	0.001770	0.187944	0.904301
H	0.054319	0.181708	0.881124
C	0.200630	0.002150	0.898719
N	0.208264	0.061666	0.865378
C	-0.000219	0.897540	0.204435
N	0.058598	0.863121	0.213596
C	0.190128	0.905959	0.000058
H	0.184417	0.882642	0.052468
C	0.903774	0.001728	0.904441
H	0.880725	0.054370	0.881463
C	0.900131	0.199134	0.898967
N	0.866471	0.207258	0.865198
C	0.902504	-0.001587	0.198289
H	0.878163	0.049862	0.196186
C	0.902879	0.193481	-0.000505
H	0.877810	0.191828	0.050818
C	0.194775	0.904701	0.901313
H	0.192733	0.880463	0.876161
C	-0.001153	0.902820	0.902663
H	0.050297	0.877905	0.878269
C	0.382549	0.284302	0.283339
C	0.449214	0.245462	0.251586
C	0.281839	0.381537	0.054416
C	0.249526	0.448489	0.057729
C	0.284123	0.050953	0.380306
C	0.247600	0.057214	0.446121
C	0.056748	0.282735	0.281677
C	0.062152	0.246614	0.246235

C	0.282072	0.381952	0.280932
C	0.243090	0.447285	0.246485
C	0.054693	0.283031	0.380638
C	0.061655	0.243453	0.446442
C	0.375767	0.280130	0.065605
C	0.441480	0.244689	0.072661
C	0.284257	0.049243	0.283110
C	0.244144	0.057071	0.250229
C	0.280914	0.281644	0.376995
C	0.245240	0.243925	0.442217
C	0.383059	0.050249	0.282992
C	0.448080	0.058852	0.249565
C	0.054377	0.382193	0.281253
C	0.061479	0.447704	0.241336
C	0.280595	0.280725	0.059081
C	0.246851	0.241603	0.066076
C	0.870541	0.967679	0.194982
C	0.805095	0.004482	0.188024
C	0.965976	0.868444	0.965970
C	0.005075	0.802258	-0.001756
C	0.968929	0.190175	0.968751
C	0.004195	0.184390	0.005468
C	0.198357	0.968149	0.867065
C	0.193872	0.000480	0.800363
C	0.967592	0.868599	0.196013
C	0.001709	0.804456	0.185636
C	0.193669	0.969394	0.967919
C	0.185207	0.002576	0.008211
C	0.868826	0.969464	0.967917
C	0.803996	0.009144	0.002527
C	0.969525	0.191678	0.869360
C	0.009021	0.183686	0.803839
C	0.965883	0.965524	0.201963
C	-0.001396	0.004727	0.195963
C	0.868499	0.197092	0.966782
C	0.801767	0.192840	0.005703
C	0.191877	0.872506	0.967296
C	0.185668	0.806705	0.002959
C	0.968120	0.968726	0.870606
C	0.005241	0.003509	0.804455
Zr	0.551642	0.103447	0.243935
O	0.659889	0.060223	0.222663
Zr	0.107548	0.552059	0.099515
O	0.065654	0.658225	0.053253
Zr	0.242135	0.101666	0.547910
O	0.223131	0.056365	0.655237
Zr	0.104198	0.237303	0.106710
O	0.059049	0.220141	0.061723
Zr	0.239387	0.553251	0.103383
O	0.220796	0.660656	0.058962
Zr	0.106453	0.101148	0.550091
O	0.062767	0.056779	0.658270

Zr	0.550317	0.239253	0.110187
O	0.656555	0.222515	0.066666
Zr	0.100762	0.105715	0.243952
O	0.054738	0.064636	0.223815
Zr	0.107147	0.234609	0.550991
O	0.063827	0.217177	0.657837
Zr	0.551444	0.106501	0.107876
O	0.658353	0.063894	0.061209
Zr	0.103241	0.553188	0.235232
O	0.056903	0.659820	0.217107
Zr	0.236077	0.101869	0.109542
O	0.217728	0.056135	0.067076
Zr	0.700518	0.145664	0.148608
O	0.593433	0.186208	0.195142
Zr	0.147652	0.701435	0.005471
O	0.193230	0.593920	0.026083
Zr	0.006688	0.147027	0.146919
O	0.027287	0.191047	0.190599
Zr	0.147297	0.006324	0.698586
O	0.190287	0.026275	0.590850
Zr	0.011689	0.699356	0.139463
O	0.029740	0.592826	0.182158
Zr	0.143197	0.143384	0.015075
O	0.190077	0.185832	0.032426
Zr	0.699268	0.013279	0.145741
O	0.592661	0.030138	0.191952
Zr	0.148969	0.141532	0.695652
O	0.193632	0.185822	0.588357
Zr	0.140148	0.010979	0.150130
O	0.182757	0.028387	0.196325
Zr	0.696392	0.148940	0.014291
O	0.588739	0.193324	0.033303
Zr	0.143467	0.700009	0.142658
O	0.186600	0.593171	0.189289
Zr	0.014159	0.141869	0.697819
O	0.031522	0.185274	0.591251
O	0.509551	0.163323	0.168646
O	0.164025	0.511076	0.159772
O	0.164875	0.159944	0.508150
O	0.161582	0.161843	0.166712
O	0.740351	0.089466	0.087834
O	0.086292	0.741656	0.082445
O	0.083037	0.085850	0.090627
O	0.090234	0.082807	0.739177
O	0.194375	0.914510	0.695014
H	0.199477	0.871647	0.729357
O	0.915333	0.197100	0.192881
H	0.872388	0.202207	0.196474
O	0.696299	0.196228	0.193848
H	0.730481	0.205355	0.192995
O	0.194698	0.696433	0.914225
H	0.195826	0.730481	0.871382

O	0.691944	0.191003	0.922450
H	0.724945	0.182633	0.881905
O	0.195017	0.918224	0.189613
H	0.212495	0.879438	0.177698
O	0.195834	0.696689	0.186098
H	0.212208	0.729605	0.177098
O	0.921545	0.189457	0.694411
H	0.879330	0.185788	0.727457
O	0.919291	0.696659	0.194238
H	0.879784	0.729573	0.211503
O	0.186132	0.196768	0.922786
H	0.176547	0.212969	0.882862
O	0.190251	0.195938	0.692146
H	0.181534	0.211400	0.725640
O	0.696394	0.920501	0.193857
H	0.729470	0.878165	0.206321
O	0.055260	0.330132	0.060323
H	0.041717	0.371616	0.065850
O	0.333698	0.059504	0.552342
H	0.375559	0.061497	0.517401
O	0.556412	0.053252	0.335150
H	0.522575	0.046497	0.378262
O	0.054564	0.553704	0.058135
H	0.037309	0.520937	0.068434
O	0.555721	0.063013	0.054949
H	0.522375	0.068439	0.041320
O	0.062286	0.326894	0.555537
H	0.067496	0.368377	0.521820
O	0.060471	0.556704	0.327490
H	0.069384	0.523702	0.367796
O	0.328123	0.061675	0.053953
H	0.367603	0.072492	0.036407
O	0.331854	0.555858	0.055037
H	0.374377	0.523604	0.041170
O	0.055656	0.055756	0.554808
H	0.048726	0.054584	0.520303
O	0.055518	0.055191	0.335458
H	0.055731	0.046277	0.378129
O	0.551543	0.332008	0.053753
H	0.517946	0.369848	0.035991
H	0.212870	0.580437	0.215430
H	0.574437	0.219250	-0.005397
H	0.209827	-0.010923	0.221833
H	-0.008051	0.211674	0.578358
H	0.219024	0.213310	0.574343
H	-0.009350	0.579171	0.209336
H	0.215891	0.212565	-0.007040
H	0.580204	-0.009688	0.217474
H	0.579587	0.213063	0.221098
H	0.216604	-0.012496	0.576696
H	-0.011344	0.219071	0.215544
H	0.220129	0.579796	-0.012714

H	0.030718	0.673588	0.256148
H	0.671228	0.039037	0.033621
H	0.038517	0.256806	0.670640
H	0.256678	0.030502	0.039882
H	0.028214	0.038390	0.262842
H	0.259523	0.674889	0.033482
H	0.035400	0.031313	0.672175
H	0.669869	0.261786	0.039038
H	0.674474	0.032465	0.261144
H	0.033369	0.259314	0.034684
H	0.262507	0.031264	0.668399
H	0.038614	0.672010	0.027509
H	0.433870	0.362149	0.169804
H	0.359826	0.433497	0.168202
H	0.046483	0.358510	0.429449
H	0.044892	0.432077	0.356853
H	0.359505	0.041873	0.166393
H	0.431826	0.043645	0.165944
H	0.168990	0.358230	0.039938
H	0.169817	0.432573	0.035944
H	0.893172	1.203119	0.819184
H	0.818739	1.207941	0.890756
H	1.208153	1.083632	0.817868
H	1.204856	1.084926	0.891809
H	0.889150	0.818321	1.080439
H	0.817903	0.892610	1.082326
H	1.082125	0.817206	1.209307
H	1.080619	0.888282	1.214103

### Acknowledgements

S.J.G. and J.B.D. gratefully acknowledge support by the Joint Science and Technology Office for Chemical and Biological Defense (JSTO-CBD).

### References

1. Rubin, H. N.; Reynolds, M. M. Functionalization of Metal–Organic Frameworks To Achieve Controllable Wettability. *Inorg. Chem.* **2017** 56 (9), 5266-5274. DOI: 10.1021/acs.inorgchem.7b00373